UiT The Arctic University of Norway

Department of Medical biology

# Long term 2D-culture of primary mouse liver sinusoidal endothelial cells (LSEC)

## A study of morphological and functional changes in LSEC *in vitro*

Basema B.A. Abujayyab

Master's thesis in Biomedicine MBI-3911, June 2023

# Abstract

Liver sinusoidal endothelial cells (LSEC) are unique and specialized cell type with high endocytic activity of bloodborne waste macromolecules. LSEC lack basal lamina and present a unique structural feature called fenestrations, which facilitate passive filtering and exchange of nutrients between blood and other liver cells. Developing LSEC cell lines is challenging with regards to preserving their morphology and functions. Therefore, the aim of this study is to optimize the conditions of a long-term 2D-culture of LSEC and examine the changes (morphology and endocytosis) over a prolonged period of time, up to 21 days.

New primary cells were isolated for each experiment from mouse livers. After conducting two pilot experiments and optimizing the initial conditions, several methods were applied to study LSEC in a long-term culture. Three different assays were performed to study the viability of LSEC. In addition, the purity of LSEC cultures was assessed by immunostaining. Two different microscopic techniques: scanning electron microscopy (SEM) and fluorescence microscopy, were utilized to investigate changes in fenestrations and cytoskeleton (actin and tubulin). Different concentrations of cytochalasin B, which prevents actin polymerization, were added to the cells to study the role of the actin cytoskeleton in LSEC fenestrations in long-term culture. Furthermore, a quantitative endocytosis assay using radiolabelled formaldehyde-treated serum albumin (FSA) was used to examine changes in endocytosis in the long-term culture. Additionally, a qualitative endocytosis assay was conducted by treating the cells with fluorescently labelled FSA, ribonuclease B (RNase B) and aggregated gamma globulin (AGG) to examine endocytosis mediated via stabilin-, mannose- and Fc-gamma IIb2 receptors, respectively.

Initial experiments revealed LSEC to have better survival for up to 8 days on fibronectin-coated plastic well plates in endothelial cell growth media (EGM). Microscopy imaging showed that a heterogeneous population of LSEC maintained monolayer and partially fenestrated morphology for up to 8 days. Both the qualitative and semi-quantitative analysis showed a decrease in the fenestrations number and an increase in the fenestrations size from day 3. In addition, an increase in the number of fenestrations was observed in LSEC treated with cytochalasin B on days 1 and 3.

FSA endocytosis showed a steep decrease in endocytosis in long-term culture for LSEC cultured in RPMI media. However, the endocytosis in LSEC cultured in EGM initially decreased until day 5, but recovered on day 8 and remained stable until day 11. Fluorescent imaging demonstrated that LSEC maintained the endocytosis via the three types of receptors examined, stabilin-, mannose- and Fc gamma IIb2 receptors, for up to 8 days.

Viability assessments demonstrated a decrease in cell number with time and an increase in the cell volume but no changes in the mitochondrial activity per cell with time. Furthermore, the purity of LSEC culture was verified to be over 97%.

The results of this study suggest that optimizing the conditions for prolonged preservation of LSEC morphology and function in long-term culture is possible. The main outcome showed that EGM allows for LSEC to maintain high viability and partially fenestrated morphology for up to 8 days and preserves endocytic functions for up to 11 days.

## Key words:

Liver sinusoidal endothelial cells (LSEC), long-term primary cell culture, endocytosis, fenestration(s), fenestra(e), scavenger receptor(s),

# Acknowledgements

This master thesis represents my final work of a master's degree in biomedicine at Department medical biology at UiT. The project was conducted at Vascular biology group (VBRG) at Department of medical biology at The Arctic University of Norway in Tromsø.

First and foremost, I would like to thank my supervisor, Karolina Szafranska. I am sincerely grateful for your advice, guidance, patience, inspiration and motivation.

Second, I would like to thank my Co-supervisors, Peter McCourt and Karen Kristine Sørensen for their help, guidance and inspiration. I am specially grateful for the welcoming environment they provided during our first meeting, which has been a constant source of motivation for me.

I would like to than McKids – Larissa, Tetyana, Christopher and Jakub. Thank you for all the support I have received and for making me feel like a member of McKids. Thank you for letting me sharing the office with you.

I extend my gratitude to the remaining members of VBRG group. Thank you for always welcoming me with a smile and including me in the group.

I would like to express my deep gratitude to my family – parents, siblings and my spouse – for all the support I have received throughout this year. It is through your support, motivation and patience that I have been able to reach this milestone.

# List of Abbreviations

| | |
|---|---|
| AGG | aggregated gamma globulin |
| BSA | bovine serum albumin |
| cpm | count per minute |
| CB | cytochalasin B |
| DAPI | 4’,6-diamidino-2-phenylindole |
| EGM | endothelial cell growth medium |
| EDTA | ethylenediaminetetraacetic acid |
| FGF | fibroblast growth factor |
| FSA | formaldehyde-treated bovine serum albumin |
| hEGF | epidermal growth factor |
| HMDS | hexamethyldisilasane |
| MACS | magnetic-activated cell sorting |
| LDH | lactate dehydrogenase |
| LSEC | liver sinusoidal endothelial cell |
| PBS | phosphate buffered saline |
| PBST | phosphate buffered saline with 0.05% Tween 20 detergent |
| PHEM | piperazine-N,N'-bis(2-ethanesulfonic acid)-(4-(2-hydroxyethyl)-1-piperazine ethanesulfonic acid)- (ethylene glycol-bis(2-aminoethylether)-N,N,N',N'-tetraacetic acid)-(magnesium chloride) buffer |
| RPMI | Rosewell Park Memorial Institute |
| PRR | pathogen recognition receptor |
| RNase B | ribonuclease B |
| SDS | sodium dodecyl sulfate |
| TCA | trichloroacetic acid |
| VEGF | vascular endothelial growth factor |

# Table of Contents

List of Figures

List of Table

# 1 Introduction

## 1.1 Liver

The liver makes up 2-3% of body weight and is the largest internal solid organ (1). It is located close to the diaphragm on the top right side of the abdominal cavity. The liver is partially protected by the ribs (2, 3). Like many other organs, there is a difference in liver size between women and men (4, 5). Men have an average liver size of 1500 g (4), while the average liver weight in women is 1300 g (5).

In humans, the liver is divided into the right and left lobes (2). The lobes are separated by the Falciform ligament (6). The right lobe is further divided into two caudate and quadrate lobes. A thin connective tissue, called Gilsson's capsule surrounds the liver (2). Figure 1.1.1 shows the anatomy of the liver.

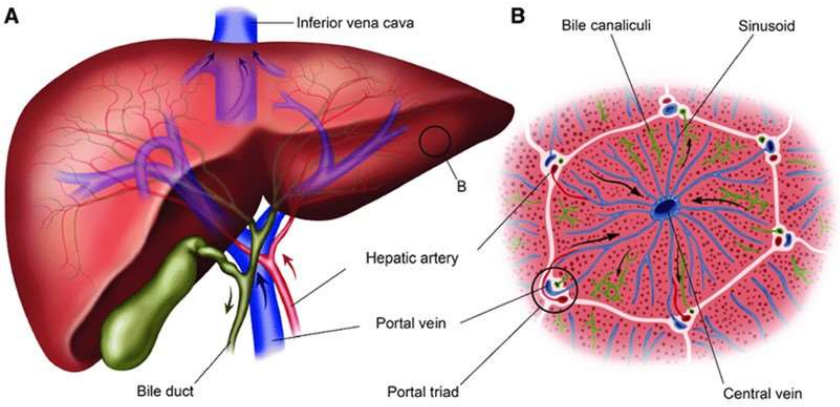


*Figure 1.1: The liver anatomy A) the liver organ and its vascular supply; B) a schematic drawing of the microanatomy of a section of the liver including the hepatic lobule. The figure is reproduced from (7) with permission.*

The liver clears the blood of many waste macromolecules and other blood-borne substances within min (2, 8). The liver is an important metabolic organ, involved in carbohydrate, lipid, protein, and drug metabolisms (8). It has both exocrine and endocrine functions (3). Exocrine functions involve the production and extraction of bile salts, while endocrine functions include synthesis, secretion, and regulation of hormones such as glucagon, insulin, somatostatin, growth hormones, and thyroid hormones, as well as synthesis and secretion of essential blood proteins, such as albumin, clotting factors, and angiotensinogen (3). The liver is composed of many different cell types that perform the specific functions associated with the liver (2, 9).

Hepatocytes, liver sinusoidal endothelial cells (LSEC), stellate cells and Kupffer cells are the major cell populations that make up the liver. Hepatocytes are also referred to as the liver parenchymal cells, while LSEC, stellate cells and Kupffer cells are referred to as non-parenchymal cells (NPCs) (2, 10, 11). In addition, there are minor populations of cells, such as leukocytes, dendritic cells, platelets, neutrophils, T cells and NK cells (12). The communication between the liver cells is important to keep them healthy and maintain their cell-specific functions (2, 13).

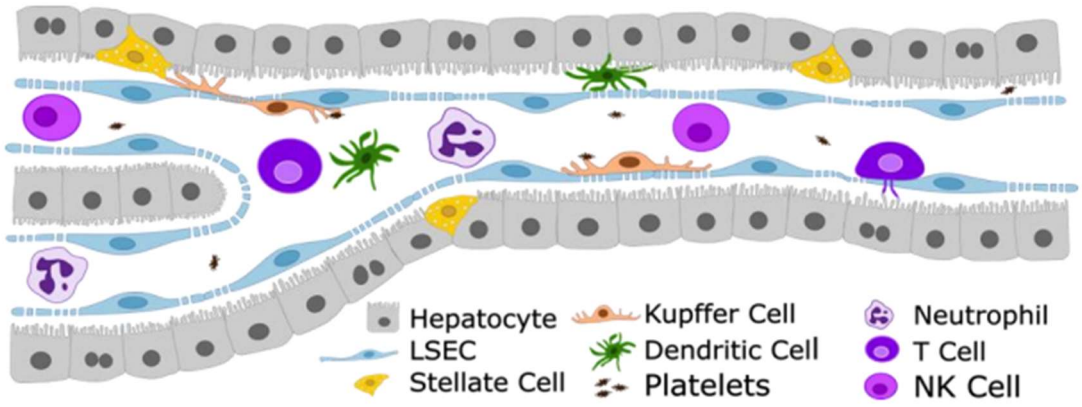


*Figure 1.2: Schematic illustration displaying the architecture of a liver sinusoid. The figure Courtesy of Karolina Szafranska, UiT, Tromsø, Norway*

Hepatocytes make up about 60% of the liver cells (14, 15) and about 80% of the liver volume due to their large size compared to other liver cells (6). Hepatocytes synthesize bile acids and proteins, as well as metabolize drugs and toxins borne by the blood. Furthermore, hepatocytes are important in maintaining glucose homeostasis in the blood by storing glycogen and metabolizing it to glucose when it is needed (10).

LSEC are fenestrated cells with a thickness range of 100 – 200 nm in the area of sieve plates (16). LSEC make up about 21% of the total cell number (15) and about 2.8% of the liver volume (6). They make up the wall of the sinusoids and the liver cells which are most exposed to the blood. The LSEC have an extraordinarily high endocytic capacity and clear the blood of various blood-borne waste substances, and exchange substrates with hepatocytes (2).

Stellate cells are located in the subendothelial space of Disse and are the main storage site of fat-soluble vitamin A (17). The cells constitute about 5.5% of the total cell number (15) and 1.4% of the liver volume (6). Stellate cells influence other liver cells and participate in liver regeneration and development in liver health conditions, while they proliferate and undergo

phenotypic changes and develop proinflammatory characteristics during inflammation (18). Stellate cells are major producers of collagen during pathological conditions such as cirrhosis and fibrosis (18). In addition, they are believed to regulate the blood flow in the sinusoids by regulating the diameter of the liver sinusoid (2, 19).

Kupffer cells are the major type of resident macrophages in the liver, and clear the blood of microorganisms and other toxic substances (20, 21). Kupffer cells are located mostly on the luminal side of the sinusoidal wall, but can also be located inside space of Disse and interact directly with stellate cells (22). Kupffer cells make up 8-12 % of the total liver cells, 2,1% of the liver volume and about 25% of the sinusoidal cells (6, 15). Kupffer cells are professional phagocytes and can take up molecules larger than 200-300 nm (23, 24, 25),while LSEC are essentially non-phagocytic and internalize macromolecules mainly via clathrin-mediated endocytosis (23, 25, 26).

### 1.1.1 Liver vasculature

One-quarter of cardiac output (at rest) enters the liver every minute (27). The liver is supplied with blood from both the hepatic artery and the portal vein (28, 29) - as shown in Figure 1.1. The composition of the blood supplied by the hepatic artery and portal vein is different. Approximately 20% of the blood comes from the hepatic artery and is highly oxygenated blood. The remaining 80% of the blood delivered to the liver comes via the portal vein from the intestine, spleen, pancreas, and abdominal cavity, and is deoxygenated (8, 28, 29). The deoxygenated blood is rich in nutrients but may also contain gut-derived pathogens (17).

The oxygenated blood and the deoxygenated blood are mixed together in the liver sinusoids (17) (Figure 1.1). Thus, the blood that passes through the sinusoids will have lower levels of oxygen than in other capillaries (30). This may be a reason why LSEC are reported to have a more anaerobic metabolism in comparison to other endothelial cells (17).

## 1.2 Liver sinusoidal endothelial cells (LSEC)

### 1.2.1 LSEC structure

LSEC form the walls of hepatic sinusoids and are considered highly specialized endothelial cells that differ from other endothelium in structure and function (17, 31, 32). LSEC have transcellular pores, called fenestrae or fenestrations, which allows for filtering the plasma of nanosized blood-borne substances. LSEC fenestrations do not have a diaphragm, and the cells lack an organized basal lamina beneath the cells (33).

#### 1.2.1.1 LSEC fenestrations

Fenestrations are an important hallmark of LSEC. The size range of the fenestrations is between 50 and 350 nm (17), and they are grouped in sieve plates (34, 35, 36). In healthy LSEC, fenestrations cover 2 – 20% of LSEC surface area (36, 37). Fenestrations provide passive size-dependent filtration, and their main function is to filter the blood/plasma before it reaches the space of Disse (38). Fenestrations facilitate the bi-directional exchange of substances ,that are smaller in diameter than the fenestrations, between the sinusoidal blood and the hepatocytes (39). Red and white blood cells and chylomicrons are too large to pass, while chylomicron remnants and small lipoproteins can pass the filter (40). Molecules that cannot pass through fenestrations, can be actively transported by LSEC (23, 24, 25).

The average size of fenestrations differs between species, but no difference between sexes was observed (17, 35). Otherwise, fenestrations are dynamic and their size changes depending on different factors (41). Increases in intrasinusoidal blood pressure can expand the size of fenestrations (42, 43). Furthermore, hormones, drugs, toxins, changes in the extracellular matrix, disease and ageing can change the diameter of fenestrations by expanding or contracting them (17, 19, 35). The changes in fenestrations diameter affect thus which substance and their amount that pass through the fenestrations and can be exchanged with hepatocytes (35).

Furthermore, some studies have found that the number and size of fenestrations can vary depending on where the cells are located in the liver. Fenestrations are larger in diameter but fewer in number in the periportal region (zone 1) compared to the centrilobular region (zone 3) which had more, but smaller fenestrations (35, 42).

#### 1.2.1.2 Cytoskeleton

LSEC morphology and function depend on various parts of the cytoskeleton (44, 45). The cytoskeleton consists of actin filaments, microtubules, and intermediate filaments, where each has its own function (46). An actin filament is formed by actin proteins or monomers, that are non-covalently bound together in a helical polymer. The actin cytoskeleton determines the shape of the cell, as well as being important for cell locomotion. Microtubules are built from tubulin heterodimer subunits that polymerize to form cylinder structures which direct intracellular transport, determine the position of the cell's membrane-enclosed organelles, and make up the spindle in cell division. Intermediate filaments are formed from intermediate filament proteins and provide mechanical strength to the cell. In the inner nuclear membrane, intermediate filaments form the nuclear lamina and protect the DNA.

The actin and microtubule cytoskeleton are dynamic and reorganize as needed. Reorganization of the cytoskeleton is particularly important during cell division where microtubules form the mitotic spindle that separates the diploid chromosomes, while actin forms a contractile ring to separate the daughter cells (46).

Each fenestrations is supported by a protein network called actin filaments (44, 45). Several studies have demonstrated that actin-disrupting agents such as cytochalasins induce extra fenestrations in LSEC (34, 35, 47). This induction of fenestrations was reported to be a reversible mechanism since LSECfenestrations after the removal of cytochalasin (35). Cytochalasin B can induce fenestrations in defenestrated LSEC in vitro (48).

### 1.2.2 LSEC functions

Clearing the blood of various circulating macromolecules by receptor-mediated endocytosis is one of the most important functions of LSEC. Some well-known macromolecules removed by LSEC are oxidized low-density lipoproteins (oxLDLs) (49, 50), degraded parts and leftover products of connective tissue, such as collagen alpha-chains, procollagen propeptides, hyaluronan, and nidogen (51, 52), and nanodrugs, in addition to small, soluble IgG immune complexes and endotoxins/ lipopolysaccharides (17). LSEC contribute to liver immune tolerance (53, 54) and are also able to remove (by endocytosis) certain viruses that gain access to the general circulation (55, 56, 57, 58)

### 1.2.2.1 Scavenger cell systems

LSEC express many receptors involved in the blood clearance of macromolecules (26). In contrast to Kupffer cells, LSEC are not phagocytic and can only take up particles that are smaller than approximately 200 nm in size, which is the size limit of clathrin-mediated endocytosis. Figure 1.3 illustrates which type of molecules LSEC can take up, as compared to Kupffer cells (26, 59).

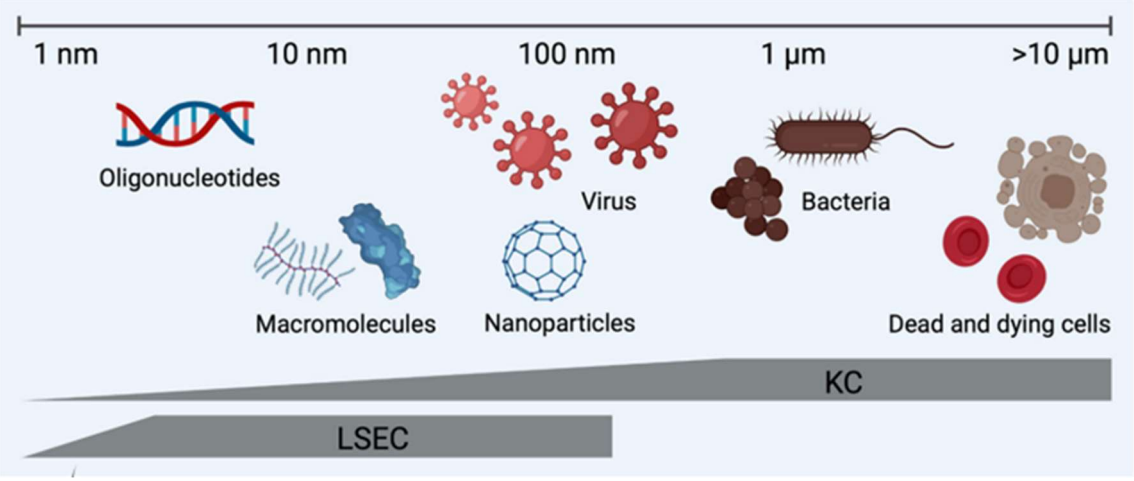


*Figure 1.3: LSEC use clathrin-mediated endocytosis to take up endogenous and exogenous nanoparticles and soluble macromolecules that are less than 200 nm in diameter while Kupffer cells mainly phagocytose particles that are larger than 200 nm. Reproduced from (26) with permission.*

While LSEC express a wide repertoire of receptors that can bind different extracellular ligands, not all receptors have a well-known function with regard to their role in endocytosis (26). The LSEC endocytosis receptors that are best studied are the scavenger receptors stabilin-1 and stabilin-2, the mannose receptor, and the Fc-gamma receptor IIb2 (reviewed in (26), and (60)).

### 1.2.2.2 Stabilin receptors

Stabilin-1 and -2 belong to scavenger receptor family class H. The scavenger receptor family consists of several different classes (61). Stabilin receptors are type I transmembrane receptors and they have various domains (61, 62) – EGF/EGF-like domains, facicilin-1 domains, an X-linked domain, a short cytoplasmic domain and a transmembrane region – (60). These domains allow them to bind to a variety of ligands including polysaccharides, such as dextran, chemically modified proteins, such as formaldehyde-treated serum albumin (FSA) (63), and

advanced glycation end-product (AGE) proteins (64), and waste products from matrix production, such as N-terminal procollagen propeptides are examples of ligands that are bound by scavenger receptors (59). The two stabilins are important for LSEC scavenging (24, 26), and the model ligand used for endocytosis studies in this thesis, FSA, binds to both stabilins 1 and 2, and is commonly used to study LSEC endocytic activity (65, 66).

#### 1.2.2.3 Mannose receptor

The mannose receptor is a pathogen recognition receptor (PRR). Mannose receptors are not only expressed in LSEC in the liver, but also in liver macrophages (Kupffer cells) (67). The receptor can also be found on subpopulations of macrophages and endothelial cells in the spleen, and lymph nodes in addition to some other cell types (68, 69, 70). The mannose receptor is a type I transmembrane receptor and belongs to the C-type lectins and the scavenger receptor family class E (26). The receptor has N-terminal extracellular region and a C-terminal intracellular region (60, 71), which means that different ligands can bind to the receptor. Ligands for this receptor are molecules released in the circulation from tissues such as lysosomal enzymes (72) (e.g ribonuclease B (RNase B) (73), C-terminal procollagen propeptides (74) collagen alpha-chains (75), tissue plasminogen activator (76), ovalbumin and mannose (68).

#### 1.2.2.4 Fc-gamma receptor IIb2

The Fc gamma receptors consist of 3 classes, most of which are type 1 transmembrane proteins (77). Fc-gamma receptor IIb2 (FcgRIIb2) is the only Fc-gamma receptor expressed by LSEC (77, 78) , and LSEC are the main carrier of this receptor in the liver (79). FcgRIIb2 is a glycoprotein and have three domains – an extracellular domain, a transmembrane domain and a cytoplasmic tail (80). The receptor's main function is to clear the blood of small, soluble blood-borne IgG antigen-complexes (17), and a model ligand for this receptor is aggregated gamma globulin (AGG) (63, 73). A study demonstrated that the human liver did not express the FcgRIIb2 throughout the whole length of the sinusoids in the hepatic lobule; expression of the receptor was absent or at low levels in periportal areasi (81). However, in rats the receptor is normally expressed in sinusoids in all parts of the hepatic lobule (67).

### 1.2.3 Primary cell culture of LSEC

Like other cells in the body, cell signalling is important for LSEC to survive and continue to perform their specific functions. Thus, LSEC are dependent on both paracrine and autocrine signalling from hepatocytes and adjacent cells (17). Therefore, long-term culture of LSEC has been challenging (82). The LSEC phenotype changes after few days in culture; they lose their fenestrations and other cell-specific markers (82).

However, LSEC cultures are never 100% pure, there is always minor contamination with other liver cells (83). Primary cultures are usually not produced by strictly sterile procedures, so there will be some risk of cell cultures getting infected by bacteria or fungi (83). Therefore, there have been several attempts to develop LSEC cell lines, however, these are missing some of the important features of the LSEC (82, 83, 84). Some have fenestrations, while others have few or the information is missing (85). Cell markers found on the cell surface of LSEC differ from one cell line to the other (85). Therefore, each cell line could be suitable to use in a specific study dependent on its characteristics but are not usable for studies of all LSEC-specific functions (84, 85).

### 1.2.4 LSEC in disease and ageing

The LSEC phenotype changes with ageing in vivo. LSEC can undergo pseudo-capillarization during the ageing process, where LSEC porosity is reduced, and the cell becomes thicker. Furthermore, LSEC in the ageing liver develop a more organized basal lamina and the collagen level is increased in the Space of Disse (59, 86, 87, 88, 89). A study by Simon-Santamaria et al. (59) showed that while the number of fenestrations and porosity in old rats was reduced compared to young rats in vivo, the diameter of the fenestrations in cells from old rats was similar to that in young rats following purification and plating (59). However, the endocytosis capacity of FSA was reduced in the LSEC from old rats compared to young rats. Impaired uptake in LSEC cavenger receptor ligands (AGE-BSA) is also reported in old mice in vivo (90).

Liver fibrosis can be caused by deletion of stabilin-1 and stabilin-2, as reported in stabilin knockout mice. Interestingly, both receptors had to be deleted to produce a marked change in

liver phenotype. The deletion of both stabilin-1 and -2 also caused kidney dysfunction in the mice (31).

A defect in LSEC that leads to reduced clearance via Fc gamma RIIb2 of circulating immune complexes may cause proinflammatory activation and autoimmune diseases such as systemic lupus erythematosus (26). Furthermore, suppression of Fc gamma receptors in the sinusoidal endothelium has been reported in liver cirrhosis in rat and human patients (91, 92).

It has been found that asthma and sarcoidosis in humans may be associated with a defect in the mannose receptor (reviewed in (26) and (93, 94)). Furthermore, a defect in the mannose receptor will weaken the immune system since the mannose receptor plays an important role in the innate immune system by mediating endocytosis of a range of exogenous molecules (pathogen recognition function), and in the adaptive immune system where it can have a role in the uptake of antigens in the LSEC that are cross-presented to cytotoxic lymphocytes (CD8+) (26, 95).

## 1.3 Microscopes

### 1.3.1 Scanning electron microscopy (SEM)

In the 1930s, Ruska (96) and Knoll (97) worked on developing scanning electron microscopes (98). Scanning electron microscopy is used to study the topography and composition of an object. The resolution in the best SEM can go down to approximately 1 nm.

SEM consists of an electron gun to generate the electron beam, a column for electrons to travel through to the sample, a deflection system, an electron detector, a chamber for the sample and a computer system (figure 1.4). The analysis of the sample starts by generating an electron beam with an electron gun. The electron beam can have 100 – 300 000 electron volts. The electrons travel through electromagnetic lenses, and a deflection system before they reach the sample. The high vacuum within the microscope prevents any interaction of the electrons with anything other than the sample. When the electron beam hits the sample, the electrons will be emitted and captured by an electron detector. There are different signals that can be emitted from the sample; secondary electrons, backscattered electrons, and x-ray/light. Secondary electron (SE) detectors, such as the In-lens-detector in the SEM microscope used in the present study, or various backscattered detectors are most commonly used for cellular imaging, where

they detect secondary electrons and backscattered electrons by scanning methods, which are converted to electric signals that will then be shown on the screen as pixels. The computer system has also a user interface (keyboard) that can be used to control how far from the sample, the energy from the electron beam and the speed.

SEM had been used to study LSEC and fenestrations. It has been used to study fenestrations size, number, frequency, and porosity. Fenestrations have a very small size and need high resolution methods to see and study them. The method in this thesis is optimized for SE. Fenestrations are more tilted to the electron beam and emit less SE than the LSEC cell body, which results in a contrast between them, where fenestrations are brighter than the LSEC cell body.

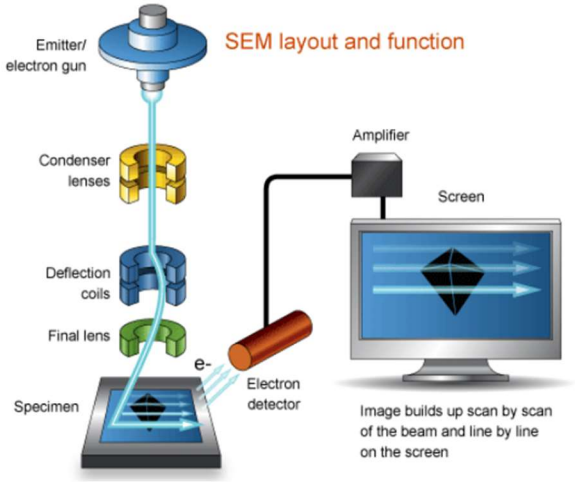


*Figure 1.4: The schematic illustration of SEM microscope. The electron beam is generated from an electron gun and travels through a deflection system, lenses, deflection coild to the vacuum chamber where the sample is scanned and results are displayed in a computer system. The figure is reproduced from (99) with permission.*

### 1.3.2 Fluorescent microscopy

In 1931, the first fluorescent microscope was developed (100). Fluorescence microscopy is based on fluorophores – molecules that have the ability to absorb light (photons) and emit it with changed wavelength (101). The principle of fluorescent microscopes is that light of a specific wavelength interacts with the fluorophores and excites them to a higher energy state, as it is described in the Jablonski diagram. Instability in the excited state results in the relaxation of the molecules back to the ground state. The molecule will then lose some of its energy, and

the excess energy will be released as light with a longer wavelength than the excitation wavelength.

Treating the cells or tissues with a fluorescently labelled protein enable the study and visualization of specific structures in cells and tissues (101). There are different types of fluorescent dyes available such as organic dyes (Alexa fluor, DAPI and FITC) or fluorescent proteins (green fluorescent protein/GFP or red fluorescent protein/RFP). The choice of fluorescent dyes is dependent on the specificity and optical properties of the fluorophores. Multicolour staining allows visualising the structures of interest at the same time and is possible due to the separation of excitation/emission wavelengths.

Fluorescent microscopes consist of light source, excitation filter, dichroic mirror, objective lens, emission filter and ocular lens. The light source could be a xenon arc lamp, mercury vapour, LED or laser. When a specific wavelength is chosen, the excitation light will pass through the dichroic mirror and reach the sample. The excited fluorophores will emit light of a longer wavelength which will be reflected by the dichroic mirror and transferred further through the emission filter to the ocular lens and/or detector to show an image. Due to the properties of light, it is possible to study structures that are not smaller than about 200 nm in ordinary light microscopes (98). Smaller structures can be visualized using super-resolution imaging techniques. By fluorescent labelling specific cytoskeletal proteins, it is possible to visualize the cytoskeleton of LSEC. For example, fluorescently labelled phalloidin is usually used to visualize actin filaments.

# 2 Aims

The “Long-term 2D-culture of primary mouse LSEC” master project is part of the EIC Pathfinder project “DeLIVERY”, funded by EU Horizon 2021. The main goal of the DeLIVERY project is to develop a long-term micro-physiological sample imaging system for the evaluation of the effects of polypharmacy in the liver. When LSEC are isolated out of the body, they gradually lose their functions, dedifferentiate, and begin to resemble other microvascular endothelial cells (25, 94, 95). The process of dedifferentiation of LSEC is not fully understood. It was reported that LSEC are activated in early culture, and immediately start to lose their fenestrated morphology, and endocytic activity (25, 94, 95) , therefore most experiments on LSEC are done the same day as their isolation. Optimization of long-term LSEC culture is one of the crucial initial tasks in the DeLIVERY project.

The specific aim of this master project was to characterize LSEC dedifferentiation *in vitro* in 2D culture with a focus on cell fenestrations and endocytic activity.

To prevent or reverse LSEC dedifferentiation in culture, different conditions such as cell culture media, substrates and surface coatings had to be optimized. The cell purity was assessed as the contamination of the other liver cells could influence LSEC function and morphology in culture. Several studies have shown the ability of actin-disrupting agents to induce fenestrations (41, 96, 97) which could have a potential effect inducing fenestrations on defenestrated cells and/or slow down the defenestration process in the long-term culture. Therefore, cytochalasin B was tested as a short, acute treatment or as a continuous media supplementation.

Furthermore, dedifferentiation also affects other LSEC features such as endocytosis. Another part of this thesis aimed to study if the observed changes in LSEC morphology in culture were correlated with or independent of any changes in endocytic activity. LSEC endocytosis was examined by measuring the uptake of fluorescently labelled and radiolabelled ligands for LSEC scavenger receptors.

# 3 Methods

## 3.1 Contributions

This project applies a wide range of techniques, and achieving independence in laboratory work was one of the major goals. Therefore, in this thesis, the majority of the methods were conducted by the thesis author, from section 3.5.2 onwards.

The person performing liver perfusion requires an animal handling course and a Federation of European Laboratory Animal Science Associations (FELASA) license. Therefore, the procedure was conducted by the experienced staff members at Vascular Biology Research Group (VBRG), Dr. Jaione Simón-Santamaría and Dr. Ruomei Li, while the author of this thesis was conducting the liver cell purification in the laboratory of VBRG.

## 3.2 Ethics statement

The animal experiments in this thesis are performed in vitro and the handling of laboratory mice was conducted according to ethical guidelines and regulations for animal research. The experimental protocol was approved by the competent institutional authority at UiT The Arctic University of Norway, which is licenced by the National Animal Research Authority at the Norwegian Food Safety Authority (Mattilsynet; Approval IDs: UiT 20/21, 09/22, to Karen Kristine Sørensen). Approximately 20 mice were used for this project.

## 3.3 Animal models

Mice are widely used in liver research as a model system to understand the functions of the liver. Despite differences in gross morphology between human and mouse liver, the microarchitecture is highly similar. In this thesis, an inbred mouse strain C57BL/6JRj of male mice (Janvier Labs, France), was used in the experiments. Inbred strains are a result of repeated sister-brother mating (102, 103) which gives stable phenotypic traits, genetic similarity, and thus more reproducible results between biological replicates (102). It is recommended to use inbred animals in pharmacological studies.

## 3.4 Animal husbandry

Mice were housed at the Department of Comparative Medicine ("Avdeling for komparativ medisin", AKM, UiT) in cages with environmental enrichments including aspen bedding, nesting material, houses, and aspen bricks. The mice received fresh water *ad libitum* and fed a standardized mouse diet, and were kept under controlled conditions – 12 h light/dark cycle, 21℃ ± 1℃ and 55% ± 1% humidity. The mice arrived at AKM at 5-6 weeks old, and the experiments were done in the following 4-8 weeks when mice weights were about 22-30 grams. They were evaluated daily by trained personnel to ensure good animal well-being.

## 3.5 Cell isolation and culture

List of all the reagents used in liver perfusion and LSEC purification can be found in Appendix A

### 3.5.1 Mouse Liver perfusion

The project is based on primary LSEC from mice. Liver perfusions were conducted on the morning of the experiment day. Before the procedure, the perfusion buffer was warmed up to 60℃ to remove dissolved gasses and avoid the formation of bubbles during perfusion of the liver. Moreover, an additional gas trap was used in the perfusion system to trap any bubbles. Mice were sacrificed by cervical dislocation, and the liver perfusion procedure was conducted post-mortem according to the protocol in (104). In short: the abdomen was cut by a midline incision and the intestines were moved to the side to expose the liver and portal vein. The cannula was placed in the portal vein, near the splenic vein branch and the liver was perfused with ~20 mL warm (37°C) calcium-free perfusion buffer to remove blood, and loosen the cell adhesions between cells (which are calcium-dependent), and then with 1,2 mg of Liberase™ (Roche, Germany) solution in 50 mL of perfusion buffer with calcium since Liberase is dependent on calcium to function. Successful perfusion and removal of the blood are indicated by the change of the liver colour from dark red to light brown. At the end of the in situ digestion of the liver, the gall bladder was removed, and the liver was cut out of the carcass and placed into a petri dish with calcium-free perfusion buffer with 1% BSA. BSA deactivates Liberase and prevents cell digestion and damage (105). The liver capsule was opened, and liver cells were shaken into the buffer and transferred into 50 mL tubes. The cell suspensions were kept at 4 ℃. For a more thorough explanation of the liver perfusion method, please refer to (104).

### 3.5.2 LSEC extraction with Magnetic-Activated Cell Sorting (MACS) beads

The liver cell suspension after perfusion consists of both parenchymal cells and non-parenchymal cells (NPCs). LSEC are the main cells of interest for this project so the high purity separation method Magnetic-Activated Cell Sorting (MACS) was applied, and the isolation protocol was based on (104). The procedure started with the removal of the hepatocytes by low-force differential centrifugation. After centrifugation, the supernatant consists of NPCs while the pellet contains hepatocytes and undigested pieces of the liver. The NPCs cell suspension was centrifuged three times at 35g x 2 min (at 4°C) and each time supernatant was collected in 50 mL tubes while keeping the cells at 4°C to prevent cell activation. However, in some experiments, one or two more centrifugations were necessary to remove all hepatocytes. Next, the supernatant was centrifuged for 10 min at 300g, and the pellet containing NPCs was resuspended in 1 mL of MACS buffer. MACS buffer contains 0,5% BSA and EDTA in PBS.

The resuspended pellet in MACS buffer was transferred to 2 mL tubes. The 50 mL tubes were washed with 1 mL MACS buffer and transferred to 2 mL tubes to transfer as many cells as possible. The cell suspension was centrifuged for 8 min at 300 g at 4°C and the pellet resuspended in MACS buffer. Positive selection was performed using superparamagnetic beads made of $Fe_3O_4$ covered with antibodies against CD146 which is an endothelial marker. The cell suspension was incubated with 15 μL of CD146 microbeads (Miltenyi Biotec, Germany) and incubated at 4°C for 25 min on a rotating device to allow CD146 beads to mix well with cells and bind to LSEC cell surface proteins.

One last time before separating cells on a magnetic stand, 1.5 mL of MACS buffer was added to the cell suspension and centrifuged for 8 min at 300 g at 4°C to remove unbound beads. The pellet containing LSEC was resuspended with 1 mL MACS buffer and added to the magnetic filter and a 70 μm pre-separation cell-strainer on the top of the column. Once the cell suspension passed through the filter column, the filter was washed with 1 mL of MACS buffer 3-4 times in total. The column was removed from the magnetic field and 2 mL MACS buffer was then added. Next, by pushing the plunger into the column the magnetically labelled cells were immediately flushed out. Counting of the cells was performed before cell seeding, followed by a centrifugation step to remove MACS buffer. The cells were then resuspended in cold media to achieve a concentration of 1 million cells per 1 mL.

### 3.5.3 Culture media and cell culture

First, two pilot experiments were performed where the cells were cultured in two different types of media: Roswell Park Memorial Institute w/L Glutamine 1640 (RPMI) (EuroClone, Italy) and Endothelial cell growth media (EGM) (Cell Applications Inc. USA). The basal medium RPMI contains essential nutrients such as amino acids, vitamins, inorganic salts, D-glucose and phenol red. While it was developed for culturing human leukemic cells it is now utilized for various cell cultures.

In comparison, EGM medium was developed to enhance attachment, spreading and proliferation of human large vessel endothelial cells. This medium is enriched with fetal bovine serum (FBS), trace elements, and antibiotics. In addition, the medium contains growth factors, excluding vascular endothelial growth factor (VEGF) according to the information from the supplier.

All cells were seeded in serum-free RPMI medium for 1-1.5 h for initial attachment. Subsequently, the medium was replaced with RPMI containing 1% FBS, or EGM. FBS contains a mixture of essential nutrients for the cells. Previous studies have reported that serum levels higher than 5% serum is lethal to LSEC (82, 106). However, the toxic effect may have been caused by impurities (endotoxins) in old batches of serum and recent data suggest that low serum is beneficial for LSEC (106, 107). Since LSEC are constantly secreting signalling molecules that are potentially important for cell survival, only half of the media was changed each day, in the present study to retain some of the signals that LSEC have already produced as well as to avoid drying the cells when media were changed.

The cells were incubated at 37°C , in an incubator (Heracell™ VIOS 160i, Thermofisher) with 5% $O_2$, and 5% $CO_2$. 5% oxygen is recommended for LSEC to enhance viability, decrease the production of pro-inflammatory mediators, and increase the production of anti-inflammatory mediators (30).

### 3.5.4 Surface coating

Before seeding, tissue culture wells were coated with fibronectin to help the LSEC to attach. Fibronectin is a glycoprotein in the extracellular matrix that promotes cell adhesion to the culture well surface and survival (108). Depending on which tissue culture plate was used, and

how large the wells were, a certain amount of fibronectin was added to fully cover the bottom of each well. Fibronectin was then pipetted out, and the remaining fibronectin in the wells was kept for at least 10 min at room temperature (RT). The wells were washed three times with PBS, before use in experiments. By washing the wells with PBS, sodium azide in fibronectin solution is washed out, which would otherwise kill the cells. Sodium azide acts as a bacteriostatic agent in the fibronectin and preserves the fibronectin solution during storage at 4°C (fibronectin precipitates if frozen).

One of the pilot experiments (the 2nd pilot experiment) involved coating the tissue culture wells with Collagen type I. Collagen type I is also commonly used in the coating of well plates used in LSEC cultures to promote cell adhesion to the wellplate surface and the survival of the cells (108). Surface coating with collagen type I followed the same protocol as fibronectin.

### 3.5.5 Cell seeding

The cells were seeded on fibronectin-coated 16well chambered coverglass (Thermofisher, USA), glass coverslips #1.5 (Thermofisher) or 24, 48 or 96 well tissue culture plates (VWR).

In the first pilot experiment, which aimed to study changes in LSEC fenestrations with SEM, 16-well chambered coverglasses were used where 75 000 cells/well were seeded in 200 µL of media. Furthermore, 80 000 cells/well were seeded on glass coverslips to study the changes in cytoskeleton.

In the second pilot experiment, which aimed to optimize the conditions for long-term culture, 16-well chambered coverglasses were used to investigate substrate material (glass) influence on LSEC (75 000 cells/well) and 48 well plates was used to examine substrate material (plastic) influence on LSEC (300 000 cells/well).

For the main experiments, well plates with plastic surfaces were used. A 24 wellplate with 500 000 cells/ well was used to study changes in fenestrations with SEM. For endocytosis assays and cytoskeleton staining assays, a 48 well plate was used containing 300 000 cells per well. Furthermore, a 48 well plate with 250 000 cells/well was used for immunostaining. For viability assessment, 96 wellplate was utilized, with each well containing 100 000 cells.

## 3.6 Pilot experiment

### 3.6.1 Description of the experiments

Two pilot experiments were conducted to optimize the protocol for keeping the cells viable for up to 8 days. The first pilot experiment was conducted on glass surfaces (16 well chambered coverglass and coverslips) and the purpose of the experiment was to compare the two media, RPMI vs EGM. The cells were fixed with McDowell's fixatives for SEM or 4% formaldehyde for light microscopy on days 1, 3, 5, and 8 – as described in sections 3.8.1 and 3.8.2.4. The staining of the cytoskeleton followed the protocol in section 3.8.2.4.

According to the results obtained in the first pilot experiment, a new pilot experiment was conducted. The purpose of this experiment was to compare media (RPMI vs EGM), surface coating (fibronectin vs collagen type I), substrate material (glass vs plastic well surfaces) and effects of changing the media (every day or every other day).

Selected wells were coated with fibronectin or collagen type I to assess the attachment capabilities of LSEC on the different substrates. Some cells were seeded on coated glass and some cells were seeded on coated plastic. Some cells were incubated in EGM and others in RPMI media. The last thing that was checked was if changing the media every day or every other day had any effect on cells.

In the second pilot experiment, the cells were fixed on days 5 and 8 with 4% formaldehyde for light microscopy to study how different conditions affect the cells in long-term primary culture. LSEC membrane was stained with Cell Mask red for 30 min in PBS.

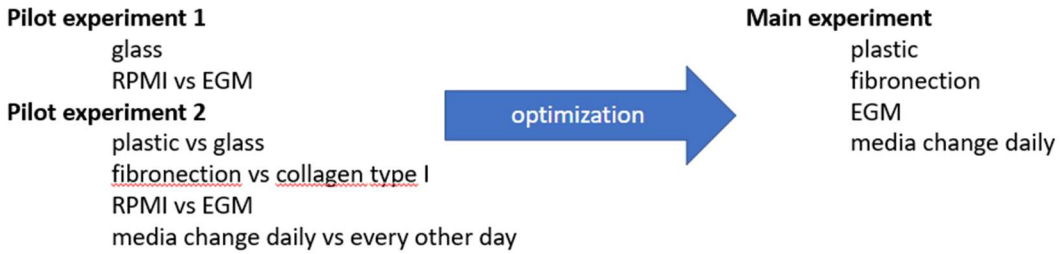


*Figure 3.1: Schematic illustration of the experiments. The purpose was to compare media (RPMI vs EGM), surface coating (fibronectin vs collagen type I), substrate material (glass vs plastic well surfaces) and effects of changing the media (every day or every other day)*

*Table 3.1 Experimental set-up for the pilot experiments.*

| **Day** | **1st pilot experiment** | **2nd pilot experiment** |
|---|---|---|
| Day 1 (3 h after LSEC isolation) | Seeding the cells and incubating the cultures for 1-1.5 h in RPMI. After 1-1.5 h in RPMI, the media for some cells was changed to EGM. Fixing the cells for SEM or light microscopy. | Seeding the cells and incubating the cultures for 1-1.5 h in RPMI. After 1-1.5 h in RPMI, the media for some cells was changed to EGM. |
| Day 2 | Change half of the media volume for the cells | Change half of the media volume for some of the cells |
| Day 3 | Fixing the cells for SEM or light microscopy. Change half of the media for the remaining cells | Change half of the media for all remaining cells |
| Day 4 | Change half of the media for the remaining cells | Change half of the media volume for some of the cells |
| Day 5 | Fixing the cells for SEM or light microscopy Change half of the media for the remaining cells | Fixing the cells for light microscopy Change half of the media for all remaining cells |
| Days 6-7 | Change half of the media for the remaining cells | Change half of the media volume for some of the cells |
| Day 8 | Fixing the cells for SEM or light microscopy. | Fixing the cells for light microscopy |

### 3.6.2 Modifications based on the pilot experiment

Based on results from the pilot experiment presented in section 4.1 the following conditions for cell cultures were selected to maintain LSEC viability and function for up to 8 days. In subsequent experiments, the cells were seeded on fibronectin-coated plastic and incubated in

EGM media, with a daily renewal of half of the media. Assays presented in sections 3.7, 3.8 and 3.9 were modified based on the pilot experiment.

## 3.7 Experimental set-up of the main experiment

To study LSEC morphology in long-term culture, the cells were cultured for up to 8 days for cells studied on SEM or fluorescent microscopy, up to 11 days for viability assays and up to 21 days for the quantitative measurement of endocytosis. The assays were performed on days 1, 3, 5, 8, 11, 21 as demonstrated in Table 3.2. The liver perfusion day was designated as day 1, and the initial assay (day 1) was performed approximately 3 h after cell seeding (Table 3.2).

*Table 3.2: Experimental set-up for the main experiment. The main experiment involved several assays performed on plastic fibronectin-coated well plates. The cells were incubated in EGM (except for $^{125}$I-labeled endocytosis assays where the cells were incubated in both EGM and RPMI).*

| **Day** | **Plan** |
|---|---|
| Day 1<br>(3 h after LSEC isolation) | Seeding the cells and incubating the cultures for 1-1.5 h in RPMI.<br>After 1-1.5 h in RPMI, the media for some cells is changed to EGM.<br>After 1 h of incubating the cells in EGM media, the assays were performed (Viability assessment and $^{125}$I-labeled endocytosis assay), or cells are fixed for SEM or light microscopy |
| Day 2 | Change half of the media volume for the remaining cells |
| Day 3 | Performing the assays (Viability assessment and $^{125}$I-labeled endocytosis assay) or fixing the cells for SEM or light microscopy.<br>Change half of the media for the remaining cells |
| Day 4 | Change half of the media for the remaining cells |
| Day 5 | Performing the assays (Viability assessment and $^{125}$I-labeled endocytosis assay), or fixing the cells for SEM or light microscopy<br>Change half of the media for the remaining cells |
| Days 6-7 | Change half of the media for the remaining cells |

| | |
|---|---|
| Day 8 | Performing the assays (Viability assessment and $^{125}$I-labeled endocytosis assay), or fixing the cells for SEM or light microscopy. |
| Day 9-10 | Change half of the media for the remaining cells |
| Day 11 | Performing the assays (Viability assessment and $^{125}$I-labeled endocytosis assay) |
| Day 12-20 | Change half of the media for the remaining cells |
| Day 21 | Performing the assay ($^{125}$I-labeled endocytosis assay) |

## 3.8 Viability assessment

To evaluate the cell health in culture, a resazurin assay was used to determine the mitochondria function, and a modification of lactate dehydrogenase (LDH) assay to assess the plasma membrane integrity and estimate the total cell volume. We also counted the number of cell nuclei in cultures after DAPI staining to study the changes in cell denstiy.

### 3.8.1 Resazurin

Resazurin Assay (Abcam, cat. Ab129732), also known as Alamar Blue assay, was used to measure the metabolic activity of viable cells. Resazurin (7- Hydroxy-3H-phenoxazin-3-one 10-oxide) is a non-fluorescent dye with a blue colour. Mitochondrial respiratory chain, specifically NAD(P)H in the presence of NAD(P)H dehydrogenase, reduces resazurin to a pink, highly fluorescent derivative, called resorufin.

The cells were seeded on fibronectin-coated plastic 96 well plates with 100 000 cells/well (in 100 µ L EGM). Following cellular seeding and incubation in EGM, resazurin was added to the cells and incubated for 2.5 h before the fluorescence of resorufin was measured in a plate reader (CLARIOstar microplate reader, BMG Labtech, excitation/emission of 545-20/600-40 nm).

### 3.8.2 Lactate dehydrogenase (LDH)

When the cell is damaged, the plasma membrane may lose its integrity, and the cell releases a cytosolic enzyme LDH. The LDH-GLO$^{TM}$ Cytotoxicity Assay (Promega) was used to analyse the LDH level in the cytoplasm of the viable cells. LDH Detection Reagent is a mix of LDH Detection Enzyme mix and Reductase substrate which contains NAD+, lactate, reductase,

reductase substrate and Ultra-Glo™ rLuciferase. Figure 3.2 illustrates the reaction between the components in the LDH Detection Reagent. If LDH is present in the medium, it will catalyze the conversion of lactate to pyruvate. NAD+ will then be reduced to NADH. NADH is utilized together with reductase substrate to generate luciferin. Ultra-Glo™ rLuciferase in the LDH Detection Reagent converts luciferin to a bioluminescent signal that can be detected by the reader.

The cells were seeded on fibronectin-coated plastic 96 well plate with 100 000 cells/well (in 100 µL EGM). The cell culture media (EGM) was changed (to remove any LDH released from dead cells) before adding 1% Triton X-100 to the cells to lyse them. The viable cells will then release LDH in the media. The assay was adapted to a 1:10 ratio, where 25 µL of the medium was added to 225 µL of the LDH freezing buffer (as described by manufacturer) The samples were frozen until the redout. After thawing the samples were mixed 1:1 with LDH Detection reagent and after 30 min luminescence was measured by CLARIOstar plate reader (BMG Labtech).

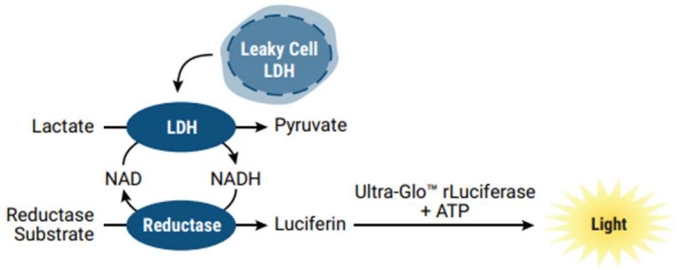


Figure 3.2: *Illustration of LDH reaction with LDH Detection Reagent. LDH Detection reagent is a mix of LDH Detection Enzyme mix and Reductase substrate which contains NAD+, lactate, Reductase, Reductase substrate and Ultra-Glo™ rLuciferase. The figure is sourced from (109).*

## 3.9 Morphological study

### 3.9.1 Sample preparation for SEM

To study the morphology of the LSEC and examine variations in the number and size fenestrations, samples were examined with SEM. The cells were cultured for up to 8 days, and samples were fixed for SEM on days 1, 3, 5 and 8. On day 1, fixation was performed 3 h after seeding to allow cells to attach well to the surface.

To preserve the ultrastructure of the cells, McDowell's fixative (a mixture of 4% formaldehyde and 1% glutaraldehyde (110), was used to crosslink proteins. After an initial 10 min fixation at RT, the samples were stored in the same fixative at 4°C until. On the day of further sample preparation the samples were washed 3 times with PHEM buffer to remove the fixative. PHEM is used because it does not contain phosphate salts (such as those in PBS) that react with osmium tetroxide which is part of the preparation protocol. The cells were then incubated for 1 h with 1% tannic acid in PHEM to protect the cells from shrinkage and preserve cell structure, and washed three times with PHEM buffer before being incubated for 1 h with osmium tetroxide in double-distilled $H_2O$. Osmium tetroxide is used to oxidize the lipids. After 1 h incubation with osmium tetroxide, the cells were washed 3 time with PHEM.

The samples were then dehydrated in ethanol to remove water. Dehydration is carried out in a graded ethanol series of 30, 60, 90, and 100 % ethanol. When 30% - 90% ethanol is added, the samples were incubated for 5 min. Next, the samples were dehydrated 4 times with 100% absolute ethanol and incubated for 5 min.

After dehydration, the samples were chemically dried with hexamethyldisilasane (HMDS) for 2 x 5 min. HMDS has a very low surface tension, acts as a crosslinker for proteins, and reduces collapsing of the specimens (111). The samples immersed in HMDS were air-dried by evaporating the HMDS.

Thereafter, the samples were mounted on aluminium stubs with silver glue or carbon tapes to avoid charging from electrons during microscopy and thus destruction of the samples and/or creation of charging-related imaging artefacts. In addition, silver glue was used on sample edges to bind sample edges with carbon tape and further reduce charging. After the silver glue was dried, the samples were coated with approximately 10 nm layer of gold/palladium alloy. The aim of the coating is to transfer the charge away from the sample surface and provide a source for secondary electrons which are the foundation for the image formation in SEM.

For storage, the samples were stored in a desiccator to keep the samples dry and prevent them from being moistened by humidity in the air as the samples need to be completely dry in SEM.

#### 3.9.1.1 SEM imaging and analysis

SEM samples were examined using Zeiss Gemini scanning electron microscope (Carl Zeiss, Germany) by using the InLens detector. The microscope was run at 2kV. Four or five overview pictures were captured from randomly selected areas, along with three or four detailed pictures. Overview pictures were obtained at 300x magnification, 12288 x 9216 resolution, and scan speed 3. Overview pictures were used to observe the overall appearance of the samples; if the cells were well attached to each other, or if there were gaps between cells. Detailed pictures provided one close-up view of a single LSEC per image. Detailed pictures were captured with the following settings; 1180x magnification, 6144 x 4608 resolution, and scan speed 5.

For semi-quantitative analysis, overview pictures were used for cell counting. Cell counter plugin was downloaded on ImageJ-/Fiji to count the cells. The counted cells were categorized into four categories: highly fenestrated, normally fenestrated, low fenestrated, or defenestrated. Highly fenestrated LSEC means that the whole cell body was covered by fenestrations and that there is almost no more space to open more fenestrations. Cells were considered as normally fenestrated if the cells exhibited a diverse array of fenestrations, while low fenestrated cells had few fenestrations that can barely be distinguished as LSEC. Defenestrated cells had intact cell bodies, but no fenestrations/sieve plates. Additionally, shrunk cells were identifies based on the distinct morphological features resembling apoptotic cells.

#### 3.9.1.2 SEM imaging and analysis

SEM samples were examined in a Zeiss Gemini scanning electron microscope (Carl Zeiss, Germany) by using the InLens detector. The microscope was run at 2kV. Four or five overview pictures were captured from randomly selected areas, along with three or four detailed pictures. Overview pictures were obtained at 300x magnification, 12288x9216 resolution, and scan speed 3. Overview pictures were used to observe the overall appearance of the samples; if the cells were well attached to each other, or if there were gaps between cells. Detailed pictures provided one close-up view of a single LSEC per image. Detailed pictures were captured with the following settings; 1180x or 1173x magnification, 6144x4608 resolution, and scan speed 5.

For quantitative analysis, overview pictures were used for cell counting. Cell counter plugin was downloaded on ImageJ-/Fiji to count the cells. The counted cells were categorized into four categories: highly fenestrated, normally fenestrated, low fenestrated, or defenestrated. Highly fenestrated LSEC means that the whole cell body was covered by fenestrations and that there is almost no more space to open more fenestrations. Furthermore, cells were considered

as normally fenestrated if the cells exhibited a diverse array of fenestrations, while low fenestrated cells had few fenestrations that can barely be distinguished as LSEC. Defenestrated cells had intact cell bodies, but no fenestrations/sieve plates.

### 3.9.2 Light microscopy

#### 3.9.2.1 Staining of cytoskeleton

The samples were examined for changes in the organization of cytoskeleton structures (microtubules and actin filaments) in LSEC. The cells were cultured on glass coverslips in the first pilot experiment, and later on plastic well plates. The staining was done by the droplet method in the first pilot experiment. The coverslips were placed in a droplet of PBST or fluorescent dye, with a volume of 100 μL to minimize the amount of dye used.

The samples were fixed (on days 1, 3, 5 and 8) with 4% buffered formaldehyde. After 10 min the fixative was removed, and samples were stored in PBS with ~0.1% formaldehyde at 4°C before further immunostaining.

On the day of staining, the samples were washed three times with PBS. Then the samples were incubated for 2 min in 0.05% Triton X-100 for permeabilization of cell membrane. Next, the samples were washed 3 times with PBST (PBS with 0.5% Tween20). Fluorescent agents are very sensitive to light and therefore immunostaining was carried out in a darkened room. The samples were stained and incubated in the dark overnight at RT with 1:100 anti-tubulin antibody (Alexa fluor 647, Santa Cruz Biotechnology, USA). The next day, 1:100 Alexa fluor 555 phalloidin (Invitrogen, Thermofisher, USA) in PBST was added to samples for 30 min to stain the actin. Afterwards, 2 mg/mL 4',6-diamidino-2-phenylindole (DAPI) (Sigma, USA) was used to stain the cell nucleus, and the samples were incubated for 15 min. In the next steps, it was important to wash away any remaining fluorescent substances. First, the samples were quickly washed 3 times with PBST, then twice with PBST with 10 min incubation for each wash. Finally, the samples were washed twice with PBST with 30 min of incubation for each wash.

In the first pilot experiment where the cover slips were used, samples were mounted on coverslips by using prolong glass antifade mounting media (Invitrogen, Thermofisher, USA). Later, when the experiments where done on plastic wells, PBST was changed to PBS for storage and imaging.

#### 3.9.2.2 Immunostaining

Fixed cells in PBS were permeabilized for 2 min with 0.1% Triton-X100. Triton-X100 is a detergent that will disrupt the cell membrane and allow the antibodies to access intracellular antigens. After that, the cells were blocked for 30 min to prevent non-specific binding of antibodies. The blocking solution contained 20% BSA with 1% in the final concentration and 3% donkey serum in PBS. After blocking, the cells were washed with PBS. By washing the cells with PBS, unbound blocking reagents are removed and that will reduce the non-specific binding of antibodies.

To study the target antigen, specific antibodies were added to the samples and incubated for 1 h. Table 3.3 demonstrates which primary antibodies were used for staining which target antigen, the host, supplier, catalogue no. and dilution. The cells were washed 3x with PBS to remove unbounded primary antibodies, as well as reduce nonspecific binding.

The next step was incubation for 30 min with a secondary antibody. Secondary antibodies used in this study are listed in Table 3.3. The secondary antibody is fluorescently labelled, and it will bind to primary antibodies to visualize the location of the target antigen. The samples were washed with PBS to reduce background staining by removing unbound secondary antibodies.

DAPI was used then to stain the nucleus. To remove unbound DAPI and avoid background staining, the samples were washed twice with PBS for 5 min.

##### 3.9.2.2.1 Fluorescent imaging and analysis

Fluorescent samples were examined in the fluorescent microscope EVOs. Images were captured from randomly selected areas, with 20x magnification or 40x magnification. To study changes in ligands uptake or receptor staining, the same setting for a ligand/a receptor was used to capture images from all the days.

Fluorescent samples were examined using the fluorescent microscope EVOs (ThermoFisher Scientific). Images were captured from randomly selected areas, with 20x magnification or 40x magnification. To study changes in ligands uptake or receptor staining, the same illumination

settings for a ligand/a receptor were used to enable the comparison between the images captured from all the days.

*Table 3.3: Primary and secondary antibodies tested.*

| **Primary antibody** | **Host Primary antibody** | **Catalog number** | **Working conc.** | **Secondary Antibody** | **Catalog number** | **Working conc.** |
|---|---|---|---|---|---|---|
| GFAP | Rabbit | Dako (Agilent) Cat # Z0335 | 1:100 | Donkey anti-goat IgG (H+L) Cross adsorbed secondary Antibody DyLight 88 | Thermofisher Cat# SA5-10026 | 1:250 |
| VSIG4 | Goat | Bio-techne Ltd Cat# AF4674-SP | 1:100 | Alexa Fluor 555 donkey anti-goat IgG (H+L) | Invitrogen Cat# A21432 | 1:250 |
| Stabilin -1 | Rabbit | ATLAS Cat# HPA005434 | 1:50 | Alexa Fluor 546 donkey anti-rabbit IgG (H+L) | Invitrogen Cat# A10040 | 1:250 |
| Stabilin – 2 | Rat | MBL life science Cat# MBL D317-3 | 1:50 | Donkey anti-Rat IgG (H+L) Cross adsorbed secondary Antibody DyLight 88 | Invitrogen Cat# SA5-10026 | 1:250 |
| CD32/ CD16/ Fc- | Goat | R&D Systems Cat#AF1460 | 1:100 | Donkey anti-goat IgG (H+L) Cross | Invitrogen | 1:250 |

| | | | |
|---|---|---|---|
| gamma receptor IIb2 | adsorbed secondary Antibody DyLight 550 | Cat# 10087 | SA5- |

## 3.10 Endocytosis assays

### 3.10.1 Qualitative (fluorescent) endocytosis assays

#### 3.10.1.1 Fluorescent labelling of FSA

To be able to visualize ligand uptake in the fluorescence microscope FSA was labelled with amine-reactive fluorescent dyes from the Alexa Fluor family. FSA (10 mg) was dissolved in 1 mL 0.1M sodium bicarbonate with pH of 8.3. Then the amine-reactive dye was dissolved in DMSO with a final concentration of 10 mg/mL. Incubation was for 1 h at room temperature, protected from light to avoid bleaching. A needle and syringe were used to inject the reaction mixture into a dialysis cassette (3500 MWCO). The dialysis cassette was placed inside a glass beaker containing PBS on a magnetic stirrer providing continuous stirring of the dialysis cassette in PBS. Any excess AF dye will come out in PBS. PBS is then changed several times until it is not coloured anymore which means that all unreacted and excess dye is removed.

#### 3.10.1.2 LSEC challenged with fluorescently labelled FSA, RNase B and AGG

In the first pilot experiment, we aimed to study changes in endocytosis throughout the time course days, fluorescently-labelled FSA was added to the samples to the final concentration of 20 μg/mL medium.

LSEC were seeded on glass coverslips and incubated in RPMI or EGM media. Samples were treated with fluorescently labelled (either with Alexa fluor 647 or Alexa fluor 488) FSA and fixed directly after a 10 min pulse with FSA or after an additional chase of 60 min (in media without FSA). Before fixing, the samples were washed with pre-warmed media to remove unbound FSA and to avoid unspecific fluorescent signals.

In the main experiment, the changes in endocytosis via the three main receptors of LSEC, stabilin-, mannose- and Fc gamma IIb2 receptors were studied throughout the days. LSEC were treated with 10 μg/mL FSA (Alexa Fluor 647), 40 μg/mL RNase B (Alexa Fluor 647) or 40 μg/mL AGG (Alexa Fluor 647).

LSEC were seeded on plastic and incubated in EGM medium. Samples were fixed directly after a 1 h pulse with ligands or after an additional chase of 2 h. Before fixing, the samples were washed with pre-warmed media to remove unbound fluorescent ligands and to avoid excessive fluorescent signalling.

### 3.10.2 Quantitative (radiolabelled)endocytosis assay

The cells in 48 well were treated for 2 h with $^{125}$I-FSA in RPMI with 1% HSA (CSL Behring GmBH, Germany). The final added radioactivity was 20,000 count per minute (cpm) per well, which corresponds to approximately 20 ng of ligand. FSA was produced and labelled at VBRG according to standardized protocols based on (112).

After 2 h of incubation, the samples were put on ice to stop the endocytosis. The media from each well was transferred to a separate tube marked with precipitate (P). Furthermore, each well was washed with 250 μL of cold PBS and transferred to the corresponding P tube.

To lyse the cells, 250 μL of 1% SDS was added to each well. After 5 min, SDS was transferred to tubes marked cell-associated (CA) to measure cell-bound radioactivity. The wells were washed with an additional 250 μL SDS and transferred to the same tubes. To each "P" tube, 750 μL of 20% TCA was added to precipitate $^{125}$I-FSA, and then the tubes were centrifuged for 10 min at 2500 rpm. The samples consist of a pellet with $^{125}$I-FSA and a supernatant with free $^{125}$I. Half of the supernatant in P tubes was transferred to new tubes marked "SN" (supernatant) to later calculate the amount of degraded FSA.

All tubes were capped with rubber lids to avoid spillage. The gamma counter machine (Packard Cobra, Perkin-Elmer, Australia, Canberra) was used to measure radioactivity in the tubes.

Cell-free controls were included in the endocytosis assay. These controls are used to assess the level of unspecific binding of ligand to the substrate, and the amount of free iodine in the supernatant that is caused by spontaneous detachment. The unspecific binding could be that

$^{125}$I-FSA stock components binding to the surface of the well, instead of the cells. Non-specific binding was accounted for by subtracting its value from the measurements in wells containing cells.

## 3.11 Testing agents for improved LSEC long-term culture

### 3.11.1 Selection of agents

Cytochalasin B ( is a mycotoxin known to induce more fenestrations in LSEC (113). The cells were treated with Cytochalasin B at different concentrations. Due to initial challenges in the optimization of the long-term cell culture protocol, only one agent was selected for further testing.

### 3.11.2 Cytochalasin B treatment

In the first pilot experiment performed on 16 well chambered coverglasses or glass coverslips, the cells were treated continuously with 2 µg/mL or 0.5 µg/mL Cytochalasin B supplemented with media, RPMI or EGM, or with 10 µg/mL acute treatment (30 min) before fixing with 4% formaldehyde for light microscopy or with McDowell's fixative for SEM. Further, the cells incubated in EGM on plastic surfaces were treated with 5 µg/mL Cytochalasin B for just studying the changes in fenestrations with SEM.*Experimental set up for LSEC treatment with* Cytochalasin B*. LSEC were seeded on fibronectin coated glass cover slips and incubated either in EGM or RPMI.*

*Table 3.4: Experimental set up for LSEC treatment with Cytochalasin B. LSEC were seeded on fibronectin coated glass cover slips and incubated either in EGM or RPMI.*

| **Days** | **0.5 µg/mL** | **2 µg/mL** | **10 µg/mL or 5 µg/mL** |
|---|---|---|---|
| Day 1<br><br>(3 h after LSEC isolation) | Seeding the cells and incubate the cultures for 1-1.5 h in RPMI.<br><br>After 1-1.5 h in RPMI, the media for some cells is changed to EGM. Both media are supplemented | Seeding the cells and incubate the cultures for 1-1.5 h in RPMI.<br><br>After 1-1.5 h in RPMI, the media for some cells is changed to EGM. Both media are supplemented | Seeding the cells and incubate the cultures for 1-1.5 h in RPMI.<br><br>After 1-1.5 h in RPMI, the media for some cells is changed to EGM. |

| | | | |
|---|---|---|---|
| | with 0.5 μg/mL Cytochalasin B<br><br>After 1 h of incubating the cells in EGM media, the cells were fixed for SEM or light microscopy | with 2 μg/mL Cytochalasin B<br><br>After 1 h of incubating the cells in EGM media, the cells were fixed for SEM or light microscopy | 30 min before fixing the cells for SEM or light microscopy, the cells were treated with 10 μg/mL or 5 μg/mL |
| Day 2 | Change half of the media containing Cytochalasin B for the remaining cells | Change half of the media containing Cytochalasin B for the remaining cells | Change half of the media volume for the remaining cells |
| Day 3 | Fixing the cells for SEM or light microscopy.<br><br>Change half of the media containing Cytochalasin B for the remaining cells | Fixing the cells for SEM or light microscopy.<br><br>Change half of the media containing Cytochalasin B for the remaining cells | 30 min before fixing the cells for SEM or light microscopy, the cells were treated with 10 μg/mL or 5 μg/mL<br><br>Change half of the media volume for the remaining cells |
| Day 4 | Change half of the media containing Cytochalasin B for the remaining cells | Change half of the media containing Cytochalasin B for the remaining cells | Change half of the media volume for the remaining cells |
| Day 5 | Fixing the cells for SEM or light microscopy.<br><br>Change half of the media containing Cytochalasin B for the remaining cells | Fixing the cells for SEM or light microscopy.<br><br>Change half of the media containing Cytochalasin B for the remaining cells | 30 min before fixing the cells for SEM or light microscopy, the cells were treated with 10 μg/mL or 5 μg/mL<br><br>Change half of the media volume for the remaining cells |

| | | | |
|---|---|---|---|
| Days 6-7 | Change half of the media containing Cytochalasin B for the remaining cells | Change half of the media containing Cytochalasin B for the remaining cells | Change half of the media volume for the remaining cells |
| Day 8 | Fixing the cells for SEM or light microscopy.<br><br>Change half of the media containing Cytochalasin B for the remaining cells | Fixing the cells for SEM or light microscopy.<br><br>Change half of the media containing Cytochalasin B for the remaining cells | 30 min before fixing the cells for SEM or light microscopy, the cells were treated with 10 µg/mL or 5 µg/mL<br><br>Change half of the media volume for the remaining cells |

## 3.12 Statical and image analysis

ImageJ Fiji software was used for image analysis to adjust contract/brightness, merge pictures, count the cells, and add scale bars (114). Results from the quantitative analysis are presented as means +/- standard deviation (SD). Statical significance was determined by running a one-sided Student's t-test in Excel. Student's t-test is used to determine if a specific condition (in this thesis – media and the treatment with Cytochalasin B) has an effect on the population of interest (LSEC). It is utilized to compare two independent groups when the data are normally distributed. It assesses whether the difference between the mean of the two groups is significant. In this thesis, t-test was used to assess if there is a significant change in parameters in the following days using a one-tailed t-test. The results were considered statically significant if the p-value was <0.05. An asterisk system is used to indicate $P < 0.05$ (*), $P < 0.01$ (**), and $P < 0.001$ (***).

# 4 Results

Two pilot experiments were performed to optimize cell media, surface coating, and choice of culture surface. The initial results in the pilot experiments were later used to select the conditions for the main experiments designed to study changes in fenestration size and number, cytoskeleton, cell viability and the scavenging system as a function of time in culture. Additionally, investigations were carried out to assess the influence of cellular treatment with Cytochalasin B on the LSEC. These treatments were primarily performed during the pilot experiment on glass surfaces to study both cell fenestrations and cytoskeleton.

The selected pictures in the figures are representative pictures. For experiments done on glass in section 4.2.2.1, data was not obtained for all treatments in some experiments.

## 4.1 Initial optimization of LSEC cell culture (pilot experiments)

In the first pilot experiment, the LSEC morphology was investigated in two different media, RPMI and EGM. The cells were seeded in 24 well plates on #1.5 glass coverslips. Half of the media volume was changed every day for 8 days. To examine changes in cell morphology, cells were fixed on days 1, 3, 5 and 8 (day 1 is the cell isolation day). Fluorescent microscopy was utilized to study changes in the actin and tubulin cytoskeleton, while SEM was used to examine changes in the number and size of fenestrations.

Similar changes were observed with both media until day 5. The cells on day 1 made a confluent monolayer, which can be observed by both fluorescent microscopy (Figure 4.1), and SEM (figure 4.2). The number of viable cells declined throughout the days. Furthermore, from day 3 on, LSEC underwent elongation and enlargement (Figures 4.1 and 4.4).

On day 8, there were marked differences between the samples kept in the two different media. In the cultures in RPMI, many/most cells had detached (figure 4.1), and the remaining cells were shrunken or disrupted as observed by SEM (figure 4.2). In the EGM cultures, there was a low number of highly enlarged cells in the culture (Figures 4.1-4.2).

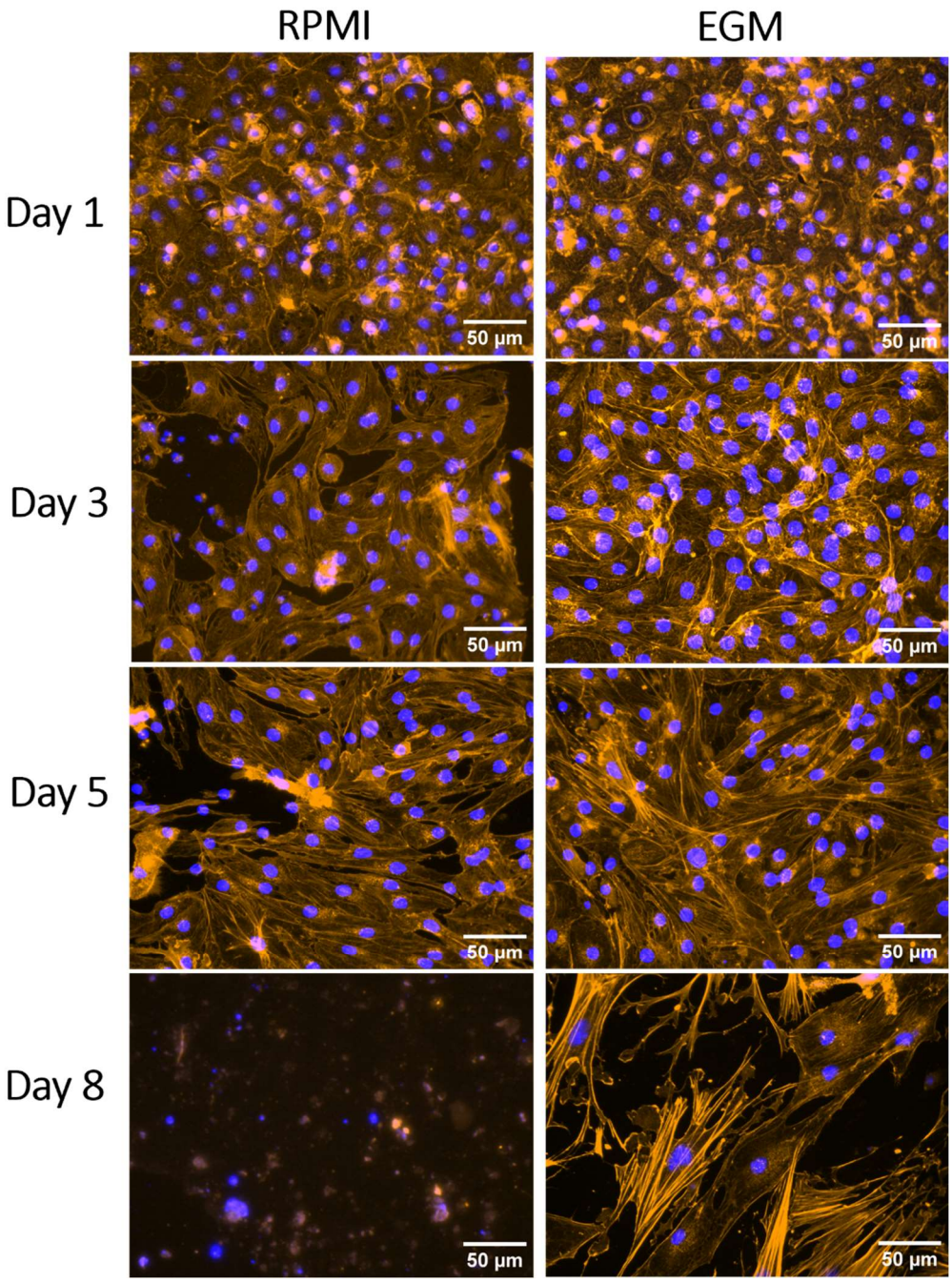


*Figure 4.1: Fluorescent images of changes in the actin cytoskeleton of LSEC. Mouse LSEC were isolated and seeded on fibronectin glass coverslips in both RPMI and EGM. The cells were fixed and stained on days 1, 3, 5 and 8. Actin cytoskeleton was stained with phalloidin 555 (orange), and cell nuclei were stained with DAPI (blue). Images are presented vertically, showing changes over time, with side-by-side comparisons of the two media. Images were obtained at 40x magnification with EVOs. Scale bar = 50 µm.*

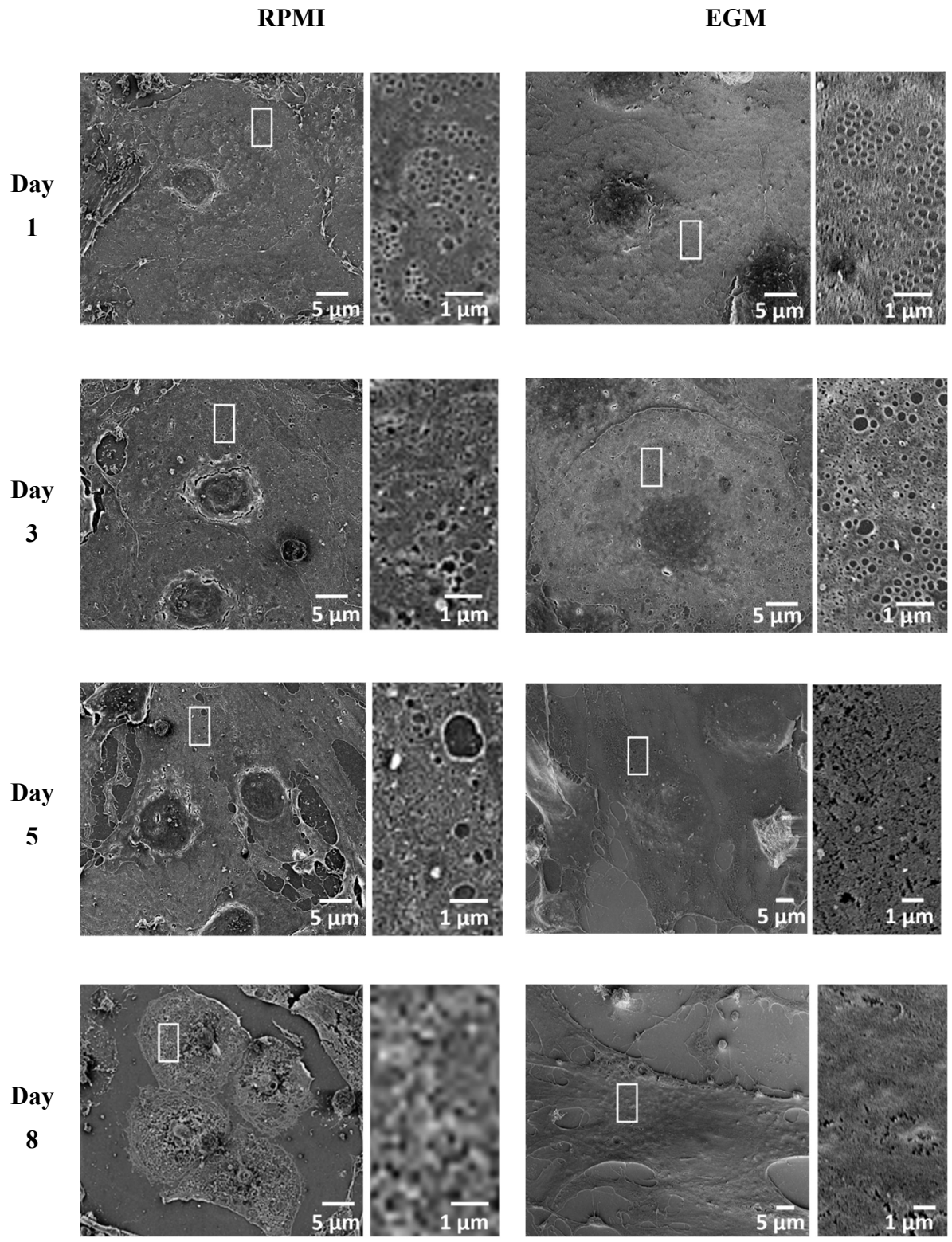


*Figure 4.2: Fluorescent images of changes in the actin cytoskeleton of LSEC. Mouse LSEC were isolated and seeded on fibronectin glass coverslips in both RPMI and EGM. The cells were fixed and stained on days 1, 3, 5 and 8. Actin cytoskeleton was stained with phalloidin 555 (orange), and cell nuclei were stained with DAPI (blue). Images are presented vertically, showing changes over time, with side-by-side comparisons of the two media. Images were obtained at 40x magnification with EVOs. Scale bar = 50 µm.SEM images of changes in fenestration status. Mouse LSEC were isolated and seeded on fibronectin-coated glass coverslips in both RPMI and EGM. The cells were fixed at days 1, 3, 5 and 8, followed by SEM sample preparation. Images are presented vertically, showing changes over time, with side-by-side comparisons of the two media. Scale bar = 5 µm.*

The same changes in the number and shape of LSEC were observed by SEM and fluorescent microscopy. On day 1, the cells exhibited numerous fenestrations in both media (figure 4.2). A decrease in the number of fenestrations was observed by day 3, accompanied by an increase in the fenestration size. Subsequently, on day 5, distinct variations were observed among the cells within samples, with some normally fenestrated cells while other cells showed marked defenestration. On day 8, LSEC cultured in RPMI underwent cell death, whereas LSEC in EGM showed some cells that appeared viable (figure 4.2, bottom row). However, the surviving cells displayed clear changes in morphology (as well as being defenestrated) and size compared to their original morphology and size on the day of the isolation.

The second experiment was designed based on the previous results to further optimize the conditions for the cells to survive for up to 8 days. The cells were seeded on either plastic or glass surfaces coated with fibronectin, or collagen type I and incubated for 5 or 8 days in RPMI or EGM media. The cells were stained with CellMask Deep Red to visualize the cell membrane, and nuclei were stained with DAPI. Figure 4.3 illustrates the LSEC morphology on day 5. Cells on plastic showed a confluent monolayer of cells in EGM, whereas there were few cells left on the glass. The same trend was observed with RPMI;  cell survival was best on plastic, however, the cultures had fewer cells than with EGM.

No clear differences were observed between fibronectin or collagen type I (data not shown). No changes were observed in wells where media was changed daily or every other day (data not shown).

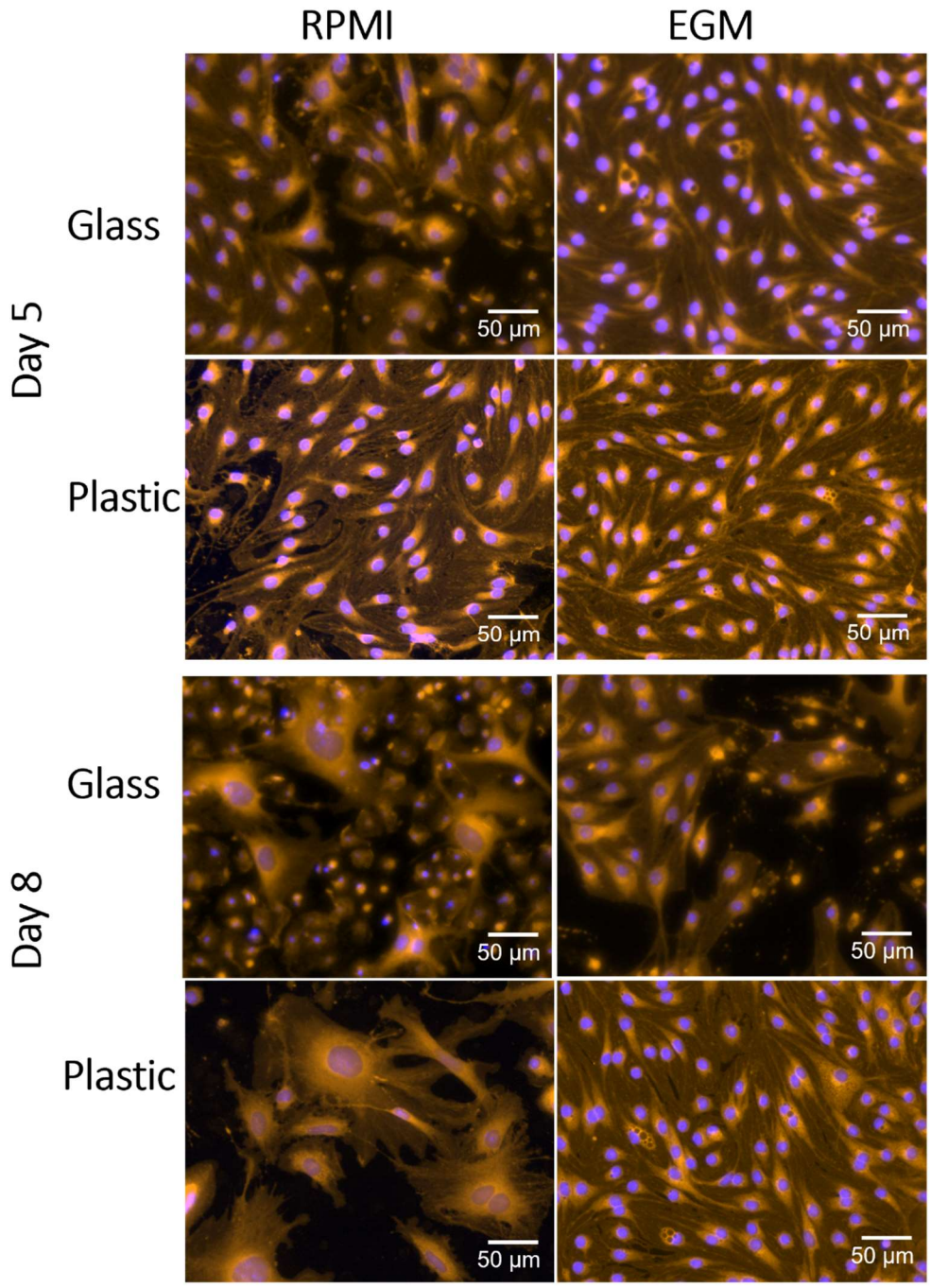


*Figure 4.3: Fluorescent images of LSEC in long-term culture. Mouse LSEC were isolated and seeded on fibronectin glass coverslips or fibronectin plastic well plate in both RPMI and EGM. The cells were fixed and stained on days 5 and 8. LSEC body was stained with Cell mask deep red (orange), and cell nuclei were stained with DAPI (blue). Images are presented vertically, showing changes between days 5 and 8 and between surface materials, with side-by-side comparisons of the two media. Images were obtained at 20x magnification on the EVOS microscope. Scale bar = 50 µm.*

### 4.1.1 The scavenging function of LSEC

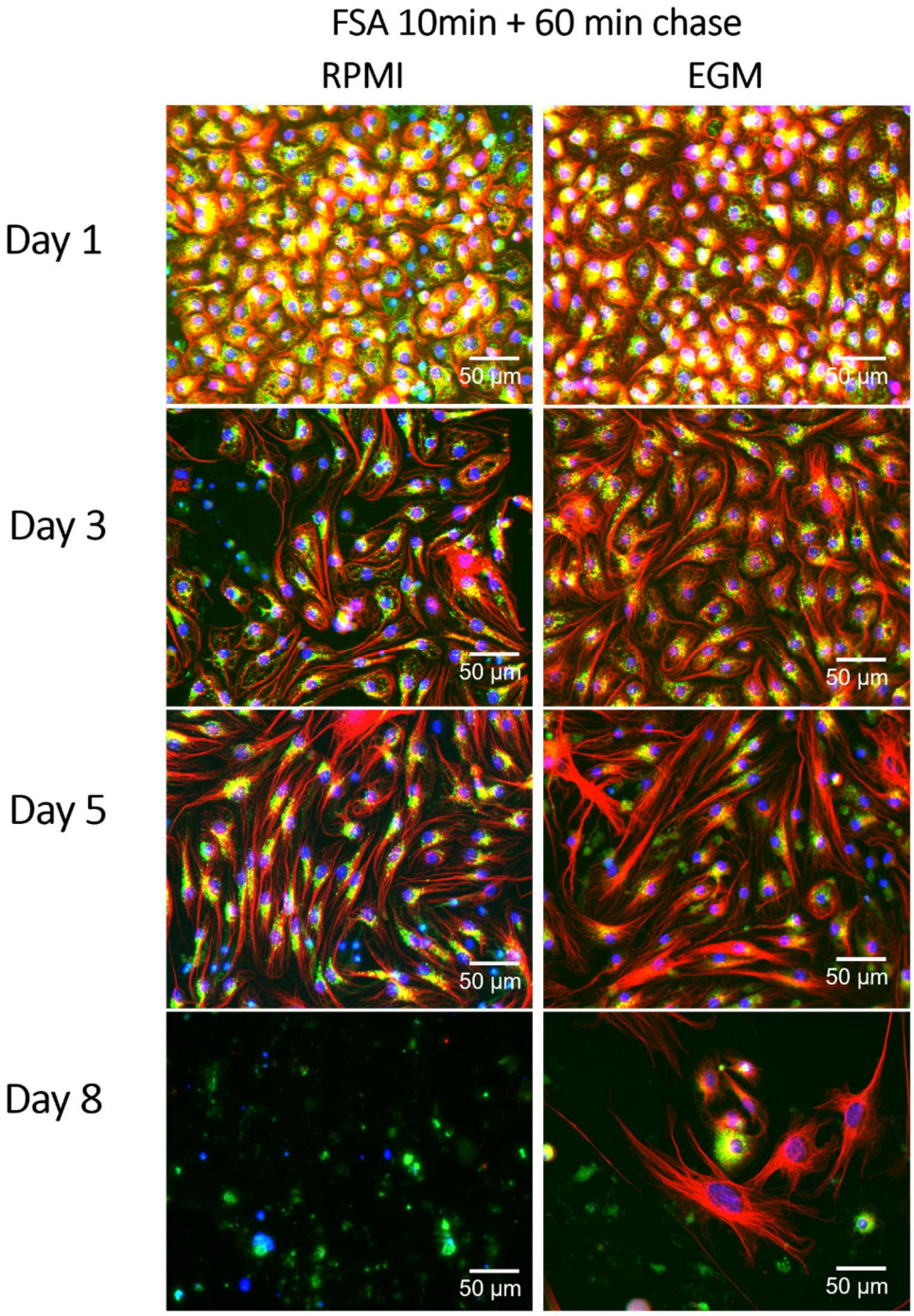


*Figure 4.4:* Fluorescence images of FSA uptake in LSEC. Mouse LSEC were isolated and seeded on fibronectin glass coverslips in both RPMI and EGM. The cells were incubated for 10 min with ligand, followed by 60 min incubation without ligand. The cells were fixed and stained on days 1, 3, 5 and 8. Tubulin was stained with α-tubulin antibody conjugated to Alexa fluor 647 (red), FSA was labelled with Alexa Fluor 488 (green) and cell nuclei were stained with DAPI (blue). The yellow colour is a result of the merging of green and red colours. Images are presented vertically, showing changes over time, with side-by-side comparisons of the two media. Images were obtained at 20x magnification with EVOs. Scale bar = 50 $\mu$m.

A qualitative analysis of LSEC scavenging function was performed by adding fluorescently labelled FSA to cells and incubating the cells for 10 min with ligand, followed by a 60 min incubation in media without FSA, before fixation of cells. FSA is taken up via the LSEC scavenger receptors stabilin-1 and stabilin-2 and is a good indicator of endocytic activity in the cells (66).

A progressive decrease in fluorescent FSA signal was observed with both media over time in culture, however uptake of FSA was still observed in nearly all cells up to day 5. The ligand accumulated in vesicles close to the nuclei. At day 8, there were nearly no surviving cells in cultures in RPMI, while a few cells in EGM still had the ability to scavenge FSA (Figure 4.4).

## 4.2 Changes in LSEC morphology in culture

Based on the results of the pilot experiments, we decided to seed the cells in main experiments on fibronectin-coated plastic wells and to plate and culture the cells in EGM. Any exceptions are indicated in the text and figures.

### 4.2.1 LSEC fenestrations

Due to the nanometer size of LSEC fenestrations, high-resolution imaging is required. To investigate changes in the number and the size of fenestrations in long-term culture, cells were fixed on days 1, 3, 5 and 8, and processed for SEM.

Figure 4.5 demonstrates typical LSEC morphology on days 1 - 8. There was an increase in the size of the cells on days 3, 5 and 8 compared with day 1. In addition, the elongation of the LSEC shape was observed from day 3 onwards. In comparison to day 1, the number of cells decreases to 89 % on day 3, and to 82% on days 5 and 8 compared to day 1 (figure 4.6). On day 1, the fenestrations were organized mostly in sieve plates. On day 3 – 5, a subset of fenestrations were organized in sieve plates; however, single fenestrations were observed. On day 8, sieve plates were rarely observed. Furthermore, on day 3 – 8, the presence of residual shadow-like structures resembling previous sieve plates was observed.

Semi-quantitative analysis of the SEM images revealed that both the number of defenestrated LSEC and well as the number of fenestrations per LSEC decreased throughout the days, as demonstrated in figure 4.5, and 4.6. Figure 4.5 shows representative SEM images from days 1-

8. On day 1, the cells expressed numerous fenestrations grouped in sieve plates, while on day 3, the fenestration number decreased but the fenestration size visibly increased. On day 5, there were observed few fenestrations and some cells or the majority of the cells were defenestrated. On day 8, nearly all cells were defenestrated, although a few cells retained some fenestrations. Moreover, an increase in the size of the fenestrations was observed throughout the days.

Figure 4.6 presents the results from the semi-quantitative analysis. On day 1, over 90% of LSEC were fenestrated. The number of cells with fenestrations decreased to 70 % on day 3, 65% on day 5 and about 50% on day 8.

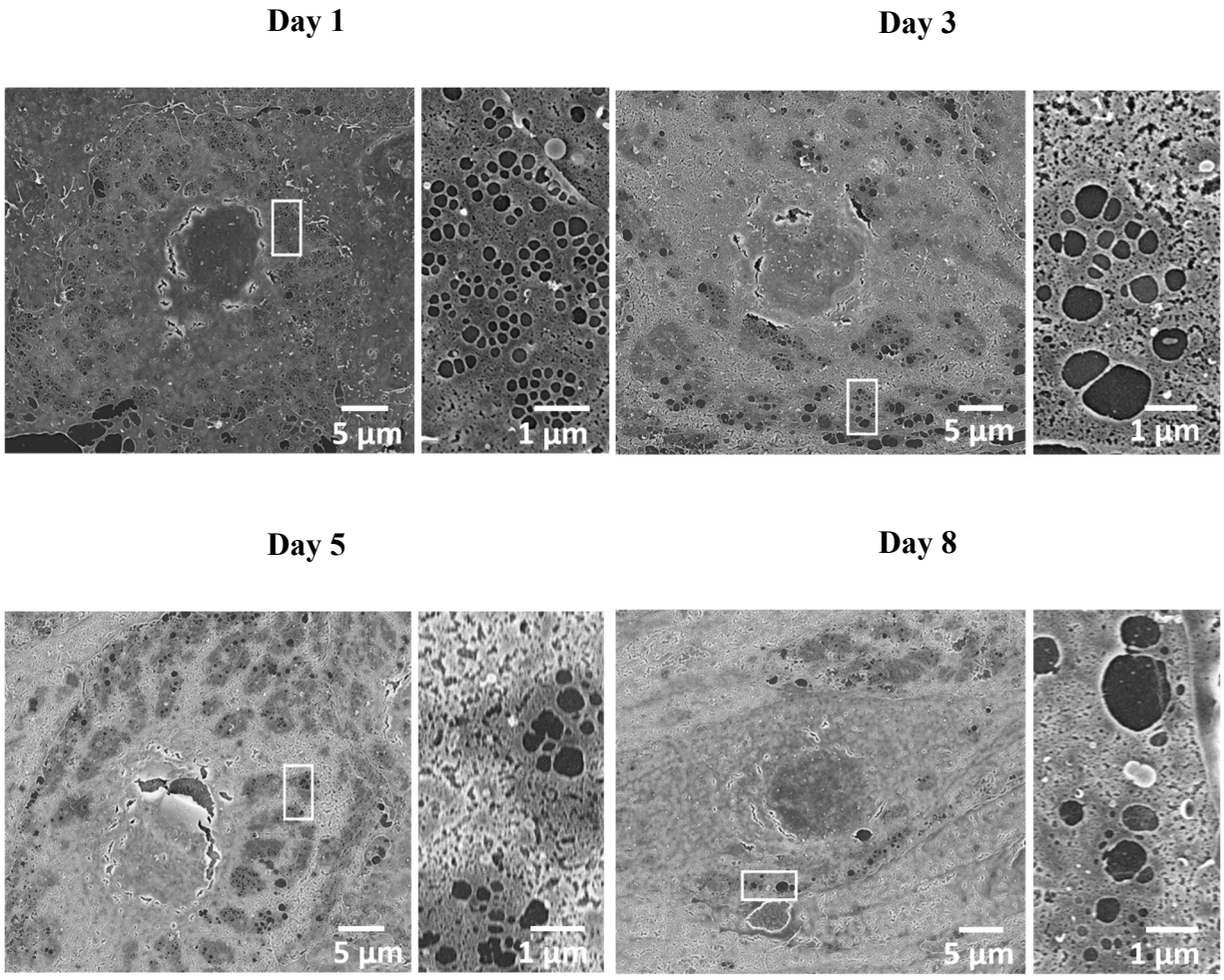


*Figure 4.5: SEM images of changes in LSEC morphology. Mouse LSEC were isolated and seeded on fibronectin-coated plastic well plate in EGM. The cells were fixed at days 1, 3, 5 and 8, followed by SEM sample preparation. Images presenting changes over time. Scale bar = 5µm.*

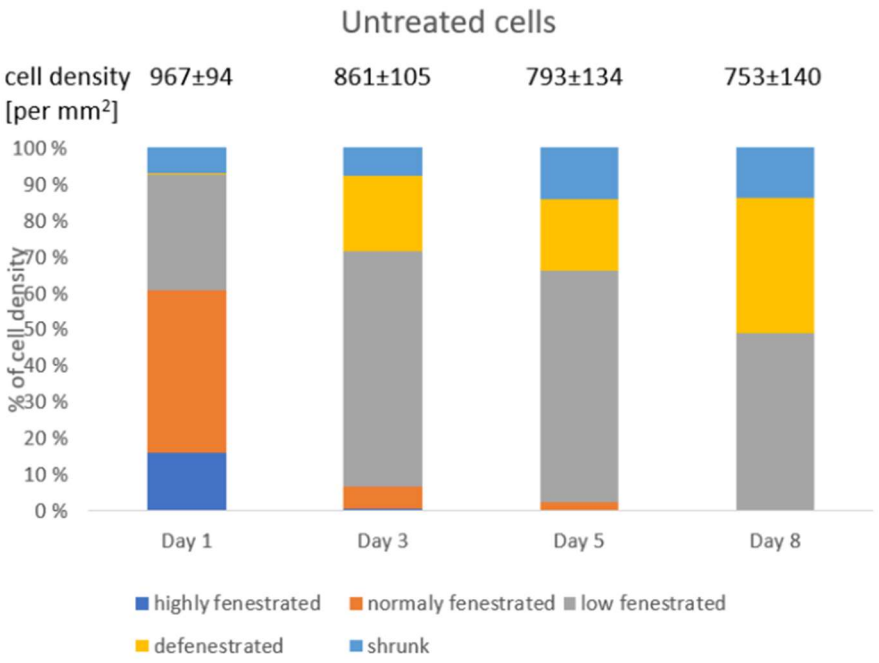


*Figure 4.6: S*emi-quantitative analysis of fenestrated cells. Mouse LSEC were isolated and seeded on fibronectin-coated plastic well plate in EGM. The cells were fixed on days 1, 3, 5 and 8 followed by SEM sample preparation. Overview pictures with size 300x400 µm were used to count the cell density and the fenestrated and defenestrated cells. The graph shows the proportion of fenestrated and defenestrated LSEC up to 8 days. Data are presented as mean ± standard deviation, n=3 independent experiments.

#### 4.2.1.1 The influence of cytochalasin B on LSEC fenestrations

The literature indicates that cytochalasin B induces more fenestrations in LSEC (115). Selected samples in the pilot experiments were treated with Cytochalasin B to study if fenestrations can be induced in long-term culture. The cells were seeded on fibronectin coated glass coverslips and continuously treated with media (EGM) supplemented with 2 µg/mL or 0.5 µg/mL of Cytochalasin B, or with 10 µg/mL for 30 min (acute treatment).

Continuous treatment with 0.5 µg/mL of Cytochalasin B exhibited numerous fenestrations on a subset of the cells on day 1 (Figure 4.7). On days 3 and 5, more fenestrated cells than in untreated control were observed, however, the size of fenestrations increased. This low Cytochalasin B concentration did not show induction of fenestrations in any LSEC on day 8.

Continuous treatment with 2 µg/mL of Cytochalasin B induced numerous fenestrations on the majority of the cells on day 1 (Figure 4.7). A subset of cells displayed an increase number of fenestrations on days 3 and 5 with an increase in the size of fenestrations. A decrease in the cell density was observed on day 5 compared with days 1 and 3. The treatment resulted in notable

disruptions in the cellular edges on days 5 and 8. Similar to the low C Cytochalasin B B concentration treatment, continuous treatment with 2 µg/mL of Cytochalasin B did not influence LSEC on day 8.

Similar observations were shown on cells treated with 10 µg/mL cytochalasin B for 30 min (Figure 4.8) induced more fenestrations were induced in the majority of the cells on day 1, and in a subset of cells on day 3 with where increase in the fenestrations size. was observed. was observed. Disruptions in cell edges gapsgaps formation were already observed on day 3. On days 5 and 7, the Cytochalasin B treatment resulted in nearly complete disruption of the cell body in the majority of cells.

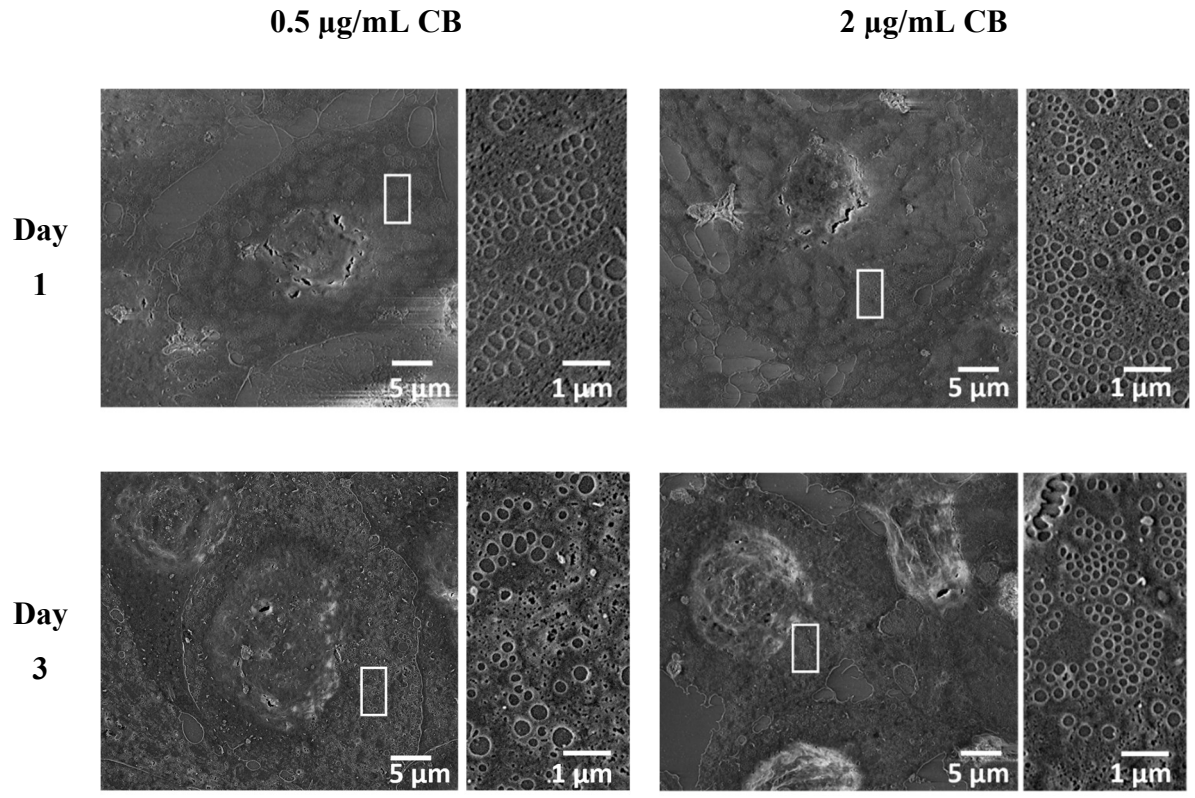

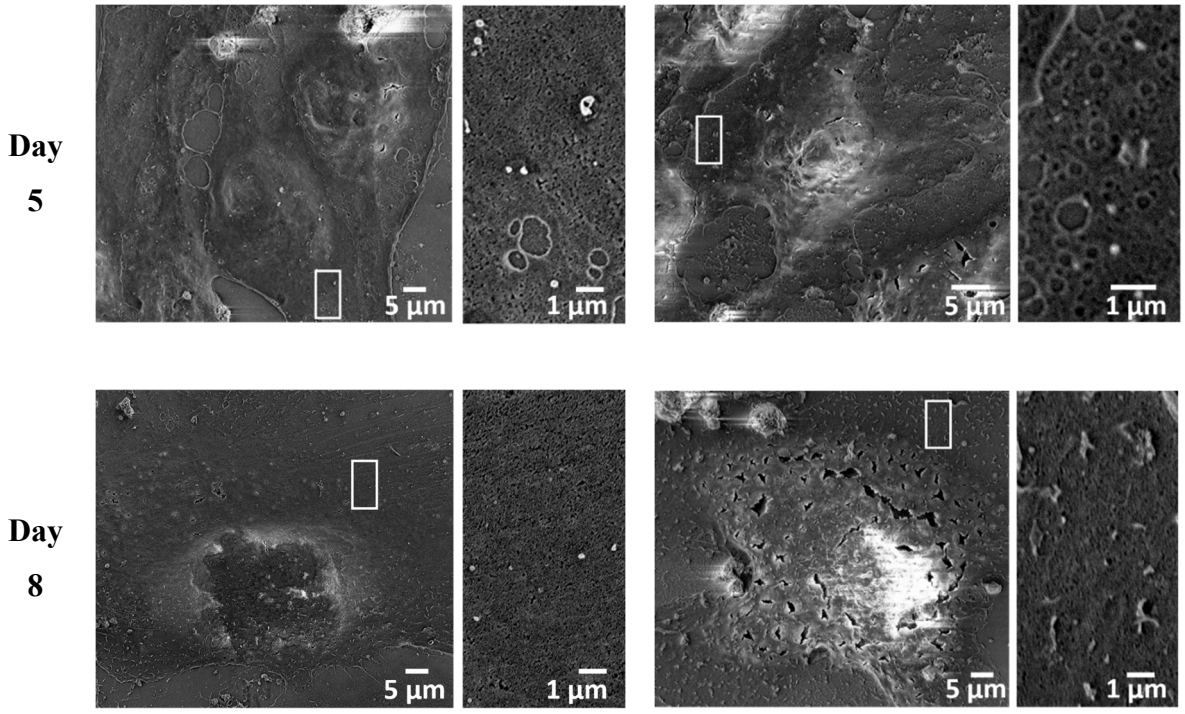


*Figure 4.7: SEM images of changes in LSEC morphology after treatment with cytochalasin B. Mouse LSEC were isolated and seeded on fibronectin-coated plastic well plate in EGM and continuously treated with EGM supplemented with 2 µg/mL or 0.5 µg/mL cytochalasin B. The cells were fixed at days 1, 3, 5 and 8, followed by SEM sample preparation. Images presenting changes over time. Scale bar = 5µm.*

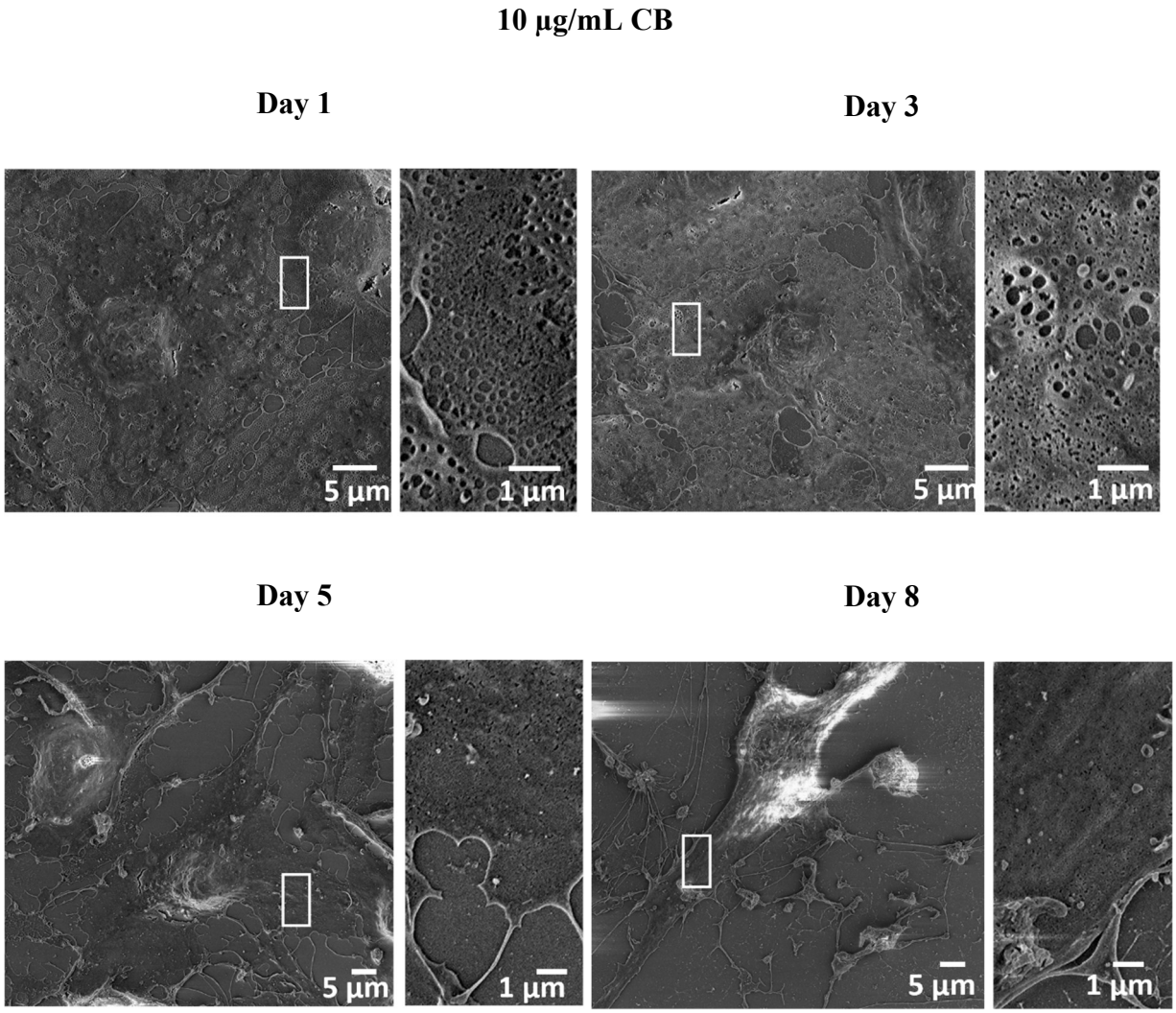


*Figure 4.8: SEM images of changes in LSEC morphology after treatment with cytochalasin B. Mouse LSEC were isolated and seeded on fibronectin-coated plastic well plate in EGM and acute treated with 10 µg/mL cytochalasin B (30 min). The cells were fixed at days 1, 3, 5 and 8, followed by SEM sample preparation. Images presenting changes over time. Scale bar = 5 µm.*

After the analysis of pilot experiments and initial optimization of cell culture conditions, new experiments were conducted on fibronectin-coated plastic well plates.LSEC were treated with 5 µg/mL Cytochalasin B for 30 min before being fixed and prepared for SEM.

Treatment with Cytochalasin B induced more fenestrations in LSEC on day 1 (Figure 4.9 and 4.10), as compared to non-treated cells (Figure 4.5 and 4.6). Almost 50% of LSEC on day 1 were highly fenestrated and there were 80% fenestrated cells in total (Figure 4.10). The total number of fenestrated cells remained stable on day 3, while there was a marked decrease in the number of highly fenestrated cells. On days 5 and 8, no highly fenestrated cells were observed while the total number of fenestrated cells was 60% and 50%, respectively. The majority of

these cells were low fenestrated while 3% was normally fenestrated cells. The rest of the cells were completely defenestrated.

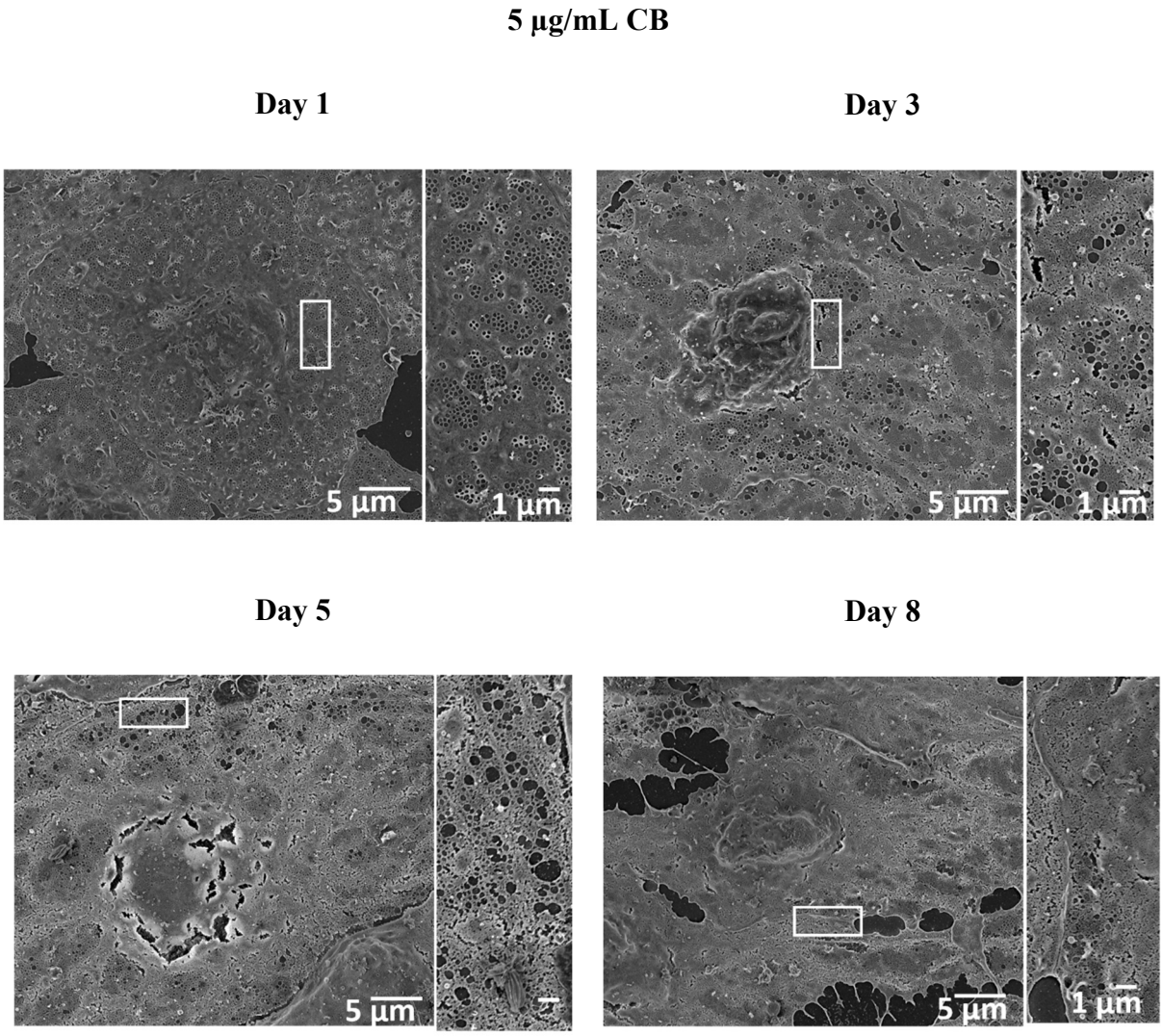


*Figure 4.9:* SEM images of changes in fenestrations after acute treatment with *Cytochalasin B*. Mouse LSEC were isolated and seeded on fibronectin-coated plastic well plate in EGM. The cells were acutely treated (30 min) with 5 µg/mL cytochalasin B on days 1, 3, 5 and 8 followed by fixing and SEM sample preparation. Images presenting changes over time. SEM used to visualize the changes. Scale bar = 5 µm. Abbreviations: CB – cytochalasin B.

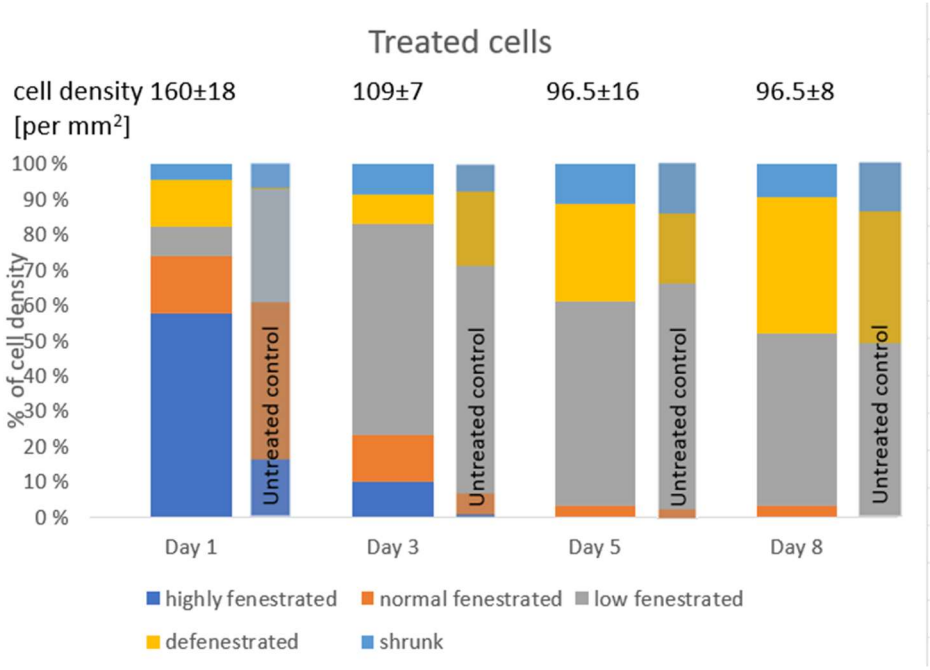


*Figure 4.10: Semi-quantitative analysis of LSEC treated with 5 µg/mL of* cytochalasin B *for 30min. LSEC were isolated and seeded on fibronectin-coated plastic well plate in EGM. The cells were fixed on days 1, 3, 5 and 8 followed by SEM sample preparation. Overview pictures with size 300x400 µm were used to count the cell density and the fenestrated and defenestrated cells. The graph shows and compares the proportion of fenestrated and defenestrated LSEC up to 8 days in treated and untreated (control) LSEC. Cell density data are presented as mean ± standard deviation, n=3 independent experiments.*

### 4.2.2 Cytoskeleton

The changes in actin cytoskeleton in LSEC over time in culture were studied by staining with phalloidin AF555. Fluorescent microscopy was used to visualize these changes.

On day 1, the actin filaments were well organized to form an intracellular mesh and a cortical ring around LSEC periphery was observed, as illustrated on figure 4.11. The thick actin fibers (stress fibers) appeared on days 5 and 8. The actin filaments became extended throughout the whole LSEC cell body. On day 8, the organization changed where the actin filaments no longer arranged at the cell periphery; the actin structure (stress fibers) is following the cell elongation. The actin filaments appeared thicker and with 3D-like structure.

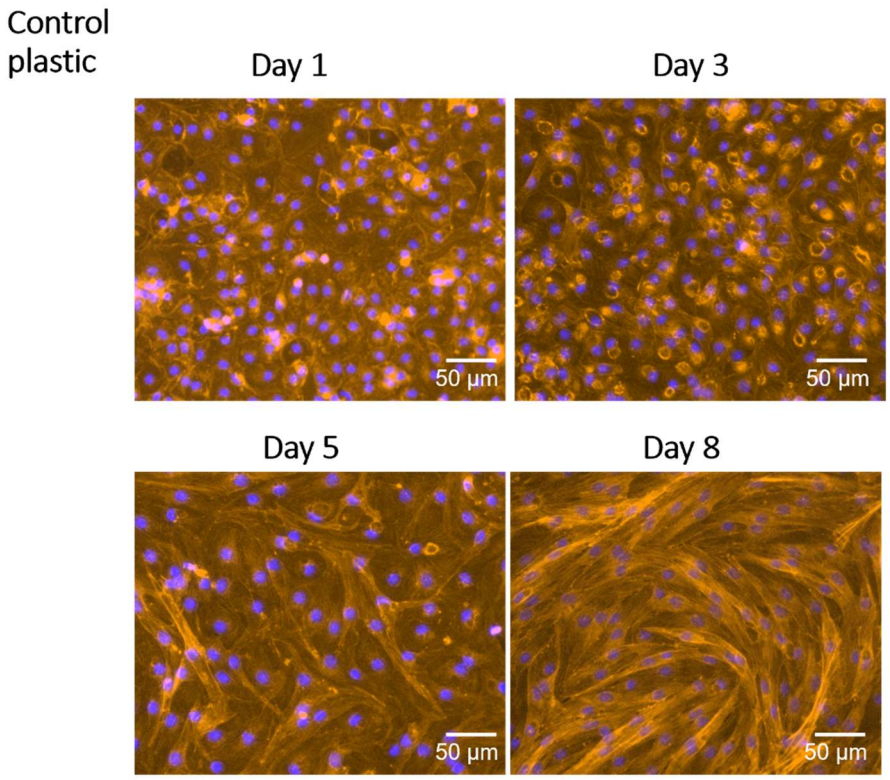


*Figure 4.11: Fluorescent images of changes in the actin cytoskeleton. Mouse LSEC were isolated and seeded on fibronectin plastic well plates in EGM. The cells were fixed and stained on days 1, 3, 5 and 8. Actin cytoskeleton was stained with phalloidin 555 (orange), and cell nuclei were stained with DAPI (blue). Images presenting changes in the cytoskeleton over time. Images were obtained at 20x magnification with EVOs. Scale bar = 50 µm.*

### *4.2.2.1* The actin cytoskeleton under the influence of *cytochalasin B*

Some samples in the pilot experiment were treated with *cytochalasin B* to study if *cytochalasin B* affected the actin cytoskeleton in long-term culture, and cells were examined by fluorescent microscopy. The cells were continuously treated with media (EGM) with 2 µg/mL or 0.5 µg/mL cytochalasin B for, or with 10 µg/mL for 30 min (acute treatment). In addition, 10 µg/mL was administered to for acute treatment (30 min) to some cells incubated in RPMI media.

Figures 4.12 and 4.13 demonstrate that in both media, after treatment with cytochalasin B, actin dots were formed. Less actin stress fibres were observed in cells after cytochalasin B treatment on days 5 and 8 compared to time-matched control cells. Since this experiment was done parallel to the first pilot experiment and the cells were cultured on glass surfaces, day 8 is not fully representative

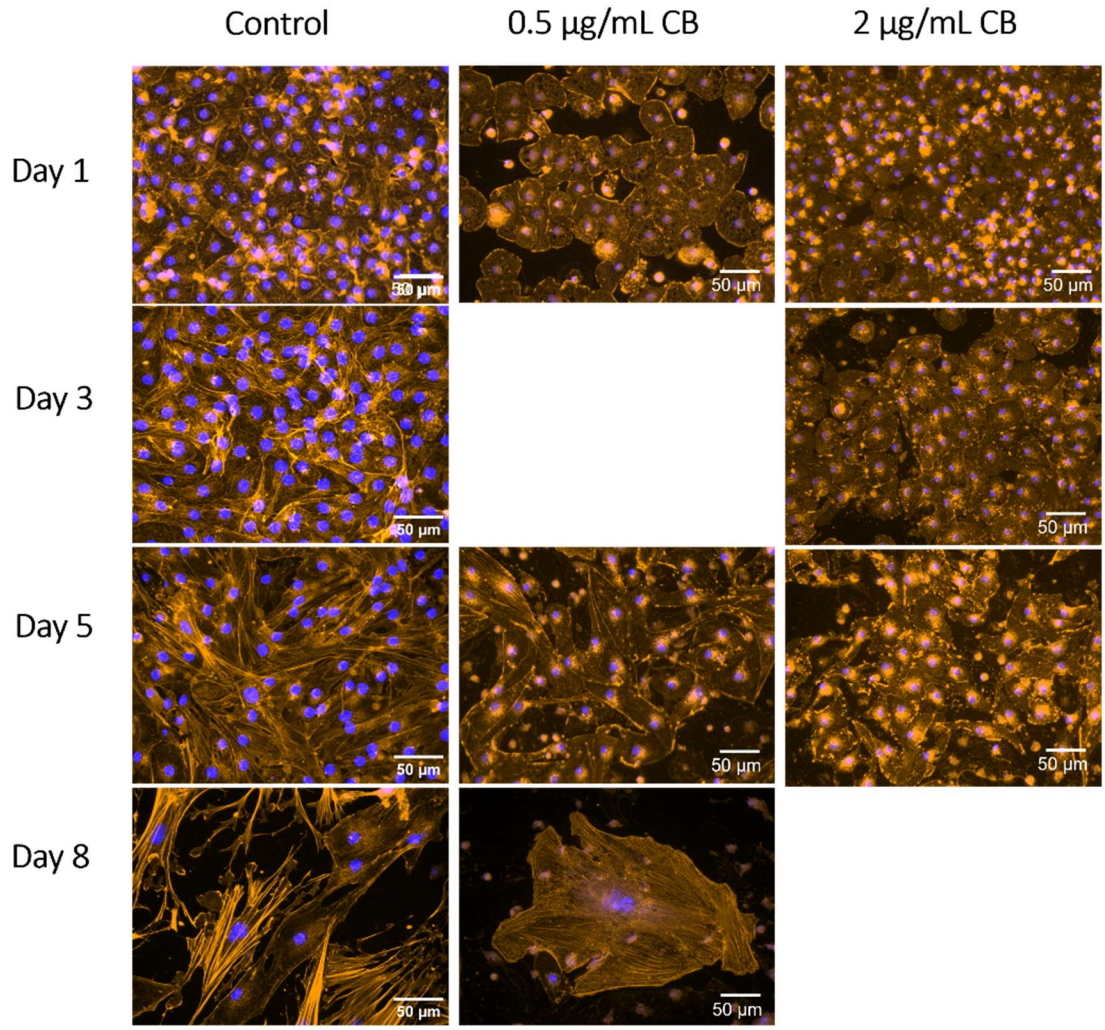


*Figure 4.12: Fluorescent images of changes of actin-stained cells after treatment with* cytochalasin B. *Mouse LSEC were isolated and seeded on fibronectin glass coverslips and continuously treated with EGM supplemented with 2 µg/mL or 0.5 µg/mL* cytochalasin B. *The cells were fixed and stained on days 1, 3, 5 and 8. The actin cytoskeleton was stained with phalloidin 555 (orange), and cell nuclei were stained with DAPI (blue). Images are presented vertically, showing changes over time, with side-by-side comparisons of control and cells with continuous treatment of 2 µg/mL or 0.5 µg/mL* cytochalasin B *in media. Due to technical error, samples from day 3 0.5 µg/mL treatment and day 8 2 µg/mL treatment could not be imaged. Images were obtained at 40x magnification with EVOs. Scale bar = 50 µm.* Abbreviations: CB – cytochalasin B.

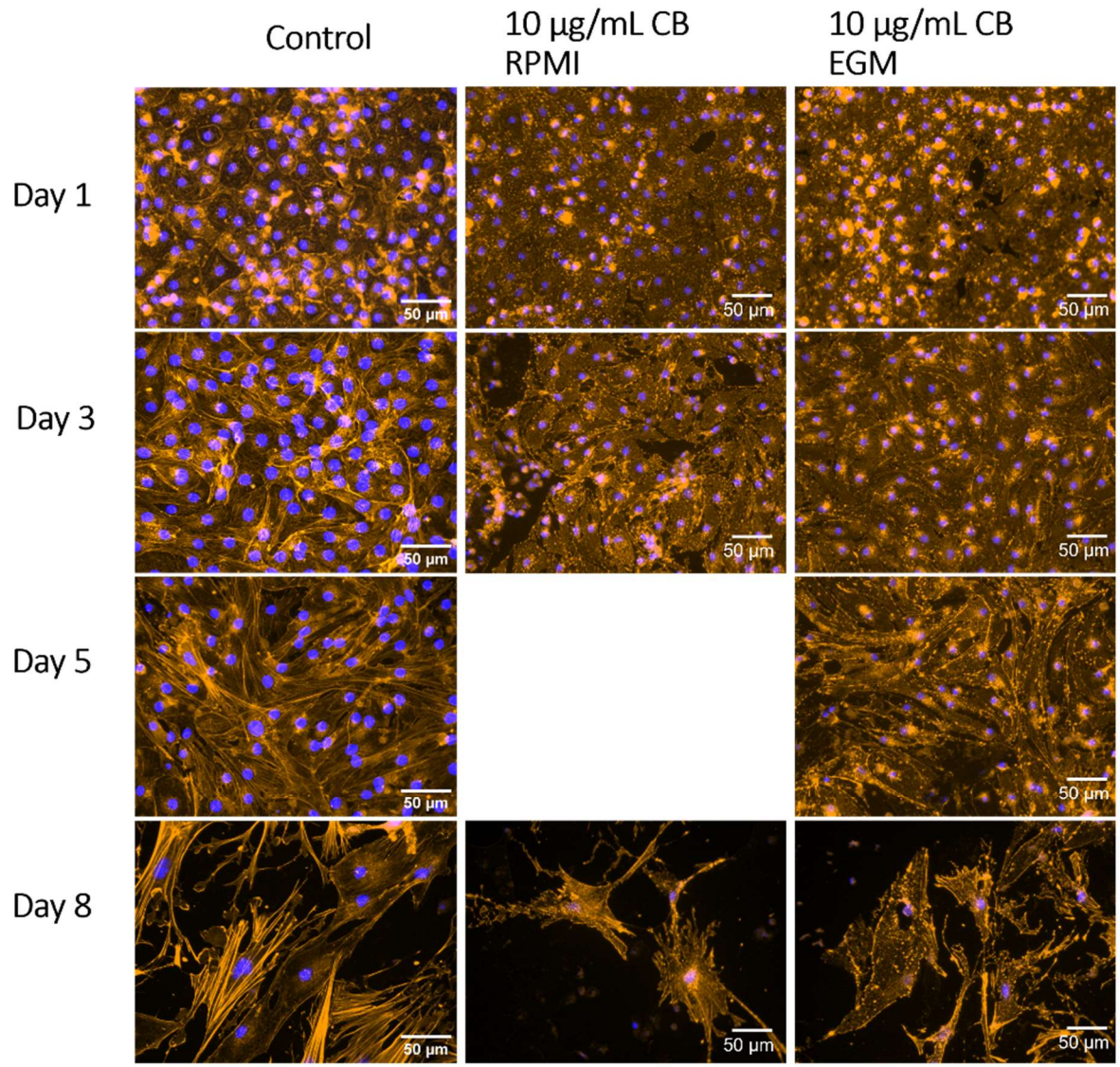


*Figure 4.13: Fluorescent images of changes of actin-stained cells after treatment with cytochalasin B . LSEC were isolated and seeded on fibronectin glass coverslips in both RPMI and EGM. The cells were acutely treated (30 min) with 10 µg/mL* cytochalasin B*, fixed and stained on days 1, 3, 5 and 8. Actin cytoskeleton was stained with phalloidin 555 (orange), and cell nuclei were stained with DAPI (blue). Images are presented vertically, showing changes over time, with side-by-side comparisons of control and cells with 30 min acute treatment of 10 µg/mL* cytochalasin B. *Images were obtained at 40x magnification with EVOs. Scale bar = 50 µm.* Abbreviations: CB – cytochalasin B.

## 4.3 Viability assays

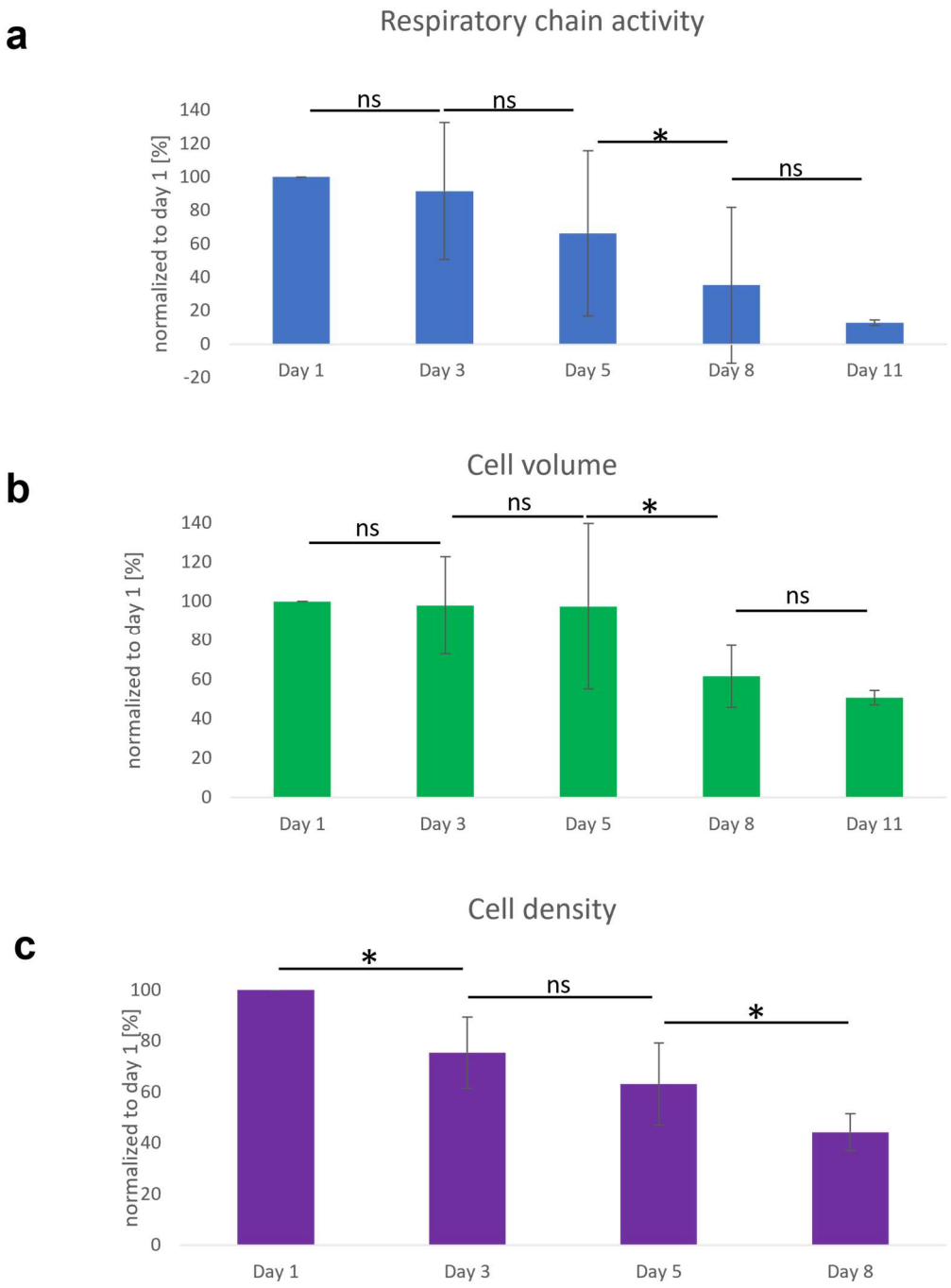


*Figure 4.14: Results of the assays evaluating LSEC health and measurements of cell numbers in culture. a) shows the results from the resazurin assay; b) the cell volume calculated based on LDH assay results, and c) the results from counting of cells stained with DAPI. Results are presented as the mean of n=3 independent experiments +/- standard deviation. Statistical significance was determined by pairwise comparisons using one-way t-test *p<0.05 **p<0.01, ***p<0.001, ns = no significance*

Three assays, a Resazurin assay, an LDH assay, and counting of cell nuclei on light microscopy images by ImageJ were performed to evaluate cell viability, or the number of cells in long-term culture. The assays were performed on days 1, 3, 5 and 8, while resazurin and LDH assays were additionally conducted on day 11. Counting cells stained with DAPI allows assessment of the number of attached cells but does not distinguish between dead and live cells.

Figure 4.14 a shows a decrease in the respiratory chain activity in LSEC in time in culture as assessed with the Resazurin assay. On day 1, the metabolic activity was the highest. Respiratry chain activity declined to 91% on day 3, 66% on day 5, 35% on day 8 and 21% on day 11.

Measurement of the release of intracellular LDH allows assessment of the volume of viable cells. Figure 4.14 b shows that LSEC volume in the samples decreased after about day 5. Cell volume was at the highest level on day 1 and remained stable at >97% until day 5. Between days 5 and 8 cell volume decreased to 61% and reached 50% on day 11.

Figure 4.14 c shows a decline in cell density from day 1 to 8. Cell density was reduced to 74% on day 3, 64% on day 5 and 43% on day 8, compared to day 1.

## 4.4 Cell purity in culture

LSEC isolation is prone to contamination with other liver cells and high contamination can possibly affect the LSEC in long-term culture. Therefore, the VSIG4 antibody was used to target and detect Kupffer cells and an antibody to GFAP was used to stain hepatic stellate cells. Since hepatocytes are significantly larger than the other liver cells, it is easy then to distinguish them in the sample and no staining was required. Based on these results, the purity of LSEC cultures was calculated to be >97%.

Figure 4.15 illustrates that some Kupffer cells, about 2%, were present in the LSEC cultures on all days. A general observation of the samples indicated a decrease in the number of Kupffer cells with the days. GFAP+ cells were not observed.

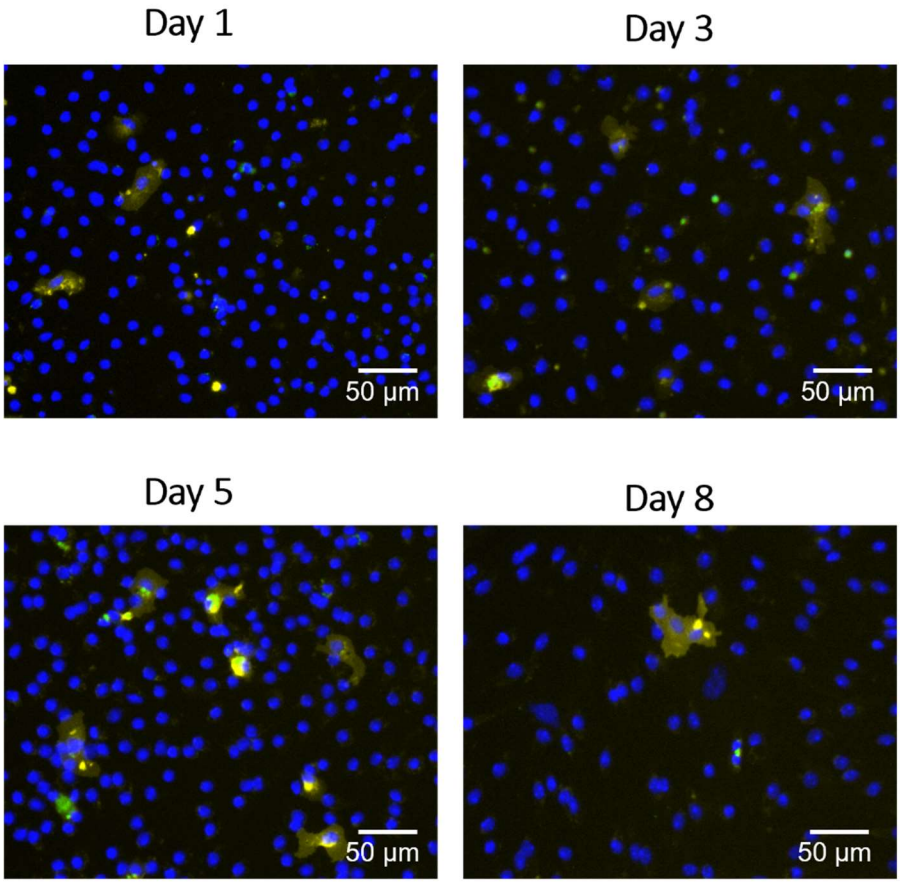


*Figure 4.15: Purity assessment of LSEC culture of a C57BL/6JRj mouse. LSEC were isolated and seeded on fibronectin plastic well plates in EGM. The cells were fixed and co-stained with markers to Kupffer cells and hepatic stellate cells on days 1, 3, 5 and 8. Kupffer cells were stained with an antibody to VSIG4 (yellow), stellate cells were labelled with the target antibody GFAP and cell nuclei were stained with DAPI (blue). Images are presented vertically, showing changes over time for the three ligands. Images were obtained at 20x magnification with an EVOS microscope. Scale bar = 50 µm.*

## 4.5 LSEC expression of scavenger receptors and Fc-gamma reseptor IIb2

To investigate the LSEC expression of stabilin-1 (Appendix D), stabilin-2 and Fc-gamma receptor IIb2 in long-term culture, the receptors were stained according to the method outlined in section 2.7.3.4. LSEC were seeded on a plastic well plate and incubated in EGM media until fixing.

Figure 4.16 demonstrates the results after antibody staining for the different receptors (antibodies are listed in Table 3.3 ). LSEC had a high expression of stabilin-2 on day 1, with a

decrease in staining intensity over time. However, the negative control lacking the primary antibody (Appendix C) displayed high unspecific binding signals.

Expression of Fc-gamma IIb2 was high up to day 3, and then the expression level decreased on day 3 and remained stable until day 8. On days 1 and 3, heterogenous expression of the Fc-gamma receptor IIb2 was observed. While, on days 5 and 8, the expressions of Fc gamma IIb2 were homogenous.

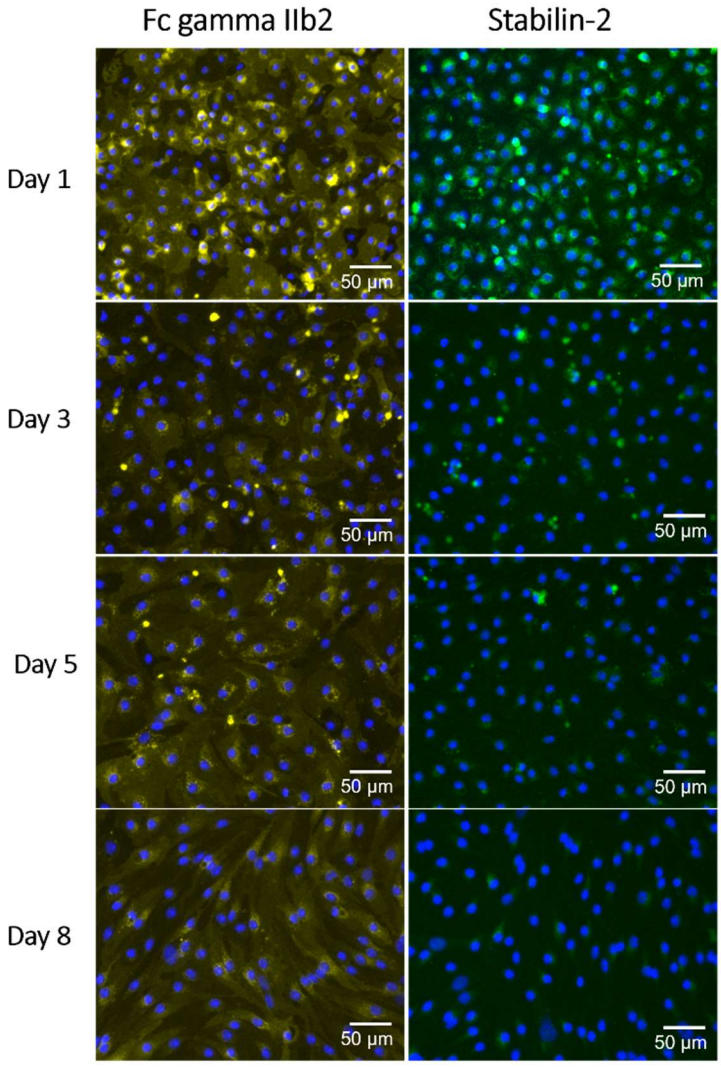


*Figure 4.16: Expression of receptors in LSEC. Mouse LSEC were isolated and seeded on fibronectin plastic well plates in EGM. The cells were fixed and single-stained on days 1, 3, 5 and 8. Stabilin-2 was stained with an anti-stabilin-2 rat antibody (green), Fc-gamma IIb2 was stained with an anti-mCD32/CD-16 antibody (yellow) and cell nuclei were stained with DAPI (blue). Images are presented vertically, showing changes over time for the three receptors. Images were obtained at 20x magnification with EVOs. Scale bar = 50 µm.*

## 4.6 Qualitative assessment of LSEC scavenging

### 4.6.1 Qualitative analysis

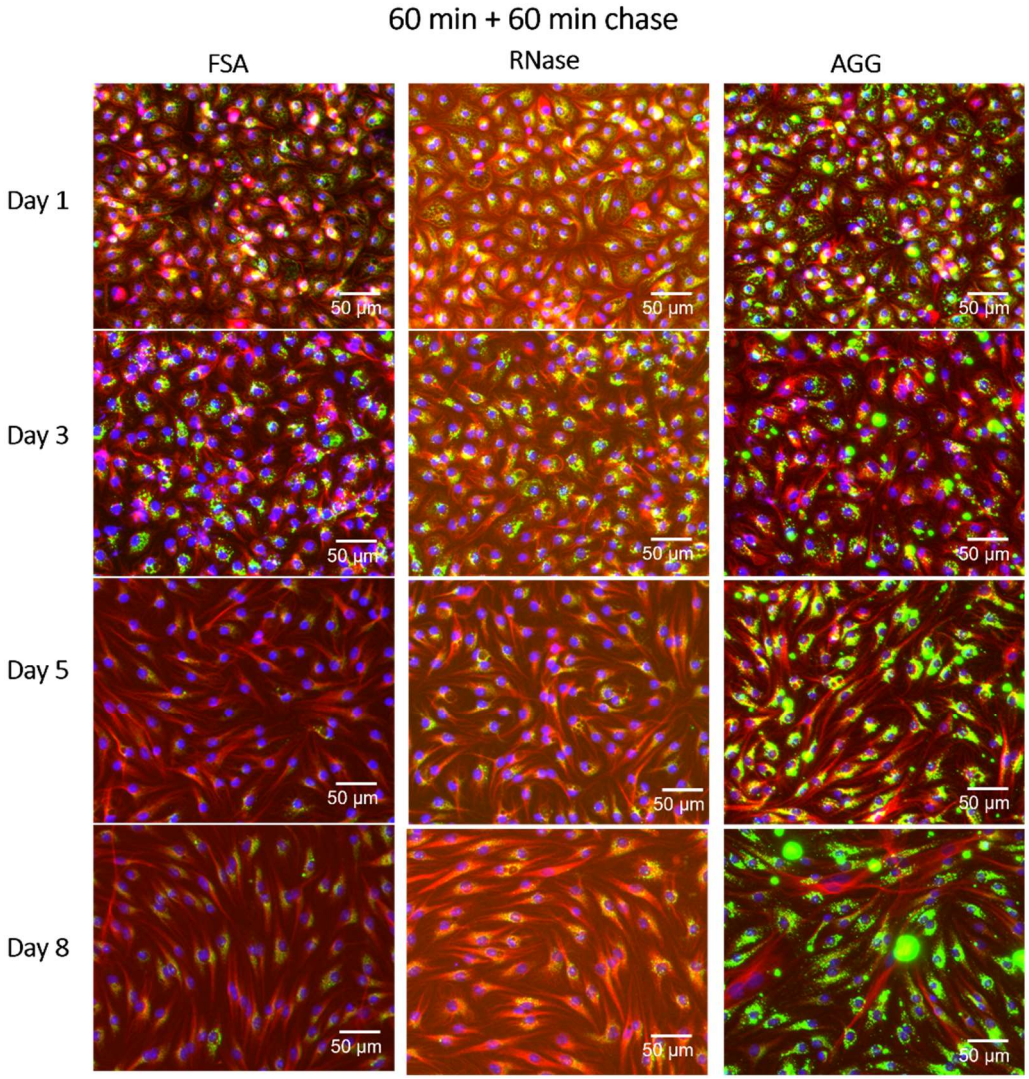


*Figure 4.17: Fluorescence images of FSA, RNase and AGG (conjugated with Alexa Fluor 647 (green)) uptake in LSEC. Mouse LSEC were isolated and seeded on fibronectin plastic well plates in EGM. The cells were incubated for 1 h with ligand, followed by 1 h incubation without ligand. The cells were fixed and stained on days 1, 3, 5 and 8. Tubulin was stained with anti β-tubulin antibody conjugated to Alexa fluor 488 (red), and cell nuclei were stained with DAPI (blue). Images are presented vertically, showing changes over time for the three ligands. Images were obtained at 20x magnification on an EVOS microscope. Scale bar = 50 u µm.*

To study the scavenger system of LSEC, LSEC were treated for 1 h (pulse) and 1 h (chase) at 37 °C with FSA, RNase B and AGG, followed by 1 h incubation in media alone, after seeding the LSEC on fibronectin-coated plastic surfaces. FSA is believed to be mainly taken up by the

receptors stabilin-1 and stabilin-2 in LSEC, while RNase B is endocytosed via the mannose receptor and AGG by Fc gamma receptors.

Figure 4.17 demonstrates the uptake of fluorescently labelled FSA, RNase B and AGG in cells at days 1-8. Following a 2 h incubation period, the ligands were observed localized around the nucleus. FSA uptake was high on days 1 and 3, decreased on day 5 and remained stable on day 8. The same trend was observed with RNase B; where RNase B uptake was high on days 1 and 3, and then decreased on day 5 and remained stable at day 8. The uptake of AGG appeared higher in cells on days 5 and 8 than on day 3. The figure shows that all the three ligands accumulated in vesicles close to the nuclei.

### 4.6.2 Quantitative analysis

To study endocytic activity in a quantitative way, $^{125}$I-FSA was added for 2 h. Figure 4.18 shows endocytosis of $^{125}$I-FSA by LSEC up to 21 days in culture. For day 1, on both media, the uptake of $^{125}$I-FSA was similar, around 45% of added ligand. The endocytosis values in figure 21 from the following days were normalized to day 1.

For cells in RPMI, the endocytosis of $^{125}$I-FSA steadily decreased with time in culture and on day 8 it reached about 13% of day 1. On day 11, endocytosis was not detectable. The ratio of cell associated and degraded FSA remained stable.

For EGM, on days 3 and 5, the endocytosis decreased to 70% and 60% of day 1 respectively. The difference between endocytosis on day 3 and 5 was not significant, but on day 8, the endocytosis increased and reached above 90% of day 1, and remained on a similar level until day 11. On day 21, the endocytosis decreased to about 20% of day 1. A small decrease in the ratio of degraded to cell associated FSA was observed on day 3, however after day 5 it returned to day 1 values. On day 21, the degradation of FSA was about 30% compared to 50% on day 1.

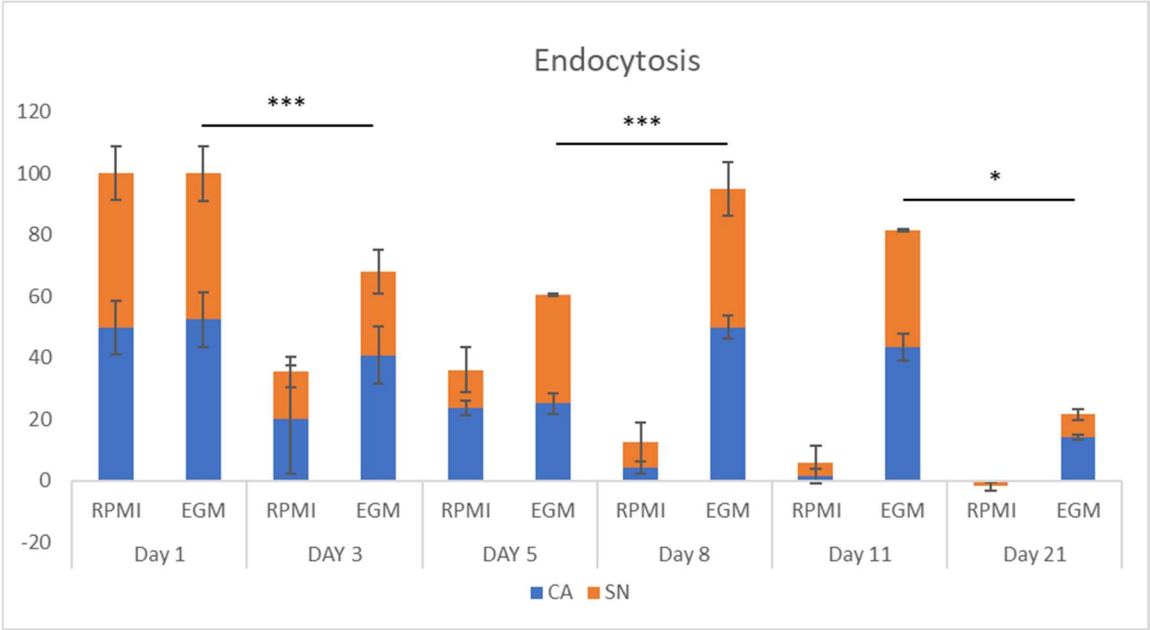


*Figure 4.18: Endocytosis of $^{125}$I-labelled FSA. Blue represents cell associated FSA, and orange represents cell degraded FSA. X-axis represents precentage of endocytosis normalized to day 1. and y-axis represents media used and the days assay was performed on. Results are presented as the mean of n=3 independent experiments +/- standard deviation. Statistical significance was determined by pairwise comparisons using one-way t-test *p<0.05 **p<0.01, ***p<0.001.*

# 5 Discussion

The project focuses on the optimization of the long-term 2D culture of LSEC and is part of EIC project DeLIVERy. One of the aims of the DeLIVERy project is to develop a long-term cell/tissue culture that will facilitate the study of cellular responses to various drugs and use it in a microfluidic device.

## 5.1 Methodological considerations

Continuous efforts are made to optimize laboratory methods to provide the best possible conditions for studying LSEC in vitro. However, these methods also have limitations.

### 5.1.1 Animal model

The ethical implications of using animals in research have always been a subject of concern. Different countries have different ethical regulations, and in this study, European ethical guidelines have been followed. Currently, there are no real alternatives to using animal cells in LSEC research, and in the present study, we used cells isolated from laboratory mice. The access to human liver samples is in general highly limited, and restricted to projects that have ethical approval for the use of human material. LSEC isolation from patient liver samples such as excess tissue from cancer resections, is also more challenging than isolation from mouse liver, which influence the viability and purity of the cells in culture (68). In long-term in vitro studies, the initial conditions of the freshly isolated cells influence successful long-term culture so using human samples from cancer resections is not feasible at this point.

In order to investigate the characteristics of liver fenestrations across animal classes, various vertebrates species have been used in LSEC research, including rodents, sheep, pigs, guinea pigs, birds, rabbits, cats, dogs and baboons (35, 116, 117). The LSEC of the examined species possess fenestrations, however, the average number per cell and fenestrations diameter varies between species (17, 35, 118). The choice of animal models depends on the type and aims of the study. Mice are commonly used in studies related to studies of fenestrations in ageing and ageing-related diseases since mice have a lifespan of 2-3 years, as well as share 99% of genes with humans (119). Similarly to humans, the fenestrations in mice are organized in sieve plates (35). However, mice have a higher average of fenestrations size and slightly lower number of fenestrations than humans (35, 115, 120)

In this study, the inbred mouse strain C57Bl/6JRj was chosen as the animal model. This is a commonly used mouse strain, with much physiological data available. Moreover, the use of inbred mice reduces variation between biological replicates, which reduces the number of animals needed. Rat LSEC isolated with the current protocol used at VBRG have lower initial viability than mouse LSEC which seems to influence the long-term culture (based on pilot experiments at VBRG).

### 5.1.2 Primary cells vs. cell lines

Most LSEC studies have been conducted using primary LSEC since it has been reported that LSEC lose their characteristics and functions after a few days from isolation (48, 121). Several attempts have been made to establish LSEC cell lines (83, 84, 122, 123, 124), however, none exhibits all the characteristics and receptors of LSEC. Most cell lines demonstrated limited receptor-mediated endocytosis and limited uptake of FSA. The cell lines reported by Zhao et al. (124) and by V. C. Cogger et al (122) showed fenestrations-like structures, but, their characteristics are far from those observed in primary cells. Therefore, it was not possible to use cell lines in this study, as the objective is to optimize the conditions to establish a long-term culture and investigate morphological and functional changes over time.

A challenge associated with the isolation of primary cells is the contamination of the cell culture with other liver cells during/after the isolation. The use of CD146 as a cell marker for endothelial cells enables effective positive selection of LSEC and minimizes contamination (104). The liver contains also other endothelial CD146+ cells however their effect on LSEC culture is believed to be minimal. On the other hand, contamination with other liver cells, such as Kupffer cells, stellate cells, and hepatocytes can influence the cell viability and functions of LSEC.

In this study, the purity of LSEC cultures was tested by immunostaining of Kupffer cells using an antibody against VSIG4 (also named CRIg), which is a reported Kupffer cell marker (67, 125), and Stellate cells using an antibody against GFAP, which is an intermediate filament-III protein expressed in quiescent and activated stellate cells in the liver (126, 127, 128). Due to the size of the hepatocytes, they were easily detectable under microscopy as significantly larger than any other liver cell type. Hepatocyte contamination was not observed in the cultures, and the cultures did not contain GFAP+ cells. The results from the immunostaining against

VISG4+ Kupffer cells indicated minimal contamination. The final purity was estimated to be 98 %, with Kupffer cells the main contamination. This is in line with a previous report (104), which showed more than 95% (up to 99%) fenestrated endothelial cells (i.e. LSEC) in cultures with CD146-MACS isolated cells, evaluated by SEM. This level of contamination is not expected to have any significant influence on LSEC function since stellate cells which would have the biggest influence were not detected.

### 5.1.3 Immunofluorescence

Immunofluorescence is used to target specific proteins in cells/tissues for a better understanding of the cell's physiology and mechanisms. In this study, a direct staining method was used to visualize tubulin, while an indirect staining method was used to detect other proteins. In the indirect method, the cells were incubated with a primary antibody to enable a specific binding with the desired target molecule and then the cells were incubated with a secondary antibody which is conjugated with a fluorophore and will bind to the primary antibody.

Fluorescence was observed in the negative control of stabilin-2 staining, indicating either autofluorescence in mouse LSEC or unspecific binding of the secondary antibody. Autofluorescence was not observed in the other samples, which suggests that unspecific binding of the secondary antibody is likely. Autofluorescence is however, reported to be a challenge in human LSEC from patient samples (129), where it was observed in all utilized fluorescence microscopy channels. However, in our study in mouse LSEC, the fluorescence in negative controls was only observed in the green channel, 500 – 550 nm when using the Donkey anti-rat IgG (H+L) Cross absorbed secondary antibody Dylight 488 as a secondary antibody for stabilin-2. According to the manufacturer's report (130), no unspecific binding of that secondary antibody was observed in the negative controls tested on A549 cells (human lung carcinoma epithelial cells). Nevertheless, the observed signal in the negative controls suggests that the blocking buffer was not functioning properly, and different blocking buffers should be tested to improve the blocking step. Another explaining could be a manufacturing error of the specific antibody batch which resulted in unspecific binding.

Photobleaching is another challenge in fluorescent techniques. Fluorophores are sensitive to light and should be kept in the dark to avoid photobleaching, which presents yet another

challenge, especially for multicolor labeling. Sequential labeling exposes samples to extra light during the process which may contribute to photobleaching before imaging. Furthermore, fluorescently labeled FSA is also prone to photobleaching during and after labeling, and therefore the fluorescently-labeled FSA was kept in darkness during the purification (dialysis) step, aliquoting, and cell treatment. A strong fluorescent FSA signal was observed in all samples suggesting a minimal influence of photobleaching.

### 5.1.4 SEM limitations

The approximate resolution limit of a standard light microscope is 200 nm. Liver fenestrations can have a size as small as 50 nm, so SEM is the optimal technique to study fenestrations in LSEC (131). The number of fenestrations can be easily be quantified from SEM images but the fenestrations size measured is prone to errors due to sample preparation steps, which could influence the results (33, 132). Over-fixation could shrink the cells, in the same manner as the use of cold fixatives (133). On the other hand, under-fixation would prevent the preservation of the cell's ultrastructure. Despite the observations of a few shrunk cells in SEM images, the LSEC morphology was well preserved in the samples, suggesting that over-fixation or under-fixation of the cells was not a problem.

Due to the high vacuum in SEM, complete dehydration of the samples is necessary. Dehydration has some disadvantages, mainly the deformation and increased size of fenestrations (131). Szafranska et al. (131) reported a significant increase of more than 30% in the size of fenestrations when measured using SEM compared with other fluorescent superresolution techniques not requiring dehydration of the samples. In this study, findings obtained on day 1 from SEM images indicated a high number of fenestrations in the cells, with a decrease in fenestrations number from day 3 as supported by previous studies (106, 121). The dehydration during SEM sample preparation could influence the size of fenestrations leading to an exaggerated increase in size observed on days 3, 5, and 8, however, it would most probably not change the observed trend. This error is also likely to be similar in untreated and treated cells, and thus not influence the comparison of groups. Wet-fixation imaging techniques could be used in future experiments to confirm the findings.

## 5.2 Long-term culture of LSEC

### 5.2.1 The effects of the culturing surface (glass vs plastic)

In this study, we initially chose to culture LSEC on glass surfaces due to the excellent optical properties of glass, facilitating high-quality microscopic imaging. Furthermore, the chemical-free and non-toxic nature of glass was hypothesized to not affect the cell cultures negatively.

In the initial pilot experiment conducted exclusively on glass, a decline in cell population and an increased number of defenestrated cells was observed. To optimize the conditions for the long-term culture of LSEC, a second pilot experiment was performed. Results from the second pilot experiment indicated better LSEC survival on plastic, with a confluent monolayer on day 8 compared to sparse enlarged cells on the glass surface. A previous report by Elvevold et al (121) showed survival of pig LSEC for up to 30 days in fibronectin-coated glass slides in (DM 110 media + 5% Tissue SS and hydrocortisone). Unfortunately, this medium is no longer available. The observed difference may be due to species differences or glass culture specifications.

One possible explanation for the different survival between glass and plastic could be that the smooth glass surface influences the functionalization of the substrate. Culturing endothelial cells requires adhesive proteins such as fibronectin or collagen. Non-uniform or not dense enough functionalization of the surface would negatively affect the cell attachment and/or growth. The differences in LSEC cultured on the glass on day 8 suggest that fibronectin/collagen coating was not efficient enough resulting in detachment and cell death. The coating parameters of glass surfaces should be assessed and optimized in the future.

### 5.2.2 The influence of cell culture media (EGM vs RPMI)

RPMI contains only essential molecules for cell survival in cultures. The composition covers 20 essential and non-essential amino acids, 6 inorganic salts, 11 vitamins, D-glucose, L-glutathione reduced, and phenol red pH indicator (134). The media has been traditionally utilized for lymphocytes cultivation.

On the other hand, the EGM was developed specifically for culturing of large blood vessel endothelial cells. According to the manufacturer, the medium contains FBS, growth factors, trace elements, and antibiotics but the exact concentrations are not revealed. The medium does not contain vascular endothelial growth factor (VEGF) which is a hormone that acts as a

mediator of paracrine signaling from hepatocytes and stellate cells to LSEC. Lack of VEGF has been previously linked to the defenestration of LSEC (135).

Nevertheless, information about another EGM from another manufacturer (136), (developed for culturing of human endothelial cells (HUVECS)), lists six growth factors in the supplement. The listed media supplementation contains human epidermal growth factor (hEGF), human fibroblastic growth factor (hFGF), human insulin-like growth factor 1 (IGF-1), hydrocortisone, ascorbic acid, heparin, and 2% FBS.

The findings from the pilot experiment demonstrated better survival of LSEC in EGM compared to RPMI. Additionally, the analysis of SEM images performed on cells seeded on plastic surfaces in EGM revealed the presence of a low number of fenestrations in the remaining cell population on day 8. LSEC is a unique and specialized endothelial cell type that is dependent on environmental stimuli to sustain its functions. The components of RPMI appear to be insufficient to maintain the viability of LSEC above 3-5 days in vitro. Although the specific growth factors or their concentrations in EGM used in this study have not been disclosed by the manufacturer, they are likely crucial for LSEC survival and preserving LSEC functions over several days in culture. We, therefore, plan to also test the defined medium from (136) and compare it with EGM that was used in the present study.

Several previous studies have been conducted in an attempt to develop a new media that can allow LSEC to survive in vitro for several days and maintain their morphology and functions in vitro (67, 121, 137). In general, these studies used basic media such as DMEM and RPMI with supplements. Elvevold developed (121) serum-free media that consisted of DMEM containing vitamins and amino acids and MCDB 110 media made for serum-free media and contained hormones, vitamins, and some growth factors, Tissue SS (serum replacement), hydrocortisone, and cholic acid. The tissue SS supplement was not specified and is unfortunately not commercially available. This media contained hydrocortisone which was reported to improve endothelial growth in culture and acts as an anti-inflammatory agent (138). Furthermore, Elvevold et al supplemented the media with three of the growth factors, EGF, IGF, and FGF, reported in EGM from (136) in addition to hydrocortisone. Li et al. (137) examined the effect of the synthetic corticosteroid dexamethasone on rat LSEC in cultures (1 μg/mL), using DMEM supplemented with ascorbic acid as a basic medium. Dexamethasone was here shown to significantly enhance cell viability compared to non-treated cells (137).

A study by De Zanger et al. (139) rat LSEC were cultured in RPMI media with phorbol myristate acetate (PMA) supplementation (added after 24 h of incubation in RPMI). PMA had positive affect on LSEC viability. Higher number of viable LSEC was observed in the samples cultured with RPMI supplemented with PMA than the control untreated samples. The cells survived for up to 7 days. However, after 72 h, the control samples showed higher number of fenestrationsper $\mu m^2$ than the sample treated with PMA with the same size of fenestrations.

### 5.2.3 LSEC viability

There are different assays to assess cell viability based on different cell functions. To examine LSEC health or cell density in culture, three different assays were conducted – Resazurin, modification of LDH release, and counting of cell nuclei (stained with DAPI without distinction for dead or live cells).

In this thesis, the results from counting the cell nuclei stained with DAPI showed a 26% decrease in cell density on day 3 (I.e. after 48h) in EGM. The cell density calculated from the semi-quantitative analysis of SEM images of LSEC cultures declined as a function of time in the culture at a similar pace as in the results from DAPI cell counting. The cell density on day 8 calculated from fluorescent microscopy images showed about a 50% decrease compared to day 1, while an approximately 30% decrease in cell density was observed from the semi-quantitative calculation of SEM images. The difference may be at least partly explained by differences in fixation protocols. Fluorescent microscopy samples were fixed for a short time (15 min) with only 4% formaldehyde and were permeabilized with detergents. This procedure weakens the cell membrane, possibly resulting in the detachment of the cell nuclei and therefore reduction in the cell density parameter. The SEM fixative contains both formaldehyde and glutaraldehyde which gives a strong irreversible fixation preventing the detachment of cell nuclei. SEM samples were additionally fixed for a prolonged time.

LSEC single-cell area increased from day 3 on. LSEC are dependent on paracrine and autocrine signals to survive and maintain their function and morphology. In the cell culture, decrease in the cell density over time contributed to gaps between LSEC. Therefore, it is suggested that LSEC cell area increase in try to come in contact with other LSEC.

The LDH assay is not a direct measurement of the cell volume, however, it provides an estimation of the total cell volume. The decline of cell density in cultures on days 3 and 5, along with the stable total cell volume on these days, indicates an increase in a single cell volume. These findings support observations in the SEM and light microscopy images where the single-cell area appeared to increase. A more direct method should be used to confirm the findings about cell volume changes, such as quantitative phase microscopy (16).

Interestingly, mitochondrial respiratory chain (measured with the resazurin assay) and cell density decreased at the same rate indicating no changes in single-cell mitochondrial respiratory chain.

## 5.2.4 LSEC morphology

### 5.2.4.1 Fenestrations

Fenestrations are a characteristic feature of LSEC, and this study aimed to examine the changes in the number and the size of fenestrations in prolonged primary culture using SEM. The findings from this study revealed that the number of fenestrations decreased over time in culture. Similar findings have been reported in previous studies (82, 140, 141), including the study conducted by Elvevold (121) which aimed to develop a new media to preserve pig LSEC functions. The authors of that study maintained the endocytosis in LSEC for up to 20 days; however, they reported the disappearance of fenestrations after 3-4 days. Di Martino et al.(48) showed defenestration of mouse LSEC after 6 days, but fenestrations were not studied on days 2-5. In Di. Martino study, LSEC were treated with 10 μg/mL cytochalasin B for 2 h. The authors also suggested that the LSEC population was heterogenous which was confirmed in the present study. A subset of defenestrated cells was observed while other cells maintained fenestrations on days 3, 5, and 8. A quantitative analysis of fenestration size was not performed, however, the remaining fenestrations became visibly enlarged after day 3.

The identification of optimal in vitro conditions for preserving fenestrations, may offer valuable insights into the preservation of fenestrations in aging and diseases.

### 5.2.4.2 Cytoskeleton

The cytoskeleton is composed of actin filaments, microtubules, and intermediate filaments. In LSEC, actin filaments provide structural support to the fenestrations and determine their shape,

while microtubules are surrounding the sieve plates. Several studies have revealed the development of actin stress fibers after several days in cultures (44, 48). In this study, an increase in stress fibers was observed in LSEC on days 5 and 8 in culture. Similar findings were also observed on day 6 in mouse LSEC by Di Martino et al. (48).

The observed increase in the cell volume, as measured indirectly by the modified LDH assay (described in Methods) corresponds with the observation of the changes in the actin cytoskeleton and loss of fenestrations with time in culture. A decrease in porosity of LSEC in culture has been reported in studies done on human liver biopsies obtained from chronic alcoholics, alcohol-fed baboons, chronic alcohol ingestion in rats, humans and rats with cirrhosis, and with aging (120, 142, 143, 144, 145). Fenestration loss related to aging was explained by the thickening of LSEC (89, 145, 146). The formation of actin stress fibers increases cell thickness, and disrupts the contact between the upper and lower cell membranes, possibly hindering the formation of fenestrations.

Several actin-disrupting agents have been identified to influence actin filaments and disrupt stress fibers (44, 48). In this study, cytochalasin B treatment led to increased formation of actin dots in the LSEC, and (re)formation of new fenestrations in a subset of LSEC in culture.

Steffan et al. (115) created a short term culture of LSEC where LSEC were treated with 10 mg/mL cytochalasin B (similar to the concentration used for acute treatment on LSEC seeded on glass surfaces in this study) for 2 h. After 15 min of incubation, they made similar observations to this study, where in a subset of cells numerous fenestrations were induced while a subset of the cells remained defenestrated. However, after 2 h of incubation, they observed new fenestrations induced in all the cells.

Several studies have suggested that actin-disrupting agents induce more fenestrations in LSEC in vitro (34, 41, 147). De Zanger et al. (139) conducted a long term culture of LSEC and administered a 2 h treatment with 10 μg/mL cytochalasin B after 72 h of culturing with RPMI supplemented with PMA, and his results provided further support to previously reported observations, demonstrating that cytochalasin B significantly induced fenestrations in LSEC.

Furthermore, Di Martino et al. (48) treated LSEC in a long-term culture with an acute dose of an actin-disrupting agent, cytochalasin D (2 μM for 30 min), and new fenestrations were formed on day 6. These findings were similar to those observed in cytochalasin B-treated LSEC in the present study. An increase in fenestrated cells was observed in all the cytochalasin B-treated

samples on all days (Figure 4.10). However, several cells were still low-fenestrated or defenestrated, especially on days 5 and 8. The reason why *cytochalasin B* did not have the same effect on all the cells in the samples, could be due to LSEC heterogeneity or influence of the cell isolation process, as suggested by Di Martino (48). Another plausible suggestions is that the fenestrations require more time (more than 30 min) to form, as it was showed in the study of Steffan where 10 μg/mL *cytochalasin B* (the same concentration used in a part of this study and in Di Martino's study) induced new fenestrations in all the cells after 2 h.

In addition to inducing new fenestrations, cytochalasin D was previously demonstrated to decrease the diameter of fenestrations (48). In this study an increase in LSEC fenestration size was observed with *cytochalasin B* treatment, however, quantitative analysis of the size of fenestrations was not performed.

Although, cytochalasin B induce new fenestrations, it has been reported to be toxic(47, 148). Semi-quantitative analysis of fenestrated cells revealed lower cell density in the samples treated with 5 μg/mL *cytochalasin B* (Figure 4.10) compared with the untreated samples (Figure 4.8). In addition, damage of cell edges was observed on LSEC continuously treated or acute treated with cytochalasin (specially in LSEC samples acute treated for 30 min with 10 μg/mL *cytochalasin B*).

### 5.2.5 Endocytosis

Most of the testing of the endocytic activity of LSEC has been performed in short-term primary cultures – usually on the day of cell isolation – due to the rapid decrease in the endocytic activity of LSEC which starts already the day after cell isolation (63, 137, 149). To best of our knowledge, most of these studies used RPMI or DMEM for cell culture. These observations were consistent with some of our findings in this study – the endocytic activity of mouse LSEC incubated in RPMI significantly decreased in time.

A study conducted by Elvevold et al. (121) on pig LSEC revealed a decline in endocytosis of FSA over time in three different media. $^{125}$I-labeled endocytosis assay was assessed on days 2, 4, and 6 after isolation. The data obtained from RPMI media showed a higher level of endocytic activity day by day than the results obtained in this study. Elvevold et al. reported endocytic activity (compared to day 1) of 85%, 55%, and 34% on days 2, 4, and 6, respectively. In

contrast, the findings from this study using RPMI on mouse LSEC indicated a decrease to 25%, 36%, and 12,5% on days 3, 5, and 8 respectively. The data from relevant literature show that the endocytic activity in cell culture decreases more rapidly in small vertebrates (such as mice and rats) in comparison to large vertebrates (such as pigs, used by Elvevold et al.) (63, 82).

Elvevold reported higher endocytic activity in the new media developed to maintain pig LSEC functions compared with RPMI media. Similar results were obtained in this study by incubating mouse LSEC in EGM. The results from this study show that cells cultured in EGM maintained high endocytic activity (of radiolabelled FSA) via scavenger receptors in mouse LSEC for up to 11 days and detectable levels for at least 21 days (Figure 4.18).

Furthermore, Elvevold et al. (121) tested the endocytic activity by supplementing the media with selected growth factors. The addition of the EGF, which is also expected to be present in EGM, enhanced the pig LSEC endocytic activity on day 1 at the highest levels – 128% higher than the similar activity in cells incubated in the new media without supplementation of growth factors. They also showed that endocytosis via tabilin-1 and -2 in LSEC incubated in media supplemented with growth factors increased over time; it was higher on day 6 than on days 4 and 2.

These findings are consistent with the results from the present study where endocytosis of $^{125}$I-FSA of mouse LSEC decreased significantly on day 3 and day 5 (Figure 4.18) but, significantly increased on day 8 (to 95% compared with day 1) and remained almost stable also until day 11 (81% compared to day 1). Similar trends were observed with fluorescently-labeled FSA where the uptake appeared higher on day 8 (more fluorescent signal) than on day 5. Correlative analysis of the endocytosis data and cell numbers in cultures, suggests that the uptake of FSA per cell increased with time in culture, especially on day 8. These data should however be repeated with cell counts done in parallel with the endocytosis assay of the same experiment in the same well plate.

The uptake of RNase B which occurs via the mannose receptor in LSEC indicated a decline in mannose receptor-mediated endocytosis after day 3. Similar observations were reported in (121), and suggest a different effect of time in culture and medium supplements on different LSEC endocytosis receptors.

We also tested LSEC uptake of fluorescently-labelled AGG, which is a model ligand for Fc-gamma receptors IIb2. LSEC showed higher uptake of AGG on day 5 compared with day 1 and

day 3. A possible reason for that could be an increase in inflammatory responses in long-term cultures as reported in (67). Similar observations are obtained from fcgRIIb2 staining – a heterogenous expression of the Fc gamma receptor was observed on days 1 and 3, while homogenous expression was observed on days 5 and 8. High signals from Fc gamma receptor IIb2 staining indicate the high expression of this receptor and corresponds with the high uptake detected by the fluorescent microscopy results.

Since endocytosis of $^{125}$I-labeled FSA was approximately similar at day 8 compared to day 1, and the fluorescent labeled ligands showed that the majority of the cells had ability to endocytose, while many cells were defenestrated at day 8, these two important features of LSEC were differently affected in vitro. These suggestions were supported by (59) which showed no correlation between endocytosis and fenestrations.

# 6 Conclusion

The focus of this project was optimizing the condition for establishing a long-term culture of mouse primary LSEC while preserving their characteristics. The results showed preserved viability and prolonged survival of LSEC in cultures with EGM compared to RPMI. The cells maintained their endocytic functions for at least 11 days in EGM on plastic surfaces. However, LSEC cell density decreased, while the cell volume and area increased in time.

Changes in the LSEC morphology were also observed in prolonged cultures. The actin cytoskeleton developed more stress fibers with time in culture. In addition, the number of fenestrations gradually decreased while the fenestration size increased (tested up to day 8). Cytochalasin B was found to disrupt the stress fibers, as well as induced new fenestrations in a subset of cells.

After 8 days, LSEC maintained the receptor-mediated endocytosis of FSA, RNase and AGG which are ligands for stabilin-1 and stabilin-2, mannose receptor, and Fc gamma receptor IIb2, respectively. Furthermore, the $^{125}$I-labeled FSA endocytosis assay showed that LSEC could scavenge and degrade FSA for at least 11 days. LSEC retain endocytic activity for a longer time than maintain fenestrated morphology which suggests that these two important features of LSEC were differently affected in vitro.

In conclusion, EGM allows for the maintenance of mouse LSEC morphology and scavenging function in vitro for longer than previously reported. These optimized conditions yield implications for the field of sinusoidal cell biology and will allow for the application of previously inaccessible techniques.

EGM represented new knowledge about optimal conditions for long-term cultures of LSEC. It enables detailed examination of LSEC morphology, functions and responses in vitro. This yield implications for the biology field.

## 6.1 Future directions

There is no truly complete study and new questions always arise as a result of the research conducted. The findings of this study add new information to our understanding of how to improve mouse LSEC primary cultures; however, there are still some unanswered questions.

The next experiments could be carried out using a media with known composition to determine the optimal conditions for prolonging LSEC morphology and function in the culture.

Endocytic capacity parallel to endocytic activity of FSA and other ligands should be studied on different days. Changes in cell density should be taken into consideration to normalize endocytosis per single cell. Furthermore, repeating the receptor staining and potential protocol optimizations could be necessary.

Comparing cell volume results with cell density results suggested an increase in the cell volume of LSEC. Therefore, a detailed study of LSEC single-cell volume by quantitative phase microscopy or atomic force microscopy could be of interest.

Previous studies aimed to examine LSEC in long-term culture reported an increase in inflammatory cytokines in the cell culture. The findings of this study revealed that LSEC had better cell health and retained their functions for several days on plastic. However, plastic is not ideal for capturing high-quality microscopic images. In addition, capturing images at 40x magnification to show more details were difficult, and all the images taken of cells cultured on plastic surfaces were captured at 20x magnification, which resulted in blurred images when cropping them to show more details. Therefore, it is necessary to explore potential solutions for culturing LSEC on glass surfaces for the long term – some alternatives could be glass coating with APTES or plasma treatment.

# References


1. Abdel-Misih SR, Bloomston M. Liver anatomy. Surgical Clinics. 2010;90(4):643-53.
2. McCuskey R. Anatomy of the liver. Zakim and Boyer's Hepatology: a textbook of liver disease. 2012;6:3-19.
3. Vernon H, Wehrle CJ, Kasi A. Anatomy, Abdomen and Pelvis, Liver. StatPearls [Internet]: StatPearls Publishing; 2021.
4. Molina DK, DiMaio VJ. Normal organ weights in men: part II—the brain, lungs, liver, spleen, and kidneys. The American journal of forensic medicine and pathology. 2012;33(4):368-72.
5. Molina DK, DiMaio VJ. Normal organ weights in women: part II—the brain, lungs, liver, spleen, and kidneys. The American journal of forensic medicine and pathology. 2015;36(3):182-7.
6. Kuntz E. Hepatology Principles and Practice: History· Morphology Biochemistry· Diagnostics Clinic· Therapy: Springer; 2006.
7. Øie CI, Mönkemöller V, Hübner W, Schüttpelz M, Mao H, Ahluwalia BS, et al. New ways of looking at very small holes–using optical nanoscopy to visualize liver sinusoidal endothelial cell fenestrations. Nanophotonics. 2018;7(3):575-96.
8. Arias IM. The liver: biology and pathobiology. Clinical Nutrition Insight. 1988;14(11):5.
9. Bouwens L, De Bleser P, Vanderkerken K, Geerts B, Wisse E. Liver cell heterogeneity: functions of non-parenchymal cells. Enzyme. 1992;46:155-.
10. Hewitt NJ, Gómez Lechón MJ, Houston JB, Hallifax D, Brown HS, Maurel P, et al. Primary hepatocytes: current understanding of the regulation of metabolic enzymes and transporter proteins, and pharmaceutical practice for the use of hepatocytes in metabolism, enzyme induction, transporter, clearance, and hepatotoxicity studies. Drug metabolism reviews. 2007;39(1):159-234.
11. Knook D, Blansjaar N, Sleyster EC. Isolation and characterization of Kupffer and endothelial cells from the rat liver. Experimental cell research. 1977;109(2):317-29.
12. MacParland SA, Liu JC, Ma X-Z, Innes BT, Bartczak AM, Gage BK, et al. Single cell RNA sequencing of human liver reveals distinct intrahepatic macrophage populations. Nature communications. 2018;9(1):4383.
13. Du W, Wang L. The crosstalk between liver sinusoidal endothelial cells and hepatic microenvironment in NASH related liver fibrosis. Frontiers in Immunology. 2022:3340.
14. Blouin A, Bolender RP, Weibel ER. Distribution of organelles and membranes between hepatocytes and nonhepatocytes in the rat liver parenchyma. A stereological study. The Journal of cell biology. 1977;72(2):441-55.
15. PERTOFT H, SMEDSRØD B. Separation and characterization of liver cells. Cell separation: Elsevier; 1987. p. 1-24.
16. Butola A, Coucheron DA, Szafranska K, Ahmad A, Mao H, Tinguely J-C, et al. Multimodal on-chip nanoscopy and quantitative phase imaging reveals the nanoscale morphology of liver sinusoidal endothelial cells. Proceedings of the National Academy of Sciences. 2021;118(47):e2115323118.
17. Sørensen KK, Simon‐Santamaria J, McCuskey RS, Smedsrød B. Liver sinusoidal endothelial cells. Comprehensive Physiology. 2011;5(4):1751-74.

18. Friedman SL. Hepatic stellate cells: protean, multifunctional, and enigmatic cells of the liver. Physiological reviews. 2008;88(1):125-72.
19. Marrone G, Shah VH, Gracia-Sancho J. Sinusoidal communication in liver fibrosis and regeneration. Journal of hepatology. 2016;65(3):608-17.
20. Bilzer M, Roggel F, Gerbes AL. Role of Kupffer cells in host defense and liver disease. Liver International. 2006;26(10):1175-86.
21. Dudek M, Lohr K, Donakonda S, Baumann T, Lüdemann M, Hegenbarth S, et al. IL-6-induced FOXO1 activity determines the dynamics of metabolism in CD8 T cells cross-primed by liver sinusoidal endothelial cells. Cell Reports. 2022;38(7):110389.
22. Bonnardel J, T'Jonck W, Gaublomme D, Browaeys R, Scott CL, Martens L, et al. Stellate cells, hepatocytes, and endothelial cells imprint the Kupffer cell identity on monocytes colonizing the liver macrophage niche. Immunity. 2019;51(4):638-54. e9.
23. Seternes T, Sørensen K, Smedsrød B. Scavenger endothelial cells of vertebrates: a nonperipheral leukocyte system for high-capacity elimination of waste macromolecules. Proceedings of the National Academy of Sciences. 2002;99(11):7594-7.
24. Smedsrød B, editor Clearance function of scavenger endothelial cells. Comparative hepatology; 2004: BioMed Central.
25. Smedsrød B, Pertoft H, Gustafson S, Laurent T. Scavenger functions of the liver endothelial cell. Biochemical journal. 1990;266(2):313.
26. Bhandari S, Larsen AK, McCourt P, Smedsrød B, Sørensen KK. The scavenger function of liver sinusoidal endothelial cells in health and disease. Frontiers in Physiology. 2021:1711.
27. Mahadevan V. Anatomy of the liver. Surgery (Oxford). 2020;38(8):427-31.
28. Blumgart LH, Belghiti J. Surgery of the liver, biliary tract, and pancreas: Saunders Elsevier Philadelphia; 2007.
29. Mccuskey RS. The hepatic microvascular system in health and its response to toxicants. The Anatomical Record: Advances in Integrative Anatomy and Evolutionary Biology: Advances in Integrative Anatomy and Evolutionary Biology. 2008;291(6):661-71.
30. Martinez I, Nedredal GI, Øie CI, Warren A, Johansen O, Le Couteur DG, et al. The influence of oxygen tension on the structure and function of isolated liver sinusoidal endothelial cells. Comparative hepatology. 2008;7:1-11.
31. Sørensen KK, McCourt P, Berg T, Crossley C, Couteur DL, Wake K, et al. The scavenger endothelial cell: a new player in homeostasis and immunity. American Journal of Physiology-Regulatory, Integrative and Comparative Physiology. 2012;303(12):R1217-R30.
32. Geraud C, Evdokimov K, Straub BK, Peitsch WK, Demory A, Dörflinger Y, et al. Unique cell type-specific junctional complexes in vascular endothelium of human and rat liver sinusoids. PloS one. 2012;7(4):e34206.
33. Wisse E. An electron microscopic study of the fenestrated endothelial lining of rat liver sinusoids. Journal of ultrastructure research. 1970;31(1-2):125-50.
34. Szafranska K, Kruse LD, Holte CF, McCourt P, Zapotoczny B. The wHole story about fenestrations in LSEC. Frontiers in physiology. 2021;12:735573.
35. Braet F, Wisse E. Structural and functional aspects of liver sinusoidal endothelial cell fenestrae: a review. Comparative hepatology. 2002;1(1):1-17.
36. Wisse E, De Zanger R, Charels K, Van Der Smissen P, McCuskey R. The liver sieve: considerations concerning the structure and function of endothelial fenestrae, the sinusoidal wall and the space of Disse. Hepatology. 1985;5(4):683-92.
37. Cogger VC, McNerney GP, Nyunt T, DeLeve LD, McCourt P, Smedsrød B, et al. Three-dimensional structured illumination microscopy of liver sinusoidal endothelial cell fenestrations. Journal of structural biology. 2010;171(3):382-8.

38. Henriksen JH, Horn T, Christoffersen P. The blood‐lymph barrier in the liver. A review based on morphological and functional concepts of normal and cirrhotic liver. Liver. 1984;4(4):221-32.
39. Warren A, Le Couteur DG, Fraser R, Bowen DG, McCaughan GW, Bertolino P. T lymphocytes interact with hepatocytes through fenestrations in murine liver sinusoidal endothelial cells. Hepatology. 2006;44(5):1182-90.
40. Naito M, Wisse E. Filtration effect of endothelial fenestrations on chylomicron transport in neonatal rat liver sinusoids. Cell and tissue research. 1978;190:371-82.
41. Zapotoczny B, Szafranska K, Owczarczyk K, Kus E, Chlopicki S, Szymonski M. Atomic force microscopy reveals the dynamic morphology of fenestrations in live liver sinusoidal endothelial cells. Scientific Reports. 2017;7(1):7994.
42. Vidal-Vanaclocha F, Barbera E. Fenestration patterns in endothelial cells of rat liver sinusoids. Journal of ultrastructure research. 1985;90(2):115-23.
43. Fraser R, Bowler L, Day W, Dobbs B, Johnson H, Lee D. High perfusion pressure damages the sieving ability of sinusoidal endothelium in rat livers. British journal of experimental pathology. 1980;61(2):222.
44. Braet F, ZANGER RD, Crabbe E, WISSE E. New observations on cytoskeleton and fenestrae in isolated rat liver sinusoidal endothelial cells. Journal of Gastroenterology and Hepatology. 1995;10(S1):S3-S7.
45. Mönkemöller V, Øie C, Hübner W, Huser T, McCourt P. Multimodal super-resolution optical microscopy visualizes the close connection between membrane and the cytoskeleton in liver sinusoidal endothelial cell fenestrations. Scientific reports. 2015;5(1):16279.
46. Alberts B, Johnson A, Lewis J, Raff M, Roberts K, Walter P. The cytoskeleton and cell behavior. Molecular Biology of the Cell 4th edition: Garland science; 2002.
47. Braet F, Soon L, Vekemans K, Thordarson P, Spector I. Actin-binding drugs: An elegant tool to dissect subcellular processes in endothelial and cancer cells. Actin-binding proteins and disease. 2008:37-49.
48. Di Martino J, Mascalchi P, Legros P, Lacomme S, Gontier E, Bioulac‐Sage P, et al. Actin depolymerization in dedifferentiated liver sinusoidal endothelial cells promotes fenestrae re‐formation. Hepatology Communications. 2019;3(2):213-9.
49. Li R, Oteiza A, Sørensen KK, McCourt P, Olsen R, Smedsrød B, et al. Role of liver sinusoidal endothelial cells and stabilins in elimination of oxidized low-density lipoproteins. American Journal of Physiology-Gastrointestinal and Liver Physiology. 2011;300(1):G71-G81.
50. Oteiza A, Li R, McCuskey RS, Smedsrød B, Sørensen KK. Effects of oxidized low-density lipoproteins on the hepatic microvasculature. American Journal of Physiology-Gastrointestinal and Liver Physiology. 2011;301(4):G684-G93.
51. Smedsrød B, Pertoft H, Eriksson S, Fraser J, Laurent T. Studies in vitro on the uptake and degradation of sodium hyaluronate in rat liver endothelial cells. Biochemical Journal. 1984;223(3):617-26.
52. Melkko J, Hellevik T, Risteli L, Risteli J, Smedsrød B. Clearance of NH2-terminal propeptides of types I and III procollagen is a physiological function of the scavenger receptor in liver endothelial cells. The Journal of experimental medicine. 1994;179(2):405-12.
53. Crispe IN, Giannandrea M, Klein I, John B, Sampson B, Wuensch S. Cellular and molecular mechanisms of liver tolerance. Immunological reviews. 2006;213(1):101-18.
54. Knolle PA, Gerken G. Local control of the immune response in the liver. Immunological reviews. 2000;174(1):21-34.

55. Øie CI, Wolfson DL, Yasunori T, Dumitriu G, Sørensen KK, McCourt PA, et al. Liver sinusoidal endothelial cells contribute to the uptake and degradation of entero bacterial viruses. Scientific Reports. 2020;10(1):898.
56. Simon-Santamaria J, Rinaldo CH, Kardas P, Li R, Malovic I, Elvevold K, et al. Efficient uptake of blood-borne BK and JC polyomavirus-like particles in endothelial cells of liver sinusoids and renal vasa recta. PLoS One. 2014;9(11):e111762.
57. Ganesan LP, Mohanty S, Kim J, Clark KR, Robinson JM, Anderson CL. Rapid and efficient clearance of blood-borne virus by liver sinusoidal endothelium. PLoS pathogens. 2011;7(9):e1002281.
58. Mates JM, Yao Z, Cheplowitz AM, Suer O, Phillips GS, Kwiek JJ, et al. Mouse liver sinusoidal endothelium eliminates HIV-like particles from blood at a rate of 100 million per minute by a second-order kinetic process. Frontiers in immunology. 2017;8:35.
59. Simon-Santamaria J, Malovic I, Warren A, Oteiza A, Le Couteur D, Smedsrød B, et al. Age-related changes in scavenger receptor–mediated endocytosis in rat liver sinusoidal endothelial cells. Journals of Gerontology Series A: Biomedical Sciences and Medical Sciences. 2010;65(9):951-60.
60. Pandey E, Nour AS, Harris EN. Prominent receptors of liver sinusoidal endothelial cells in liver homeostasis and disease. Frontiers in Physiology. 2020;11:873.
61. PrabhuDas M, Bowdish D, Drickamer K, Febbraio M, Herz J, Kobzik L, et al. Standardizing scavenger receptor nomenclature. The Journal of Immunology. 2014;192(5):1997-2006.
62. Politz O, Gratchev A, McCOURT PA, Schledzewski K, Guillot P, Johansson S, et al. Stabilin-1 and− 2 constitute a novel family of fasciclin-like hyaluronan receptor homologues. Biochemical Journal. 2002;362(1):155-64.
63. Elvevold KH, Nedredal GI, Revhaug A, Smedsrød B. Scavenger properties of cultivated pig liver endothelial cells. Comparative hepatology. 2004;3(1):1-11.
64. Araki N, Higashi T, Mori T, Shibayama R, Kawabe Y, Kodama T, et al. Macrophage scavenger receptor mediates the endocytic uptake and degradation of advanced glycation end products of the Maillard reaction. European journal of biochemistry. 1995;230(2):408-15.
65. Blomhoff R, Eskild W, Berg T. Endocytosis of formaldehyde-treated serum albumin via scavenger pathway in liver endothelial cells. Biochemical Journal. 1984;218(1):81-6.
66. Eskild W, Smedsrød B, Berg T. Receptor mediated endocytosis of formaldehyde treated albumin, yeast invertase and chondroitin sulfate in suspensions of rat liver endothelial cells. The International journal of biochemistry. 1986;18(7):647-51.
67. Bhandari S, Li R, Simón-Santamaría J, McCourt P, Johansen SD, Smedsrød B, et al. Transcriptome and proteome profiling reveal complementary scavenger and immune features of rat liver sinusoidal endothelial cells and liver macrophages. BMC Molecular and Cell Biology. 2020;21(1):1-25.
68. Magnusson S, Berg T. Extremely rapid endocytosis mediated by the mannose receptor of sinusoidal endothelial rat liver cells. Biochemical Journal. 1989;257(3):651-6.
69. Linehan SA, Weber R, McKercher S, Ripley RM, Gordon S, Martin P. Enhanced expression of the mannose receptor by endothelial cells of the liver and spleen microvascular beds in the macrophage-deficient PU. 1 null mouse. Histochemistry and cell biology. 2005;123:365-76.
70. Martens JH, Kzhyshkowska J, Falkowski‐Hansen M, Schledzewski K, Gratchev A, Mansmann U, et al. Differential expression of a gene signature for scavenger/lectin receptors by endothelial cells and macrophages in human lymph node sinuses, the primary sites of regional metastasis. The Journal of Pathology: A Journal of the Pathological Society of Great Britain and Ireland. 2006;208(4):574-89.

71. Ezekowitz R, Sastry K, Bailly P, Warner A. Molecular characterization of the human macrophage mannose receptor: demonstration of multiple carbohydrate recognition-like domains and phagocytosis of yeasts in Cos-1 cells. The Journal of experimental medicine. 1990;172(6):1785-94.
72. Elvevold K, Simon‐Santamaria J, Hasvold H, McCourt P, Smedsrød B, Sørensen KK. Liver sinusoidal endothelial cells depend on mannose receptor‐mediated recruitment of lysosomal enzymes for normal degradation capacity. Hepatology. 2008;48(6):2007-15.
73. de Haan W, Øie C, Benkheil M, Dheedene W, Vinckier S, Coppiello G, et al. Unraveling the transcriptional determinants of liver sinusoidal endothelial cell specialization. American Journal of Physiology-Gastrointestinal and Liver Physiology. 2020;318(4):G803-G15.
74. Smedsrød B, Melkko J, Risteli L, Risteli J. Circulating C-terminal propeptide of type I procollagen is cleared mainly via the mannose receptor in liver endothelial cells. Biochemical Journal. 1990;271(2):345-50.
75. Smedsrød B, Johansson S, Pertoft H. Studies in vivo and in vitro on the uptake and degradation of soluble collagen α1 (I) chains in rat liver endothelial and Kupffer cells. Biochemical Journal. 1985;228(2):415-24.
76. Smedsrød B, Einarsson M, Pertoft H. Tissue plasminogen activator is endocytosed by mannose and galactose receptors of rat liver cells. Thrombosis and haemostasis. 1988;59(03):480-4.
77. Mousavi SA, Sporstøl M, Fladeby C, Kjeken R, Barois N, Berg T. Receptor‐mediated endocytosis of immune complexes in rat liver sinusoidal endothelial cells is mediated by Fc $\gamma$ RIIb2. Hepatology. 2007;46(3):871-84.
78. Lovdal T, Brech A, Kjeken R, Smedsrod B, Berg T. Receptor-mediated and fluid phase endocytosis in hepatic sinusoidal cells. Cells of the Hepatic Sinusoid. 2001;8:125-31.
79. Ganesan LP, Kim J, Wu Y, Mohanty S, Phillips GS, Birmingham DJ, et al. FcγRIIb on liver sinusoidal endothelium clears small immune complexes. The Journal of Immunology. 2012;189(10):4981-8.
80. Roghanian A, Stopforth RJ, Dahal LN, Cragg MS. New revelations from an old receptor: immunoregulatory functions of the inhibitory Fc gamma receptor, FcγRIIB (CD32B). Journal of leukocyte biology. 2018;103(6):1077-88.
81. Strauss O, Phillips A, Ruggiero K, Bartlett A, Dunbar P. Immunofluorescence identifies distinct subsets of endothelial cells in the human liver. Scientific reports. 2017;7(1):1-13.
82. Elvevold K, Smedsrød B, Martinez I. The liver sinusoidal endothelial cell: a cell type of controversial and confusing identity. American Journal of Physiology-Gastrointestinal and Liver Physiology. 2008;294(2):G391-G400.
83. Huebert RC, Jagavelu K, Liebl AF, Huang BQ, Splinter PL, LaRusso NF, et al. Immortalized liver endothelial cells: a cell culture model for studies of motility and angiogenesis. Laboratory investigation. 2010;90(12):1770-81.
84. Parent R, Durantel D, Lahlali T, Sallé A, Plissonnier M-L, DaCosta D, et al. An immortalized human liver endothelial sinusoidal cell line for the study of the pathobiology of the liver endothelium. Biochemical and biophysical research communications. 2014;450(1):7-12.
85. Poisson J, Lemoinne S, Boulanger C, Durand F, Moreau R, Valla D, et al. Liver sinusoidal endothelial cells: Physiology and role in liver diseases. Journal of hepatology. 2017;66(1):212-27.

86. Le Couteur DG, Fraser R, Cogger VC, McLean AJ. Hepatic pseudocapillarisation and atherosclerosis in ageing. The Lancet. 2002;359(9317):1612-5.
87. Le Couteur DG, Warren A, Cogger VC, Smedsrød B, Sørensen KK, De Cabo R, et al. Old age and the hepatic sinusoid. The Anatomical Record: Advances in Integrative Anatomy and Evolutionary Biology: Advances in Integrative Anatomy and Evolutionary Biology. 2008;291(6):672-83.
88. Le Couteur DG, Cogger VC, McCUSKEY RS, De Cabo R, Smedsrød B, Sorensen KK, et al. Age‐related changes in the liver sinusoidal endothelium: A mechanism for dyslipidemia. Annals of the New York Academy of Sciences. 2007;1114(1):79-87.
89. McLean AJ, Cogger VC, Chong GC, Warren A, Markus AM, Dahlstrom JE, et al. Age‐related pseudocapillarization of the human liver. The Journal of Pathology: A Journal of the Pathological Society of Great Britain and Ireland. 2003;200(1):112-7.
90. Ito Y, Sørensen KK, Bethea NW, Svistounov D, McCuskey MK, Smedsrød BH, et al. Age-related changes in the hepatic microcirculation in mice. Experimental gerontology. 2007;42(8):789-97.
91. Muro H, Shirasawa H, Kosugi I, Ito I. Defect of sinusoidal Fc receptors and immune complex uptake in CCl4-induced liver cirrhosis in rats. Gastroenterology. 1990;99(1):200-10.
92. Muro H, Shirasawa H, Kosugi I, Nakamura S. Defect of Fc receptors and phenotypical changes in sinusoidal endothelial cells in human liver cirrhosis. The American journal of pathology. 1993;143(1):105.
93. Hattori T, Konno S, Takahashi A, Isada A, Shimizu K, Shimizu K, et al. Genetic variants in mannose receptor gene (MRC1) confer susceptibility to increased risk of sarcoidosis. BMC medical genetics. 2010;11(1):1-6.
94. Hattori T, Konno S, Hizawa N, Isada A, Takahashi A, Shimizu K, et al. Genetic variants in the mannose receptor gene (MRC1) are associated with asthma in two independent populations. Immunogenetics. 2009;61:731-8.
95. March S, Hui EE, Underhill GH, Khetani S, Bhatia SN. Microenvironmental regulation of the sinusoidal endothelial cell phenotype in vitro. Hepatology. 2009;50(3):920-8.
96. Ruska E. Die elektronenmikroskopische abbildung elektronenbestrahlter oberflächen. Zeitschrift für Physik. 1933;83(7-8):492-7.
97. Knoll M. Aufladepotentiel und sekundäremission elektronenbestrahlter körper. Z techn Phys. 1935;16:467.
98. Bell LS. Forensic Microscopy for Skeletal Tissues: Methods and Protocols: Springer; 2012.
99. Mohammed A, Abdullah A, editors. Scanning electron microscopy (SEM): A review. Proceedings of the 2018 International Conference on Hydraulics and Pneumatics—HERVEX, Băile Govora, Romania; 2018.
100. Masters BR. History of the optical microscope in cell biology and medicine. eLS. 2008.
101. Lichtman JW, Conchello J-A. Fluorescence microscopy. Nature methods. 2005;2(12):910-9.
102. Chebib J, Jackson BC, López-Cortegano E, Tautz D, Keightley PD. Inbred lab mice are not isogenic: genetic variation within inbred strains used to infer the mutation rate per nucleotide site. Heredity. 2021;126(1):107-16.
103. Casellas J. Inbred mouse strains and genetic stability: a review. animal. 2011;5(1):1-7.
104. Elvevold K, Kyrrestad I, Smedsrød B. Protocol for Isolation and Culture of Mouse Hepatocytes (HCs), Kupffer Cells (KCs), and Liver Sinusoidal Endothelial Cells (LSECs) in

Analyses of Hepatic Drug Distribution. Antisense RNA Design, Delivery, and Analysis: Springer US New York, NY; 2022. p. 385-402.
105. Green CJ, Charlton CA, Wang L-M, Silva M, Morten KJ, Hodson L. The isolation of primary hepatocytes from human tissue: optimising the use of small non-encapsulated liver resection surplus. Cell and Tissue Banking. 2017;18(4):597-604.
106. Krause P, Markus PM, Schwartz P, Unthan-Fechner K, Pestel S, Fandrey J, et al. Hepatocyte-supported serum-free culture of rat liver sinusoidal endothelial cells. Journal of hepatology. 2000;32(5):718-26.
107. Hansen B, Melkko J, Smedsrød B. Serum is a rich source of ligands for the scavenger receptor of hepatic sinusoidal endothelial cells. Molecular and cellular biochemistry. 2002;229:63-72.
108. Zhang Y, He Y, Bharadwaj S, Hammam N, Carnagey K, Myers R, et al. Tissue-specific extracellular matrix coatings for the promotion of cell proliferation and maintenance of cell phenotype. Biomaterials. 2009;30(23-24):4021-8.
109. LDH-Glo™ Cytotoxicity Assay Internet: Promega; [Available from:
110. McDowell EM, Trump B. Histologic fixatives suitable for diagnostic light and electron microscopy. Archives of pathology & laboratory medicine. 1976;100(8):405-14.
111. Braet F, De Zanger R, Wisse E. Drying cells for SEM, AFM and TEM by hexamethyldisilazane: a study on hepatic endothelial cells. Journal of microscopy. 1997;186(1):84-7.
112. Markwell MAK. A new solid-state reagent to iodinate proteins: I. Conditions for the efficient labeling of antiserum. Analytical biochemistry. 1982;125(2):427-32.
113. Braet F, De Zanger R, Kalle W, Raap A, Tanke H, Wisse E. Comparative scanning, transmission and atomic force microscopy of the microtubular cytoskeleton in fenestrated liver endothelial cells. Scanning Microscopy. 1995;1996(10):18.
114. Schindelin J, Arganda-Carreras I, Frise E, Kaynig V, Longair M, Pietzsch T, et al. Fiji: an open-source platform for biological-image analysis. Nature methods. 2012;9(7):676-82.
115. Steffan AM, Gendrault JL, Kirn A. Increase in the number of fenestrae in mouse endothelial liver cells by altering the cytoskeleton with cytochalasin B. Hepatology. 1987;7(6):1230-8.
116. Fraser R, Cogger VC, Dobbs B, Jamieson H, Warren A, Hilmir SN, et al. The liver sieve and atherosclerosis. Pathology. 2012;44(3):181-6.
117. OHATA M, TANUMA Y, ITO T. A transmission electron microscopic study on sinusoidal cells of guinea pig liver, with special reference to the occurrence of a canalicular system and “pored domes” in the endothelium. Archivum histologicum japonicum. 1984;47(4):359-76.
118. Snoeys J, Lievens J, Wisse E, Jacobs F, Duimel H, Collen D, et al. Species differences in transgene DNA uptake in hepatocytes after adenoviral transfer correlate with the size of endothelial fenestrae. Gene therapy. 2007;14(7):604-12.
119. Simon 3 EBIBEGNKAMERAGSGSAU-VAW, 5 RGiBIAJFGRPG, 6 BAP, 7 NCfBIARCDMHWMDRSV, 8 DoMAMPL, 9 DoMGASEDETRAUC, et al. Initial sequencing and comparative analysis of the mouse genome. Nature. 2002;420(6915):520-62.
120. Horn T, Christoffersen P, Henriksen JH. Alcoholic liver injury: defenestration in noncirrhotic livers—a scanning electron microscopic study. Hepatology. 1987;7(1):77-82.
121. Elvevold K, Nedredal GI, Revhaug A, Bertheussen K, Smedsrød B. Long-term preservation of high endocytic activity in primary cultures of pig liver sinusoidal endothelial cells. European journal of cell biology. 2005;84(9):749-64.
122. Cogger VC, Arias IM, Warren A, McMahon AC, Kiss DL, Avery VM, et al. The response of fenestrations, actin, and caveolin-1 to vascular endothelial growth factor in SK

Hep1 cells. American Journal of Physiology-Gastrointestinal and Liver Physiology. 2008;295(1):G137-G45.
123. Matsumura T, Takesue M, Westerman KA, Okitsu T, Sakaguchi M, Fukazawa T, et al. Establishment of an immortalized human-liver endothelial cell line with SV40T and hTERT. Transplantation. 2004;77(9):1357-65.
124. Zhao X, Zhao Q, Luo Z, Yu Y, Xiao N, Sun X, et al. Spontaneous immortalization of mouse liver sinusoidal endothelial cells. International journal of molecular medicine. 2015;35(3):617-24.
125. Helmy KY, Katschke KJ, Gorgani NN, Kljavin NM, Elliott JM, Diehl L, et al. CRIg: a macrophage complement receptor required for phagocytosis of circulating pathogens. Cell. 2006;124(5):915-27.
126. Morini S, Carotti S, Carpino G, Franchitto A, Corradini SG, Merli M, et al. GFAP expression in the liver as an early marker of stellate cells activation. Italian Journal of Anatomy and Embryology= Archivio Italiano Di Anatomia Ed Embriologia. 2005;110(4):193-207.
127. Shang L, Hosseini M, Liu X, Kisseleva T, Brenner DA. Human hepatic stellate cell isolation and characterization. Journal of gastroenterology. 2018;53:6-17.
128. Gard AL, White FP, Dutton GR. Extra-neural glial fibrillary acidic protein (GFAP) immunoreactivity in perisinusoidal stellate cells of rat liver. Journal of neuroimmunology. 1985;8:359-75.
129. Larsen AK, Simón-Santamaría J, Elvevold K, Ericzon BG, Mortensen KE, McCourt P, et al. Autofluorescence in freshly isolated adult human liver sinusoidal cells. European Journal of Histochemistry: EJH. 2021;65(4).
130. Donkey anti-Rat IgG (H+L) Cross-Adsorbed Secondary Antibody, DyLight™ 488 Internet: ThermoFisher; [Available from:
131. Szafranska K, Neuman T, Baster Z, Rajfur Z, Szelest O, Holte C, et al. From fixed-dried to wet-fixed to live–comparative super-resolution microscopy of liver sinusoidal endothelial cell fenestrations. Nanophotonics. 2022;11(10):2253-70.
132. Braet F, Wisse E. AFM imaging of fenestrated liver sinusoidal endothelial cells. Micron. 2012;43(12):1252-8.
133. Hayat M. Fixation for electron microscopy: Elsevier; 2012.
134. Composition of RPMI 1640 w/ L-Glutamine Internet: EuroClone; [Available from:
135. DeLeve LD, Wang X, Hu L, McCuskey MK, McCuskey RS. Rat liver sinusoidal endothelial cell phenotype is maintained by paracrine and autocrine regulation. American Journal of Physiology-Gastrointestinal and Liver Physiology. 2004;287(4):G757-G63.
136. EGM™ Endothelial Cell Growth Medium BulletKit™ Internet: Lonza; [Available from:
137. Li R, Bhandari S, Martinez-Zubiaurre I, Bruun J-A, Urbarova I, Smedsrød B, et al. Changes in the proteome and secretome of rat liver sinusoidal endothelial cells during early primary culture and effects of dexamethasone. Plos one. 2022;17(9):e0273843.
138. Huber B, Czaja AM, Kluger PJ. Influence of epidermal growth factor (EGF) and hydrocortisone on the co‐culture of mature adipocytes and endothelial cells for vascularized adipose tissue engineering. Cell biology international. 2016;40(5):569-78.
139. De Zanger R, Braet, F., Arnez Camacho, M.R. and Wisse, E. Prolongation of hepatic endothelial cell cultures by phorbol myristate acetate. 1997.
140. Braet F, Wisse E, Probst I. The long-term culture of pig liver sinusoidal endothelial cells: the Holy Grail found. European journal of cell biology. 2005;84(9):745-8.
141. DeLeve LD, Maretti-Mira AC, editors. Liver sinusoidal endothelial cell: an update. Seminars in liver disease; 2017: Thieme Medical Publishers.

142. Mori T, Okanoue T, Sawa Y, Hori N, Ohta M, Kagawa K. Defenestration of the sinusoidal endothelial cell in a rat model of cirrhosis. Hepatology. 1993;17(5):891-7.
143. Mak KM, Lieber CS. Alterations in endothelial fenestrations in liver sinusoids of baboons fed alcohol: a scanning electron microscopic study. Hepatology. 1984;4(3):386-91.
144. Fraser R, Bowler L, Day W. Damage of rat liver sinusoidal endothelium by ethanol. Pathology. 1980;12(3):371-6.
145. Le Couteur DG, Fraser R, Kilmer S, Rivory LP, McLean AJ. The hepatic sinusoid in aging and cirrhosis: effects on hepatic substrate disposition and drug clearance. Clinical pharmacokinetics. 2005;44:187-200.
146. Le Couteur DG, Cogger VC, Markus AM, Harvey PJ, Yin Z-L, Ansselin AD, et al. Pseudocapillarization and associated energy limitation in the aged rat liver. Hepatology. 2001;33(3):537-43.
147. Braet F, de Zanger R, Seynaeve C, Baekeland M, Wisse E. A comparative atomic force microscopy study on living skin fibroblasts and liver endothelial cells. Microscopy. 2001;50(4):283-90.
148. Cytochalasin B Ready Made Solution from Drechslera dematioidea Internet: Sigma; [Available from:
149. Braet F, De Zanger R, Sasaoki T, Baekeland M, Janssens P, Smedsrød B, et al. Assessment of a method of isolation, purification, and cultivation of rat liver sinusoidal endothelial cells. Laboratory investigation; a journal of technical methods and pathology. 1994;70(6):944-52.

# Appendix

Appendix A - MaterialsIn this section I present the main materials used in different protocols.

## List of the materials

**Compounds used in Endocytosis essay**

| Compounds | Supplier | Catalog number |
|---|---|---|
| Albumin- Alburex | CSL Behring GmBH | 078216 |
| Bovine serum albumin (BSA) | VWR | 0332-100G |
| Iodine-125 Radionuclide | PerkinElmer | NEZ033A005MC |
| PBS | Meck | D8662-500ML |
| SDS (1% solution) | ThermoFisher | AM9823 |
| Trichloroacetic acid (TCA) | Merck | 8223420250 |

**Perfusion buffers used in mouse liver perfusion**

| Compounds | Supplier | Catalog number |
|---|---|---|
| Bovine serum albumin fraction V | Sigma-Aldrich | 10735086001 |
| CaCl2x2H2O | Sigma-Aldrich | C7902 |
| HEPES | Sigma-Aldrich | H3375 |
| Human Fibronectin protein, CF | Biotech Brand/R&D systems | 1918-FN-02M |
| Kaliumklorid (KCl) | Sigma-Aldrich | 529552 |
| Liberase enzyme | Roche | 5401127001 |
| Natriumhydroksid (NaOH) | Sigma-Aldrich | S5881 |
| Natriumklorid (NaCl) | Sigma-Aldrich | S9888 |

**Compounds used in LSEC extraction with MACS-beads (mouse)**

| Compounds | Supplier | Catalog number |
|---|---|---|
| autoMACS® Rinsing Solution | Miltenyi Biotec | 130-091-222 |
| CD146 (LSEC) MicroBeads mouse | Miltenyi Biotec | 130-092-007 |
| MACS BSA Stock Solution | Miltenyi Biotec | 130-091-376 |

**Compounds used in preparation of samples for light microscopy**

| Compounds | Supplier | Catalog number |
|---|---|---|
| Alexa Fluor™ 555 Phalloidin | Thermofisher | A34055 |
| Anti-α Tubulin Antibody (B-5-1-2) Alexa Fluor® 647 | SantaCruz | sc-23948 AF647 |
| Cytochalasin B,Ready Made Solution, 10 mg/mL in DMSO | Sigma-Aldrich | C2743-200UL |
| DAPI (6-diamidino-2-phenylindole) | Sigma-Aldrich | D8417 |
| PBS | Meck | D8662-500ML |
| Prolong glass antifade mountant | Thermofisher | P36982 |
| Triton X-100 | Sigma-Aldrich | X100 |
| Vectashield Antifade mounting media | Vector labratories | H-1400 |

**Compounds used in media**

| Compounds | Supplier | Catalog number |
|---|---|---|
| Endothelial Cell Growth Medium (EGM) | Ceu Applications lnc. | 211-500 |
| RPMI 1640 with L-Glutamine | EuroClone | ECB2000L |

**Compounds used in fluorescent labeling of FSA**

| Compounds | Supplier | Catalog number |
|---|---|---|
| Alexa fluor 647 carboxylic acid | Intrivogen | A20006 |
| Thermo Scientific Slide-A-Lyzer Dialysis Cassettes | MWCO | 66330 |

## Buffers and reagents prepared at VBRG

**PHEM buffer (4x concentrate)**: Add 36.24 g PIPES to 225 mL sterile Milli-Q. Raise the pH to 6.9 with 5 M NaOH and add 13 g HEPES, 7.6 g EGTA, and 1.98 g $MgSO_4$. PH is adjucted to 7.0 with 10 M KOH. To a final volume who is 500 mL, add sterile Milli-Q to it. PHEM-buffer prepared by Randi at KAM.

**Tris-buffered saline**: 0.05 M Tris, 0.1 M NaCl, pH 7.4.

# Appendix B - Protocols

## Protocol 1: LSEC extraction with MACS-beads (mouse)

After primary cell extraction from mice, cells come in 50 mL transport buffer

1. Centrifuge 35g (400 rpm) for 2 min at 4°C (acceleration/deceleration max)
2. Collect supernatant by pouring out/pipette à to get rid of hepatocytes
3. Centrifuge 35 g (400 rpm) for 2 min at 4°C (acceleration/deceleration max)
4. Collect supernatant by pouring out/pipette à fewer hepatocytes
5. Centrifuge 35 g (400 rpm) for 2 min at 4°C (acceleration/deceleration max). If the pellet is very, very small à step 6. But if the pellet is still big à one more centrifugation
6. Gently collect supernatant with a pipette into new tubes

è Buffer with 1% BSA (can use either MACS buffer or perfusion buffer) can be added for the centrifugation step - counterweight

7. Centrifuge 300 g for 10 min at 4°C (acceleration/deceleration max)
8. Take off the supernatant (magic sucker) and resuspend the pellet in 1 mL MACS buffer

MACS buffer = 2.5 mL BSA + 47,5 ml rinsing solution buffer – 1:20 dilution

Remember – we have 20% BSA, not 100% - we make 1% BSA solution from 20% BSA!

9. Transfer the resuspended pellet to Eppendorf tubes
10. Take another 1 mL MACS buffer and wash the falcon tube and transfer it to the Eppendorf tube.
11. Centrifuge 300 g for 8 min at 4°C (small centrifuge, cold room)
12. Discard supernatant
13. Resuspend pellet in 150 µL of MACS buffer
14. Add 15 µL of CD146 beads
15. Incubate for 25 minutes in the cold room on the "rotating device"
16. Add MACS up to 1 – 1,5 mL solution – fill up the Eppendorf tube
17. Centrifuge 300 g for 8 min at 4°C (small centrifuge, cold room)
18. while waiting – prepare the magnetic stand, holder, columns, and MACS purple filter
19. Put the column and filter in the magnetics holder and rinse with MACS buffer 1 mL
20. Centrifugation – step 17 – is done à discard supernatant and resuspend the pellet in 1 mL of MACS buffer
21. Add cell suspension into the column/filter
22. Wash the column 3 times with MACS buffer 1 mL – wait 5 min before the next wash
23. Remove the column from the magnetic holder

24. Pipette 1 mL MACS buffer onto the column and immediately flush out the magnetically labeled cells by firmly pushing the plunger into the column
25. Count LSECs – cells are in 2 mL now
26. Centrifuge 300 g for 8 min at 4°C
27. Seed cells on well plates or coverslips

Counting cells
Using the Burker counting method

Seeding cells – SEM and fluorescent microscopy
1. Write down the volume for each sample – we need it when we calculate the number of cells in the total volume.
2. take 10 µL of the cell suspension to cell counting
3. Centrifuge the cell suspension – 7 min
4. Count the cells
5. After centrifugation – add 1 mL of RPMI media (without serum) to the pellet and resuspend
6. Add 1 mL media for each 1 million cells – 7 million cells --> adding 7 mL media in total to the cells
Use RPMI media – even if the cells will be incubated in EGM media later.
7. Seed cells – seeding cells in the well plates or on coverslips
Well plates used
8. Incubate the cells for 1 h
9. Use the microscope to see if the cells have attached
10. If the cells look good and have attached, then remove media and add EGM or new RPMI
11. Incubate cells – incubate Day 1 cells for 2 h before fixing

## Protocol 2: Preparation of samples for light microscopy

1. 3x wash with PBS
2. Add 400 µL 0.05% Triton X-100 and incubate for 2 min
3. 3x wash with PBST
4. Add 100 µL anti-tubulin antibody (Alexa fluor 647) and incubate overnight

Dilution – 1:100 à 17 µL: 1700 µL

5. Add 100 µL actin phalloidin 555 nm and incubate for 30 minutes

Dilution – 1:100 à 17 µL: 1700 µL

6. Add 100 µL DAPI and incubate for15 minutes

if you have to make it –Add 100 ul 70% EtOH to one DAPI tube. Transfer to a 50 mL tube. And then add PBS to 50 mL.

7. 3x washes with BST
8. 2x washes with PBST – incubate in 10 minutes
9. 3x washes with PBST – incubate in 30 minutes
10. Mount the coverslips on the cover glass – the mounting media used is prolong glass antifade mountant

Label the cover glasses

# Appendix C - How cytochalasin B affects endocytosis

The aim was to assess the influence of *cytochalasin B* on endocytosis. Some cells were pre-treated in 30 min with cytochalasin and then rinsed before incubating for 2 h with $^{125}$I-labeled FSA. The cells were also pre-treated with other concentrations for 30 min with *cytochalasin B* and then incubated with $^{125}$I-labeled FSA for 2 h without rinsing *cytochalasin B*.

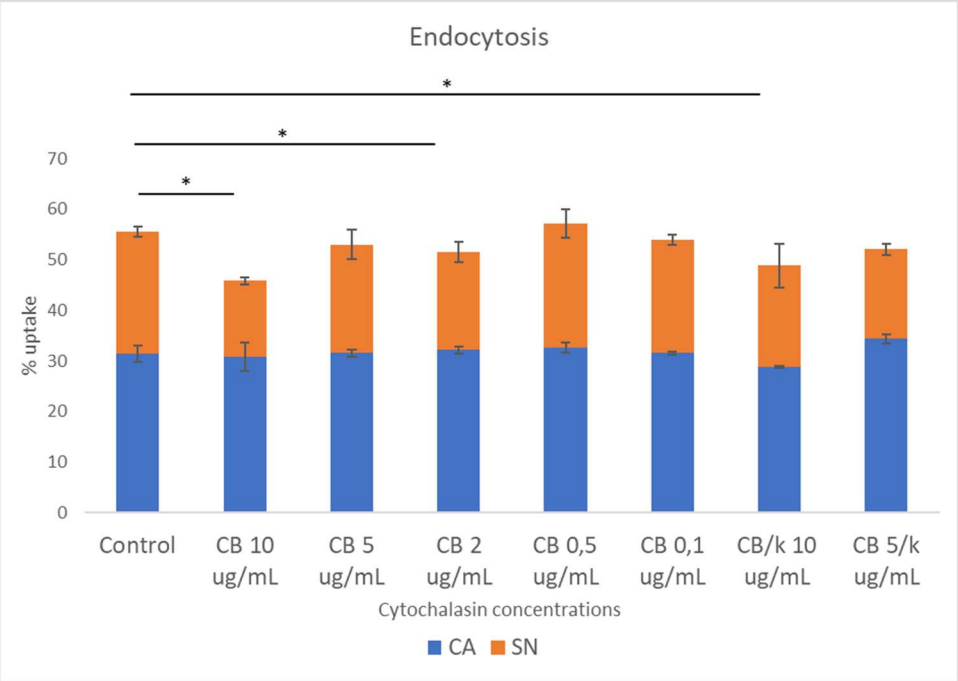


*Figure 1: Endocytosis of $^{125}$I-labelled FSA after treating with Cytochalasin B on day 1. Blue represents cell associated FSA, and red represents cell degraded FSA. CB/k represents rinsing the wells from cytochalasin before adding of $^{125}$I-labeled FSA. While the remaining samples, $^{125}$I-labeled FSA was added with continuously treatment with Cytochalasin B Results are presented as the mean of n=1 independent experiments +/- standard deviation. Statistical significance was determined by pairwise comparisons using one-way t-test *p<0.05 **p<0.01, ***p<0.001. Abbreviations: CB - cytochalasin B.*

# Appendix D – Stabilin-1 immunostaining and negative control of the immunofluorescence

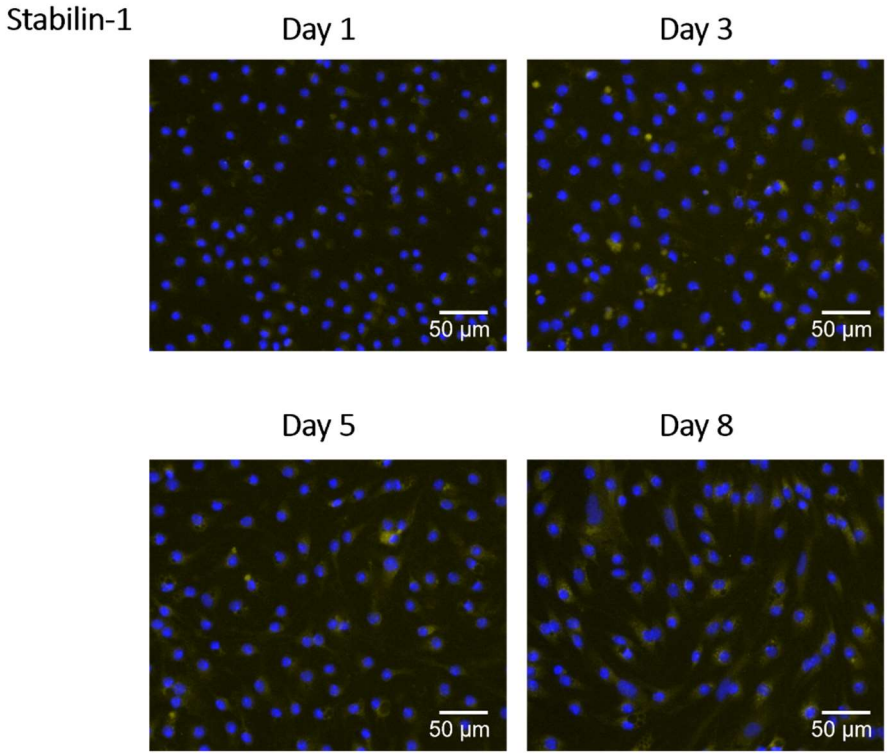


*Figure 2: Expression of receptors in LSEC. Mouse LSEC were isolated and seeded on fibronectin plastic well plates in EGM. The cells were fixed and single-stained on days 1, 3, 5 and 8. Stabilin-1 was stained with an anti-stabilin-1 rat antibody (yellow) and cell nuclei were stained with DAPI (blue). Images are presented vertically, showing changes over time for the receptors. Images were obtained at 20x magnification with EVOs. Scale bar = 50 µm.*

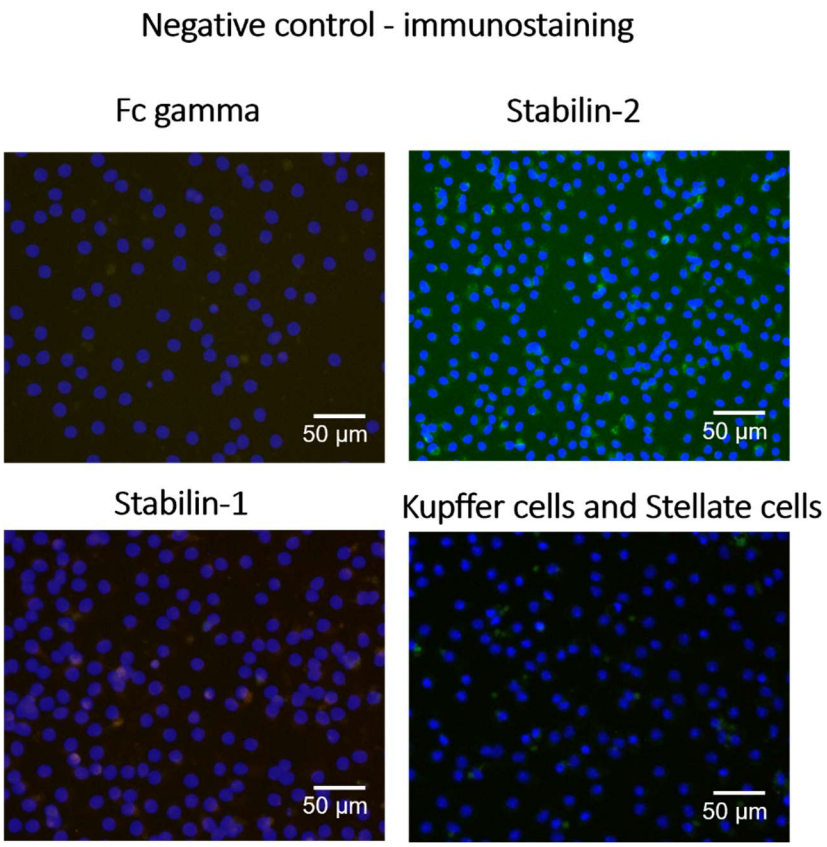


*Figure 3: Negative controls. Mouse LSEC were isolated and seeded on fibronectin plastic well plates in EGM. The cells were fixed and single-stained on days 1, 3, 5 and 8. Stabilin-1 was stained with an anti-stabilin-1 rat antibody (yellow), Stabilin-2 was stained with an anti-stabilin-2 rat antibody (green), Fc-gamma IIb2 was stained with an anti-mCD32/CD-16 antibody (yellow) and cell nuclei were stained with DAPI (blue). Images are presented vertically, showing changes over time for the receptors. Images were obtained at 20x magnification with EVOs. Scale bar = 50 µm.*